University of Calgary

PRISM Repository **https://prism.ucalgary.ca**

The Vault Open Theses and Dissertations

2014-10-14

Roles of the ING1 Epigenetic Regulator in Breast Cancer

Thakur, Satbir

Thakur, S. (2014). Roles of the ING1 Epigenetic Regulator in Breast Cancer (Doctoral thesis, University of Calgary, Calgary, Canada). Retrieved from https://prism.ucalgary.ca. doi:10.11575/PRISM/27691 http://hdl.handle.net/11023/1930

Downloaded from PRISM Repository, University of Calgary

UNIVERSITY OF CALGARY

Roles of the ING1 Epigenetic Regulator in Breast Cancer

by

Satbir Singh Thakur

A THESIS

SUBMITTED TO THE FACULTY OF GRADUATE STUDIES

IN PARTIAL FULFILMENT OF THE REQUIREMENTS FOR THE

DEGREE OF DOCTOR OF PHILOSOPHY

GRADUATE PROGRAM IN BIOCHEMISTRY AND MOLECULAR BIOLOGY

CALGARY, ALBERTA

OCTOBER, 2014

© Satbir Singh Thakur 2014

Abstract

ING proteins are epigenetic "readers" that can target various chromatin modifying complexes to chromatin. They are involved in various cellular processes such as DNA repair, apoptosis and cellular senescence. This study focuses on examining the potential role of ING1 as a therapeutic agent and prognostic marker for breast cancer.

We began by asking whether dysregulating epigenetic pathways with different chemical inhibitors could show synergistic effects with ING1 on killing cancer cells. We tested whether ING1 could synergize better with chemotherapeutics that target the same epigenetic mechanism or a different epigenetic mechanism. Combination treatment of ING1b with LBH589 (HDAC inhibitor) showed synergy, but the combination of ING1b with 5azaC (DNMT inhibitor), thus targeting two distinct epigenetic mechanisms, was more effective. Adenoviral delivery of ING1b combined with 5azaC also inhibited cancer cell growth in a xenograft model and led to tumor regression. These data showed that targeting distinct epigenetic pathways in our model was more effective in blocking cancer cell line growth than targeting the same pathway with multiple agents.

Since ING1 expression is frequently repressed in breast carcinomas, but its mechanistic role in breast cancer development and metastasis was unknown, we analyzed ING1 levels in patient samples and correlated it to patient outcome. We also studied the effects of altering ING1 levels in metastasis assays *in vitro* and mouse metastasis model *in vivo*. ING1 levels were lower in tumors compared to adjacent normal breast tissue and correlated with tumor size and distant recurrence. ING1 could also predict disease-specific and distant metastasis-free survival in these patients. Decreasing levels of ING1

increased, and increasing levels decreased migration and invasion of MDA-MB231 cells *in vitro*. ING1 overexpression also blocked cancer cell metastasis *in vivo* and eliminated tumor-induced mortality in mouse models.

Lastly, we determined if ING1 expression could predict breast cancer patient outcome. We found that stromal cell expression of ING1 showed an inverse correlation with patient survival. ING1 also correlated with tumor grade in these patients and multivariate analysis showed that ING1 was an independent prognostic marker in the breast cancer cohort we tested. This study provides important pre-clinical data that could help establish ING1 as a prognostic and therapeutic agent for breast cancer.

Acknowledgements

I would like to express my sincere gratitude to my supervisor and mentor, Dr. Karl Riabowol for providing me with the opportunity to pursue my doctoral studies under his guidance. His constant support, encouragement and belief in me have been the major reasons that have brought this project to its fruition. The freedom Dr. Riabowol provided, to try my own ideas in his laboratory has taught me to think independently and bravely face difficulties.

I would also like to thank my committee members Dr. Aru Narendran and Dr. Olga Kovalchuk for their support and guidance throughout the program. Their valuable advice and suggestions were really helpful to the work I did. I would also like to thank Dr. Oliver Bathe and Dr. Samuel Benchimol for agreeing to serve as examiners on my thesis and Dr. William Brook for serving as neutral chair.

This work would not have been possible without the support of various collaborations that I had during my stay in the department. I would like to thank Dr. Don Fujita, Dr. Frank Jirik, Dr. Don Morris, Dr. Joe Dort, Dr. Tony Magliocco and Dr. Alex Klimowicz for collaborating with us and providing reagents and suggestions for experiments. Special thanks to Dr. Manoj Mishra and Dr. Arvind Singla for their guidance regarding experiments and life in general.

Past and present members of the Riabowol lab have been instrumental in making this work possible. I would like to thank Dr. Pinaki Bose for his guidance and support during the early days in the lab. I would also like to thank Annie and Donna for the help

regarding reagents and managing the lab. Thanks to Arash, Mahsa, Yang and Alex for their friendship and support in the lab.

Staying in Calgary would not have been possible without my friends. Thanks to Abhishek, Saurav, Soumya, Kunal, Ranjan, Manoj, Sabarish and Sarvan for the good time and I look forward to a lifetime of friendship and working together.

I would like to acknowledge financial support from the Alberta Cancer Foundation for the studentship they provided during my doctoral study.

Special thanks to my Mom and my Sister for their constant care, encouragement and support throughout my life. Thanks for listening to me and supporting me during my frustrations and difficulties. Lastly, and most importantly, thanks to my Master without whom I hold no existence.

Table of Contents

List of Tables

List of Figures

List of Abbreviations

Units of measure

bp	- Base pair
cm	- Centimeters
°C	- Degrees centigrade
g	- Gram
Kg	- Kilogram
mg	- Milligram
ml	- Milliliter
mM	- Millimolar
M	- Molar
ng	- Nanogram
pfu	- Plaque forming units
µg	- Microgram
µl	- Microliter
µM	- Micromolar

Chemical compounds/buffers/solutions

CsCl	- Cesium chloride
DAPI	- 4,6-Diamidino-2-phenylindole
EDTA	- Ethylenediamine-tetraacetic acid
PBS	- phosphate buffered saline
SDS	- sodium dodecyl sulphate
Tris	- Tris(hydroxymethyl)aminomethane

Nucleic Acids

DNA	- Deoxyribonucleic acid
cDNA	- Complimentary deoxyribonucleic acid
RNA	- Ribonucleic acid
mRNA	- Messenger ribonucleic acid
miRNA	- Micro ribonucleic acid
siRNA	- Small interfering ribonucleic acid

General

5azaC	- 5-azacytidine
AML	- Acute myeloid leukemia
AR	- Androgen receptor

ATCC - American Type Culture Collection
ATM - Ataxia telangiectasia mutated
BRCA1 - Breast cancer 1
CAFs - Cancer associated fibroblasts
CK - Cytokeratin
CpG - Cytosine-phosphate-Guanine
Cys - Cysteine
DMEM - Dulbecco's minimal essential media
EGF - Epidermal growth factor
EGFP - Enhanced green fluorescent protein
EGFR - Epidermal growth factor receptor
FBS - Fetal bovine serum
FGFR - Fibroblast growth factor receptor
GADD45 - Growth arrest and DNA damage inducible 45
GFP - Green fluorescent protein
H2AX - H2A histone family, member X
HEK293 - Human embryonic kidney 293 cells
HER - Human epidermal growth factor receptor
His - Histidine
IGFR - Insulin like growth factor receptor
luc - Luciferase
MMP - Matrix metalloproteinase
MOI - Multiplicity of infection
mTOR - Mammalian target of rapamycin
NBS1 - Nibrin; Nijmegen breakage syndrome1
NF-κB - Nuclear factor kappa B
PAGE - Polyacrylamide gel electrophoresis
PARP - Poly-ADP ribose polymerase
PCNA - Proliferating cell nuclear antigen
PDGF - Platelet derived growth factor
PDGFR - Platelet derived growth factor receptor
PIK3CA - Phosphatidylinositol-4,5-bisphosphate 3-kinase catalytic subunit alpha
PI3K - Phosphoinositide 3-kinase
PTEN - Phosphatase and tensin homolog
SAHA - Suberoyl anilide hydroxamic acid
SMA - Smooth muscle actin
TGFβ - Transforming growth factor-β
UV - Ultraviolet
VEGF - Vascular endothelial growth factor

CHAPTER 1: INTRODUCTION

1.1 Cancer introduction and epidemiology

A human body is made up of ~ 37 trillion cells that form tissues and organs (Bianconi, Piovesan et al. 2013). Each of these cells in the body is governed by the genes expressed in them in order to grow, perform their particular functions, replicate and in some instances die. Under normal conditions, cells obey these programmed orders and follow a highly regulated cycle of replication and death. 'Cancer' is a general term which refers to a condition when the cells begin to grow and reproduce in an unregulated manner. This loss of control on cellular processes generally occurs due to mutations in the genes regulating them. These cells divide to form tumors which may be benign (non-cancerous; do not spread to other organs) or malignant (cancerous; spread to other organs).

Carcinogenesis is a multistep process in which cells gradually become malignant through a progressive series of alterations. Generally, carcinogenesis has been described to occur in 3 main steps namely: Initiation, Promotion and Progression. During initiation, a single cell acquires mutations which bypass the cellular repair machinery, leading to abnormal proliferation. The mutant cell proliferation leads to outgrowth and promotion of a clonal population with more acquired mutations increasing the likelihood of forming a tumor. In the third step, tumor progression continues and additional mutations occur within cells of the tumor population. Some of these mutations confer a selective advantage to the cell which allows the cell and its descendants to become dominant within the tumor population, which is known as clonal selection. New clones of tumor cells evolve from parental cells due to mutations that confer a selective advantage to them. This selection continues throughout tumor development, allowing tumors to continuously become more aggressive and increasingly malignant. These mutations occur

in a number of pathways often referred to as the “hallmarks of cancer” (Hanahan and Weinberg 2000). Epigenetic alterations are also believed to be the key initiating events in carcinogenesis. Epigenetic aberrations, unlike genetic mutations, are potentially reversible and can be restored to their normal state by epigenetic therapy makes them promising and therapeutically relevant for cancer treatment.

Cancer figures among the leading causes of death worldwide, accounting for over 8 million deaths annually, approximately 4.7 million (57%) in males and 3.5 million (43%) in females (GLOBOCAN 2012). In Canada, cancer is the leading cause of death (Figure 1A) and is responsible for nearly 30% of all deaths (De, Dryer et al. 2013). Although there are more than 100 different types of cancers described, cancers of the lung, liver, stomach, colon and breast, cause the most cancer deaths each year. The most frequent types of cancers differ between men and women. Whereas lung cancer is the most frequent cause of cancer death in men, women have the highest incidence of and mortality, from breast cancers (Figure 1B, C).

In spite of various treatment protocols, screening and awareness programs currently available for various cancers, cancer incidence is predicted to increase to 22 million within the next two decades worldwide. According to 2013 Canadian Cancer Statistics, in Canada alone, it is expected that 2 in 5 Canadians will develop cancer in their lifetimes with males having a 46% and females having 41% lifetime probability of developing cancer. Considering this alarming increase in cancer incidence and mortality that may, in part be attributed to increased predicted lifespan, new treatment strategies and agents that may help in the treatment of cancer that have minimal side effects and could increase the survival of cancer patients are clearly needed.

Figure 1: Cancer incidence worldwide

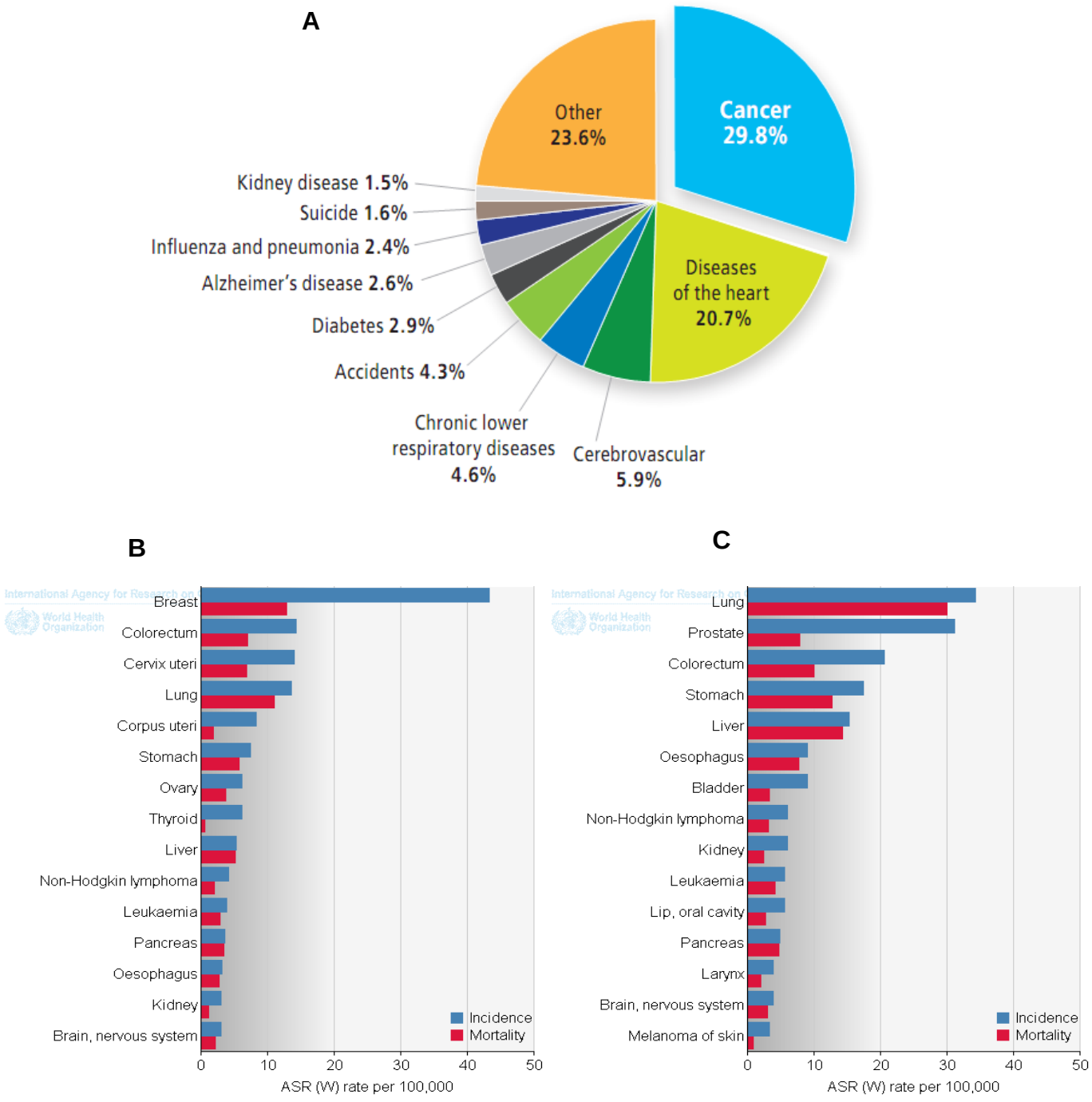

(**A**) Proportion of deaths due to cancer and other causes in Canada (Statistics Canada, 2009). Estimated age-standardized incidence and mortality rates in (**B**) women and (**C**) men (GLOBOCAN 2012).

1.2 Breast cancer epidemiology

Breast cancer is the most commonly occurring cancer in women around the world and comprises almost one third of all female malignancies (Richie and Swanson 2003). It is second only to lung cancer in cancer caused mortalities and is the leading cause of death due to cancer in women. There were an estimated 1.67 million new breast cancer cases diagnosed in 2012 worldwide. It is the most common cancer in women both in more and less developed regions with slightly more cases in less developed (883,000 cases) than in more developed (794,000) regions (GLOBOCAN 2012).

There are many risk factors that correlate with the incidence and prevalence of breast cancer in women. These are broadly classified as reproductive or lifestyle and dietary factors (Ban and Godellas 2014).

Reproductive factors

This category is comprised of factors such as age, exogenous hormones and other genetic factors that influence the probability of breast cancer incidence in women. Age is one of the major factors that also plays a role in many other physiological events during a women's lifetime such as menarche, pregnancy, breastfeeding and menopause. As in all other cancers, it has been observed that the risk of breast cancer development increases with increasing age of women (Yasui and Potter 1999) with post-menopausal women having a significantly higher risk of developing breast cancer. Longer lifetime exposure to hormones like estrogen also have a direct correlation with breast cancer incidence (Kelsey, Gammon et al. 1993) which may explain the increased risk of breast cancer with early and late onset of menarche and menopause, respectively, in women (Trichopoulos,

MacMahon et al. 1972). Breastfeeding, which suppresses ovulation and thus reduces estrogen levels in a women's body is also known to reduce the risk of breast cancer (Byers, Graham et al. 1985). It has also been reported that women who have had no children or who had their first child after 35 years of age have a slightly higher risk of breast cancer. Having many pregnancies and becoming pregnant at a young age appears to reduce breast cancer risk (Lambe, Hsieh et al. 1994; Russo, Moral et al. 2005).

Exposure to exogenous hormones, particularly estrogen and progestin, increase the risk of breast cancer development. Women using oral contraceptive pills having these hormones in the formulation are reported to be at slightly higher risk of breast cancer (Hunter, Colditz et al. 2010). It has also been observed that post-menopausal use of hormone replacement therapy is associated with an increased risk of breast cancer in women (Chlebowski, Kuller et al. 2009).

About 5-10% of breast cancers appear to be hereditary and having a familial history of breast cancer is a well-known risk factor (Stratton and Rahman 2008). Although the most common cause of hereditary breast cancer is an inherited mutation in the *BRCA1* or *BRCA2* tumor suppressor genes, mutations in other tumor suppressors such as p53, PTEN etc., are also known to put carriers at high risk of breast cancer (Evans and Howell 2007; Walsh and King 2007). Genes specifically involved in DNA repair and cell cycle regulation such as *ATM*, *CHEK2*, *NBS1* and *RAD50* are also associated with a 2-fold to 4-fold increased risk of breast cancer in women (Walsh and King 2007). Having a personal history of breast cancer also increases the risk of developing new cancers at new sites in women (Hartmann, Sellers et al. 2005).

Lifestyle and dietary factors

Apart from various reproductive and genetic factors contributing to risk of breast cancer in women, there are some factors depending on the type of lifestyle and diet of a person that may incur increased risk of developing breast cancer. These include use of alcohol and tobacco, lower physical activity and obesity. There are numerous reports that show a linear relationship between increased risk of cancer development and these factors (Smith-Warner, Spiegelman et al. 1998; Friedenreich, Bryant et al. 2001; Kobayashi, Janssen et al. 2013). Numerous dietary factors have been studied as potential breast cancer risk factors such as soy, fat, fruit and vegetable intake and carbohydrate and antioxidant intake (Yamamoto, Sobue et al. 2003; Prentice, Caan et al. 2006). Till now, results involving these dietary factors have been conflicting and no conclusive evidence is present that may establish direct links to increase breast cancer incidence (Ban and Godellas 2014). Radiation exposure occupational or for medical purposes, is also known as a breast cancer risk factor with women exposed at a young age (20 or less) having higher risk compared with women exposed after age 40 (Land, Tokunaga et al. 2003). Other factors such as race and ethnicity are also known to influence the risk of breast cancer in women as notable differences exist in both incidence and mortality among women from different races and ethnic backgrounds (SEER cancer statistics).

1.3 Classification of Breast Cancer

Breast cancer is a complex and heterogeneous disease in nature with various morphologic and biological features, behaviors, and responses towards therapy. Breast cancer classification systems, in the past, have been based on mere histological assessment and

clinical staging which includes variables such as gross tumor size, lymph node stage, and extent of tumor spread. With advancement in molecular techniques and increased knowledge of breast cancer biology, expression of proteins like the estrogen receptor (ER), progesterone receptor (PR) and over-expression or amplification of the human epidermal growth factor receptor 2 (HER2) were included in the classification system (Vuong, Simpson et al. 2014). Based on the combination of both classical histopathological and biological prognostic and predictive variables, patients are now stratified into different risk groups, which can help in determining the treatment strategies based on the group they fall into.

Histologically, breast cancer is divided into *in situ* (ductal and lobular) and invasive disease which further has more than 21 subtypes based upon morphological variations (Vuong, Simpson et al. 2014). They are also assigned scores by pathologists on characteristics like proportion of tubule formation, degree of nuclear pleomorphism and the mitotic count. The scores are then combined to give a grade (1, 2 or 3), where grade 1 tumors are most differentiated and have good clinical outcome and grade 3 are the least, having high recurrence rate and poor outcomes (Rakha, Reis-Filho et al. 2010). Combining both clinical and pathological information histologically, breast cancers are staged according to tumor size (T), the status of regional lymph nodes (N) and spread to distant metastatic sites (M), thus forming the TNM system (Edge and Compton 2010).

Based upon the biomarkers (ER, PR and HER2) clinically used worldwide, breast cancers are currently divided into luminal (luminal A or B), HER2 enriched or basal-like type. Luminal tumors are generally ER-positive, with luminal A tumors being low grade, PR-positive and HER2-negative. Luminal B tumors are high grade, PR-positive or

negative and either HER2-positive or negative and have a high mitotic index as measured by Ki-67 score (Cheang, Chia et al. 2009).

Basal-like tumors are most diverse amongst different types of breast cancers with respect to characteristics like histopathological features, mutation profiles, response to chemotherapy, metastatic behavior and survival rates (Vuong, Simpson et al. 2014). These tumors are ER-negative, HER2-negative and are also characterized by expression of proteins like cytokeratin (specifically cytokeratin 5 and 6), EGFR, c-KIT, FOXC1, frequent *p53* mutations and a high proliferation index. They are mostly grade 3 tumors and show aggressive clinical behavior (Badve, Dabbs et al. 2011). Approximately 10–15 % of all the breast cancers detected are negative for ER, PR and HER2 and are called triple-negative breast cancers (TNBC). Basal-like breast cancers are a subset of TNBC and patients with this type of tumor have a very poor prognosis; currently there is no targeted therapy available for their treatment (Valentin, da Silva et al. 2012).

The HER2 group is defined by high expression of HER2 and related genes. This group comprises tumors that are generally grade 2 or 3 and that have poor prognosis. Due to amplification or protein over-expression of HER2, these types of tumors are predicted to respond to systemic treatment with a humanized anti-HER2 specific monoclonal antibody (Trastuzumab; Herceptin). HER2 positivity is seen in 13–20 % of invasive breast cancers, which can be hormone receptor positive or negative (Slamon, Clark et al. 1987; Vuong, Simpson et al. 2014).

Apart from these subtypes mentioned above, a normal-like subtype is also believed to exist which is characterized by expression of genes associated with adipose

tissue and other stromal cell types. This group is not yet clearly defined and is thought by some groups to represent normal breast cell contamination in tumor samples rather than being a real breast cancer subtype (Vuong, Simpson et al. 2014).

Attempts have been made in the recent past to define the subtypes of cancers using both immunohistochemistry (IHC) and genomic techniques and new subtypes have emerged since the initial description of different types of breast cancer. These subtypes include claudin low (TNBC, enrichment of immune response genes), molecular apocrine (ER-negative, AR-positive) and interferon related groups (Farmer, Bonnefoi et al. 2005; Prat, Parker et al. 2010). In a more recent study, three new classes of breast cancer have been suggested based on the expression of a panel of ten biomarkers (ER, PR, CK5/6, CK7/8, EGFR, HER2, HER3, HER4, p53 and Mucin1) determined by IHC. These classes have been named as luminal N, basal p53-altered and basal p53-normal (Green, Powe et al. 2013). The significance and clinical value of the classification of tumors belonging to these newly described classes is still to be confirmed.

Recently, a novel molecular stratification of the breast cancer population was suggested using techniques like genomic DNA copy number arrays and integrative clustering analysis of 2000 different primary breast tumors. The analysis resulted in defining ten novel molecular subgroups of breast cancer using the top ranking 1000 genes whose expression levels were significantly affected by copy number change. These copy number alterations had marked effects on the expression of genes within these regions which included known and putative drivers of tumorigenesis (Curtis, Shah et al. 2012). All the subgroups thus formed had well characterized whole genome copy number profiles with distinct clinical outcomes. Table 1 shows the major attributes of various

breast cancer subtypes currently classified in the clinic along with their suggested integrative clustering.

Although gene expression profiling and other genomic based approaches to classify breast carcinoma have played a great role in determining these new subtypes, the presence of breast cancer biomarkers is generally determined by using immunohistochemical techniques in the clinic, specifically due to IHC currently being much less expensive and less time consuming.

Table 1: Molecular subtypes of Breast Cancer.

Clinical Subtype	Grade	ER Status	HER2 Status	Integrative Cluster	Key Molecular Features
Luminal A	1-2	+	-	2, 3, 4, 7, 8	Mutations in *PIK3CA*, *MAP3K1*,*GATA3*, *FOXA1*; high expression of *ESR1*, *XBP1*
Luminal B	2-3	+/-	-/+	1, 2, 6, 9	Mutations in *p53*, *PIK3CA*; amplification of *Cyclin D1*, *MDM2*; loss of *ATM*
HER2	2-3	+/-	+	5	Mutations in *p53*, *PIK3CA*; amplification of *HER2*, *Cyclin D1*; high expression of *EGFR*, *FGFR4*
Basal	3	-	-	4, 10	Loss of *BRCA1*, *RB1*; activation of *FOXM1*

Table showing integrative clustering and key molecular feature of subtypes of tumors currently recognized in clinic.

1.4 Therapies for Breast Cancer

Depending upon the type and stage of breast cancer, a variety of therapeutic paths can be followed. These include localized interventions such as surgery and radiation therapy or systemic treatments such as chemotherapy, hormonal or HER2 therapy which can be used alone or in combination. In the recent past, a major research focus has been on developing targeted therapies having improved efficacies and minimal side effects for subgroups of patients.

The description of various molecular subtypes of breast cancer and identification of the genetic alterations and signaling pathways that drive these cancers, has helped researchers worldwide in developing a number of successful molecular targeted agents that are used clinically, resulting in better patient survival with minimal side effects. Among these therapeutics are tyrosine kinase inhibitors (TKIs) which are directed against membrane growth factor receptors (HER, IGFR, FGFR etc.), inhibitors of intracellular growth signaling pathways (PI3K, AKT, mTOR etc.), angiogenesis inhibitors, and agents targeting the DNA repair machinery (Higgins and Baselga 2011).

Hormone receptor positive (ER and PR-positive) breast cancers have been successfully targeted with drugs such as Tamoxifen, aromatase inhibitors and Fulvestrant which target estrogen and have resulted in improved survival in women with early and advanced breast cancer (Robertson, Llombart-Cussac et al. 2009; Gradishar 2010). Cancers are known to develop compensatory proliferative pathways if a pathway is blocked using a therapeutic, due to cross-talk between various membrane receptors and their subsequent signaling pathways downstream. It has been observed that tumors that

are HER2 and ER-positive show poor response when treated with estrogen targeting therapeutics alone. To overcome such situations, combinatorial approaches have been made to target different pathways simultaneously. For example, patients with ER and HER2-positive tumors treated with Trastuzumab or Lapatinib (anti HER2 TKI) and aromatase inhibitor have shown a significant increase in survival (Johnston, Pippen et al. 2009; Kaufman, Mackey et al. 2009).

HER2 is regarded as an acceptable therapeutic target by oncologists worldwide. Trastuzumab which is a monoclonal antibody against HER2, in combination with cytotoxic chemotherapy has drastically changed the prognosis of patients with HER2-overexpressing breast cancer. For patients whose disease has progressed following Trastuzumab treatment, Lapatinib (dual HER1 and HER2 TKI) has been approved for treatment (Baselga and Swain 2009). Since the initial use of Trastuzumab as a single agent, a lot of novel approaches have been reported using modified versions of the antibody with significant positive response from patients. for example, Trastuzumab-DM1 (T-DM1) which is an antibody-drug conjugate consisting of Trastuzumab covalently bound via a linker to DM1, (the antimicrotubule chemotherapeutic Maytansine) was reported to show positive response in patients with advanced HER2-postive breast cancer (Krop, Beeram et al. 2010). This is an interesting strategy as this might be an alternative to systemic chemotherapy that shows severe side effects in patients. Pertuzumab which is another recombinant humanized monoclonal antibody against the dimerization domain II of HER2 has also been used successfully in combination with Trastuzumab in preclinical models (Baselga, Gelmon et al. 2010), and clinical trials are ongoing involving combined administration of Pertuzumab with T-DM1

in patients with metastatic breast cancer (Phillips, Fields et al. 2014).

Pathways such as PI3K/AKT/mTOR is known to be critical for growth of a variety of normal and cancer cells including breast cancers. Targeting these pathways is difficult in cancers as their inhibition elicits compensatory activation of multiple survival routes (Serra, Scaltriti et al. 2011). Despite this, clinical trials are ongoing combining inhibitors of mTOR with agents like aromatase inhibitors and monoclonal antibodies against proteins like IGF1R (Baselga, Semiglazov et al. 2009). In another study the mTOR inhibitor Everolimus was combined with Paclitaxel and Trastuzumab in patients with HER2-overexpressing metastatic breast cancer pretreated with Trastuzumab alone, which resulted in improved anti-tumor activity and overall response to therapy (Andre, Campone et al. 2010).

Triple negative breasts cancers are generally regarded as most aggressive type of breast cancer. Unlike some of the other subgroups, these types of cancers do not possess any validated target for therapy, which makes them difficult to treat. Considering that the majority of TNBC have *BRCA1* mutations, studies have been undertaken aimed at targeting the DNA repair machinery with agents such as Olaparib and Iniparib that are PARP inhibitors (Tutt, Robson et al. 2010; O'Shaughnessy, Osborne et al. 2011), but to date, results have been mixed. Another strategy to target EGFR in TNBC using the monoclonal antibody Cetuximab along with Cisplatin has also been considered and is currently in phase III clinical trials (Baselga 2010).

Current treatment options for breast cancer are primarily directed towards less toxic targeted therapies that can be patient specific. Today, due to the understanding of

different drivers of carcinogenesis in different cancer types, targeted therapeutic options are available for nearly all breast cancer subtypes (Higgins and Baselga 2011). The major hurdle in complete treatment of breast cancer as well as other cancers still remains in the acquisition of resistance to individual targeted treatment, which provides a major challenge and opportunity for development of novel therapeutics to be used in combination approaches and additional biomarkers of response prediction.

1.5 Epigenetics and cancer

Epigenetics is the study of heritable changes in gene expression that occur independent of changes in primary DNA sequence. Transcriptional silencing of genes via epigenetic mechanisms is a hallmark of cancer cells and epigenetic mechanisms are now firmly established as important contributors to tumorigenesis. The epigenomic landscape in a normal cells undergoes extensive rearrangement in cancer. Epimutations, along with widespread genetic alterations, play an important role in cancer initiation and progression (Sharma, Kelly et al 2010). Epigenetic changes result in global dysregulation of gene expression profiles which may contribute to the development and progression of diseases like cancer. Particularly these alterations can lead to silencing of tumor suppressor genes independently or in conjunction with genetic mutations and may serve as the second hit for cancer initiation according to the ‘two-hit’ model proposed by Alfred Knudson (Sharma, Kelly et al 2010).

In addition to inactivating tumor suppressors, epigenetic alterations can also promote cancer progression by activating oncogenes. Since epigenetic alterations, like genetic mutations, are mitotically heritable, they are selected for in a rapidly growing

cancer cell population and confer a growth advantage to tumor cells resulting in their uncontrolled growth. Multiple cellular targets, such as tumor suppressors, cell cycle regulators, differentiation regulators, and DNA repair genes are silenced by epigenetic mechanisms. Cancer cells display diverse sets of genetic alterations and epigenetic changes that alter patterns of gene expression to drive the initiation and development of a large number of tumor types (Sharma, Kelly et al. 2010). Epigenetic changes, being heritable, can drive cancer progression by conferring growth advantages and resistance to apoptosis among other factors. Four major forms of epigenetic regulation currently known are: DNA methylation (Suzuki and Bird 2008), histone modification (Kouzarides 2007), nucleosome positioning (Jiang and Pugh 2009) and noncoding RNA (Zhang, Pan et al. 2007).

Noncoding small (~22bp) microRNAs (miRNAs) regulate gene expression by post transcriptionally silencing target genes via the RNA induced silencing complexes (RISC) (Pratt and MacRae 2009). Genes that are regulated by miRNAs include protooncogenes and tumor suppressors, so miRNAs can either promote or inhibit the development of cancers. Alterations of particular, and downregulation of global miRNAs, have been reported in various subsets of tumors (Ventura and Jacks 2009), suggesting that miRNAs may prove useful in treating particular cancer types. The major hurdle in utilising this epigenetic modification for cancer treatment is in its delivery to tumor cells.

Nucleosome repositioning involves relocating nucleosomes, largely in promoter regions of genes and changing the composition of the histones in the core octamers. Based upon the repositioning, this epigenetic process may increase expression of some genes by releasing the DNA in that region and making it more accessible to transcription

factors while decreasing of some others by the opposite phenomenon of increasing nucleosome density.

The next category of epigenetic modification, and one that is a target of developing therapies involves regulation of nucleosome stability by covalent modification of tails of core histones by phosphorylation, methylation, acetylation, ubiquitination or sumoylation (Jenuwein and Allis 2001). In particular, the N-terminal region of the histones (the histone 'tails') plays a major role in transcriptional regulation by acetylation and deacetylation of various lysines within these regions. The acetylation state of histones is reversibly regulated by two classes of enzymes, histone acetyltransferases (HATs) and histone deacetylases (HDACs) (Archer and Hodin 1999; Brown and Strathdee 2002). In general, transcriptional activators bind and recruit HATs and are associated with acetylated chromatin, while transcriptional repressors and co-repressors interact with HDACs and their binding to promoters correlates with loss of histone acetylation. Acetylation, mediated by multi-protein complexes containing HATs, or by inhibiting the activity of the HDACs, neutralizes the positive charge associated with the ε-amino group of conserved lysine residues in the histone tails. This is thought to make the nucleosome-DNA structure less stable, thereby facilitating access of a variety of factors including transcription and replication factors to DNA. In addition to histones, HDACs also deacetylate non-histone proteins involved in transcription (p53, p73, E2F1, c-Jun, GATA1, RelA, and NF-κB), hormone response (AR and ER), nuclear transport (importin-α7), cytoskeletal structure (α-tubulin), DNA repair (Ku70), DNA structure (WRN), signal transduction (β-catenin), and the heatshock/chaperone response (HSP90) (Marks, Rifkind et al. 2001; Johnstone 2002). Aberrant histone deacetylation contributes

to tumorigenesis through the recruitment of HDACs to the promoter regions of tumor suppressor genes. They also contribute through chromosomal translocations, occurring in certain tumor types, which give rise to oncogenic fusion proteins resulting in inappropriate recruitment of HDACs to certain gene promoters involved in differentiation (Marks, Rifkind et al. 2001; Johnstone and Licht 2003).

Another major mechanism of epigenetic regulation in vertebrates is the pattern of distribution of the covalent modification of cytosines by methylation in the genome. It has been linked to the suppression of highly repetitive transposable elements (Suzuki and Bird 2008) and particularly targets CpG rich areas which makeup ~60% of human gene promoters (Wang and Leung 2004). In a normal cell, repetitive regions, transposons and imprinted gene promoters are heavily methylated, which are accompanied by repressive histone marks such as H3K9 methylation that together form a silent chromatin state. However, during tumorigenesis, tumor suppressor gene promoters with CpG islands become methylated, resulting in the aberrant silencing and in contrast, the repetitive sequences, transposons and imprinted gene promoters become hypomethylated resulting in their aberrant activation which contributes to cancer progression (Sharma, Kelly et al. 2010). Different CpG sites are methylated in different tissues, creating a pattern of methylation that is gene and tissue specific (Razin and Riggs 1980). This pattern creates a layer of information that helps confer upon a genome its specific cell type identity. The DNA methylation pattern is copied by independent enzymatic machinery, the DNA methyl transferases (DNMT). DNA methylation patterns in vertebrates are distinguished by their tight correlation with chromatin structure. Active regions of the chromatin, which enable gene expression, are associated with hypomethylated DNA, whereas

hypermethylated DNA is generally packaged into inactive chromatin (Razin and Cedar 1977). DNA methylation silences gene expression either by interfering with the binding of transcription factors (Comb and Goodman 1990; Inamdar, Ehrlich et al. 1991) or by attracting methylated DNA-binding proteins (MBDs), which recruit other proteins such as SIN3A and histone modifying enzymes which leads to formation of a closed chromatin configuration and silencing of gene expression.

1.6 Epigenetic drugs in cancer

Cancer cells accumulate genetic and epigenetic changes that alter gene expression to drive tumorigenesis (Sharma, Kelly et al. 2010) and epigenetic silencing of tumor suppressor, cell cycle, differentiation and DNA repair genes contributes to tumorigenesis (Kim, Bang et al. 2006). Epigenetic abnormalities that are commonly found in human tumors can often be exacerbated or reversed by pharmacologic inhibitors, such as HDAC inhibitors and DNA methylation inhibitors, making them more susceptible to other cancer treatments. One of the histone modifications showing promise as a target for cancer treatment is acetylation (Atadja 2011). Acetylation is increased by HDAC inhibitors like sodium butyrate, resulting in decondensation of heterochromatic DNA and increased sensitivity to DNAse (Candido, Reeves et al. 1978). HDAC inhibitors that are showing promising effects in clinical trials such as LBH589 (Panobinostat), are pan-deacetylayse inhibitors, being capable of inhibiting all HDACs that require Zn as a cofactor (Atadja 2009). It is interesting to note that the molecular target of the HDAC inhibitor suberoylanilide hydroxamic acid (SAHA) was recently identified as ING2, a stoichiometric member of the Sin3 HDAC complex (Smith, Martin-Brown et al. 2010),

suggesting that targeting of the INGs themselves may prove useful in combination with other chemotherapeutic agents.

DNA methylation can be modified pharmacologically and cancer was the first disease proposed as a therapeutic target (Szyf 1994). DNA methylation is altered in cancers by hypermethylation of tumor suppressor genes, aberrant expression of DNMTs and hypomethylation of unique genes and repetitive sequences. The three most commonly used catalytic inhibitors of DNMTs and hence, DNA methylation, are the nucleoside analogs 5-azacytidine (5azaC), 5-aza-deoxycytidine (5azaCdR) and Zebularine. 5azaC and its deoxy analog 5azaCdR are FDA approved for treatment of myelodysplastic syndromes (Kuendgen and Lubbert 2008). When 5′-azacytosine is incorporated into DNA in place of cytosine, DNMT is trapped on DNA (Wu and Santi 1985) resulting in passive loss of DNA methylation in the nascent strand. While positive responses with tolerable adverse effects were reported in clinical trials for hematological malignancies (Oki, Aoki et al. 2007), success in solid tumors has been elusive, which may be due to ineffective delivery, dosing or scheduling (Soriano, Yang et al. 2007). Different strategies for combining 5azaC with other chemotherapeutic agents or chromatin modifiers such as HDAC inhibitors are currently being tested in solid tumors in a number of clinical trials.

Recently, Miravirsen, a 15 nucleotide locked nucleic acid–modified antisense oligonucleotide, which is complementary to and specific for the 5′ region of the microRNA miR-122 has been used in a study involving patients with chronic infection of Hepatitis C virus (Janssen, Reesink et al. 2013). Chronic Hepatitis C virus infection is a major cause of liver cirrhosis, liver failure, and hepatocellular carcinoma and is the

leading indication for liver transplantation. miR-122 is a highly abundant miRNA expressed in the liver and is essential for the stability and propagation of Hepatitis C viral RNA (Henke, Goergen et al. 2008). Miravirsen administration to patients with chronic Hepatitis C virus infection resulted in significant virologic response. This is the first report involving miRNAs, a type of epigenetic alteration, showing a therapeutic effect by targeting a noncoding host miRNA for treatment of viral infection, which is known as one of the causes of hepatic cancer.

Table 2 shows various compounds targeting different epigenetic regulatory mechanisms and ongoing clinical trial status for them.

Table 2: Compounds targeting various epigenetic regulatory mechanisms.

Epigenetic Mechanism	Compound	Clinical Trial status	FDA approval
Nucleosome remodelling	None		
Noncoding RNAs; microRNAs	Miravirsen	I, II	
DNA Methylation	Azacytidine	I, II, III	Approved, MDS
	Decitabine	I, II, III	Approved, MDS
	Dihydroazacytidine	I, II	
	5-fluorodeoxycytidine	I, II	
	Zebularine		
	Epigallocatechin gallate	I, II, III	Approved, genital warts
	Hydralazine	I, II, III	Approved, hypertension
Histone modifications	Sodium butyrate	I, II	Approved, urea disorder
	Phenyl butyrate	I, II	
	Valproic acid	I, II, III	Approved, epilepsy
	Romidepsin	I, II	Approved, CTCL
	Entinostat	I, II, III	
	MGCD-0103	I, II	
	TSA		
	Belinostat	I, II, III	Approved, PTCL
	SAHA	I, II, III	Approved, CTCL
	Panobinostat	I, II, III	Under review (multiple myeloma)

Different compounds affecting various epigenetic mechanisms and their status in clinical trials. MDS (Myelodysplastic syndrome); CTCL (Cutaneous T-cell lymphoma); PTCL (Peripheral T-cell lymphoma)

1.7 Cancer Cell Metastasis

Metastasis is a multistep process by which tumor cells disseminate from their primary site and form secondary tumors at a distant site. It is responsible for around 90% of cancer associated mortality and is a poorly understood component of cancer pathogenesis. The cells undergoing metastatic dissemination (Figure 2) from a primary tumor locally invade the surrounding tissue and enter the microvasculature of the lymph and blood systems which is referred as "intravasation". In order for cells to successfully metastasize, they need to survive and translocate through the bloodstream to the microvessels of distant tissues. Upon reaching distant sites conducive to their growth, cells exit from the bloodstream (a phenomenon referred to as "extravasation") and adapt to the new microenvironment of these tissues and "colonize" to form macroscopic secondary tumors (Chaffer and Weinberg 2011). Thus, the metastatic process can be conceptually organized into two major phases, namely physical translocation of a cancer cell from the primary tumor to the microenvironment of a distant tissue and its colonization at the distant site (Chaffer and Weinberg 2011).

During the first phase, where the cells translocate, individual cells or small groups of cancer cells break away from the primary tumor and initiate the metastatic process. These cells acquire the ability to degrade and move through the extracellular matrix of the surrounding tissue toward blood and lymphatic vessels for their escape to distant secondary sites. Although the cells invade both the lymphatic and blood vessels, spread to anatomically distant sites seems to occur primarily through the blood (Hanahan and Weinberg 2000).

Cancers generally originate from epithelial tissue. This tissue is characterized by cells tightly bound to neighboring cells and to underlying basement membranes by various junctions which immobilize them into sheets. These physical constraints restrain both normal epithelial cells and benign cancers. During tumor progression and metastasis, cancer cells liberate themselves from the above mentioned associations and begin to mobilize by dissolving underlying basement membranes and start invading adjacent stromal compartments, thus acquiring a phenotype which resembles cells of mesenchymal origin (Thiery and Sleeman 2006). This phenomenon is termed the Epithelial to Mesenchymal Transition (EMT) and is the underlying reason for the invasive property of the cancer cells which empowers them to both intravasate and subsequently extravasate.

Interaction between cancer cells and neighboring stromal cells is essential for activation of the EMT process (Yang and Weinberg 2008). Advanced cancers generally induce an inflammatory microenvironment and stroma infiltrated with fibroblasts and various immune cells such as granulocytes and macrophages which release EMT-inducing signals. The cancer cells respond to these signals by activating expression of certain transcription factors like Snail1, Twist1/2, and Zeb2 that proceed to orchestrate EMT programs in these cells (Chaffer and Weinberg 2011). EMT during cancer progression is characterized by certain molecular signatures like downregulation of the genes encoding various epithelial junction proteins, such as E-cadherin, α-catenin, and γ-catenin at both mRNA and protein levels. E-cadherin is regarded as a gatekeeper of the epithelial state and loss of E-cadherin function is necessary, though not sufficient for EMT to occur (Tsai and Yang 2013). Intermediate filaments also switch from cytokeratin

to vimentin during EMT and increased vimentin levels are an important marker during EMT. Some other proteins required for cell migration also get induced during this event such as fibronectin, PDGF/PDGFR autocrine loop (Eckert and Yang 2011) and surface proteins like N-cadherin, CD44 (Kuo, Su et al. 2009) and integrin β6 (Bates, Bellovin et al. 2005). Signaling pathways such as TGF-β, Wnt, Notch and growth factor receptor signaling cascades, have also been implicated in the EMT process and the TGF-β pathway appears to be a primary inducer of EMT (Katsuno, Lamouille et al. 2013).

In order to gain access to the blood and lymphatic vessels, cancer cells need to degrade and invade the basement membrane and extracellular matrix which is carried out by upregulation of various matrix degradation enzymes during the EMT such as MMP-1, MMP-2, and MMP-3 and MMP-9 (Olmeda, Jorda et al. 2007; Ota, Li et al. 2009).

Once cells attain access to the vasculature, they face the major hurdle of surviving in the blood flow due to opposing immunological and physical hurdles. In animal models, it has been shown that only 0.01% or fewer of the cancer cells entering the circulation develop into metastases (Chambers, Groom et al. 2002). Cancer cells in circulation express tissue factor protein on the surface which acts as an attractant for platelets (Camerer, Qazi et al. 2004). The platelets covering the surface of the circulating cancer cells occlude the cell surface marker antigens and prevent their detection by immune cells and protect the cells from shearing forces of blood circulation.

According to Paget's “seed” vs. “soil” hypothesis compatibilities between circulating cancer cells (the seed) and certain distant sites (the soil) may explain the homing of circulating cells to specific organs (Paget 1989). The circulating tumor cells

can arrive at their destination and colonize to form secondary tumors. They can home to specific organs by getting lodged in the capillaries due to size constraints or by interactions through specific adhesion molecules that enable them to adhere to microvessels of these organs. They may also respond to a gradient of chemoattractant arising from a particular tissue (Chaffer and Weinberg 2011). Gene expression patterns of the cancer cells also govern their subsequent localization to different sites. Certain gene signatures have also been defined in breast tumor xenografts that can predict homing of breast cancer cells specifically to organs like lung, bone, or brain (Kang, Siegel et al. 2003; Chaffer and Weinberg 2011). This suggests that cancer cells in the primary tumor can acquire specific genomic profiles that may target them to particular organs to form metastatic growth.

The second phase of the metastatic cascade occurs when circulating cancer cells extravasate to new sites and form subsequent secondary tumors at these sites. Distant metastatic sites are largely non-permissive for the growth of newly arrived cancer cells, as most of the translocated cells undergo apoptosis within 24 hours of extravasation (Fidler 1970). Successful colonization occurs when incoming cancer cells attain the ability to acquire mitogenic stimulation from growth factors and cytokines from the microenvironment, which allows them to self-renew and recruit the necessary supporting stroma with appropriate blood supply. It has been observed that certain released factors from the primary tumor like VEGF-A, can help form a pre-metastatic niche at certain sites that generates a microenvironment conducive to the survival of cancer cells (Kaplan, Riba et al. 2005). The incoming cancer cells may first experience a period of dormancy while they adapt to their new microenvironment. Once the dormant cells have adapted,

they may progress to form small lesions (micrometastasis) where their size is kept in check due to a balance in proliferation, apoptosis and phagocytosis by the host-tissue immune system. To develop into larger lesions (macrometastasis) and form secondary tumors, an adequate blood supply is needed and thus angiogenic signals are expressed by the growing cancer cells. A rapidly expanding macrometastasis is an outcome of successful colonization of cancer cells which can further serve as a source of secondary metastases whose spread may be limited to certain subset of sites in the body or they may alternatively colonize to distinct tissue types.

Figure 2: The Metastatic Cascade

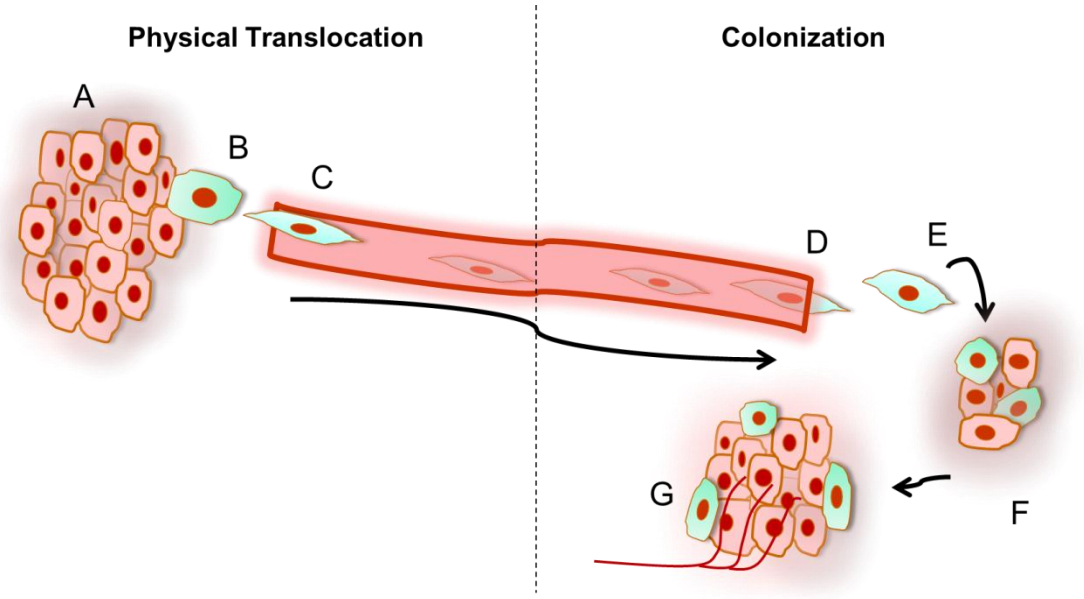

Metastasis occurs in two major processes; Physical Translocation, where cells from the primary tumor detach and translocate to distant organs; Colonization, where the translocated cells grow to form secondary tumors. **(A**) Primary tumor. (**B**) Acquisition of invasive phenotype by EMT. (**C**) Local invasion and intravasation into blood vessels. The circulating cancer cells enter into the blood stream and transit to distant organs. (**D**) Circulating cancer cells extravasate and invade parenchyma of distant tissue. (**E**) Cells adapt to the new environment but remain in a dormant state. (**F**) Dormant cells develop into micrometastases via growth in response to growth cues from the host tissue. (**G**) Micrometastases develops into macrometastases with recruitment of blood supply for the growing tumor mass.

1.8 Tumor-stroma interactions

Progression of tumors towards a malignant phenotype is not exclusively dependent on the autonomous properties of cancer cells, but is also influenced by the surrounding stroma. Tumor microenvironment which includes the extracellular matrix, surrounding blood vessels, endothelial cells, cancer-associated fibroblasts (CAFs), macrophages and other inflammatory cells, plays an important role in cancer progression. As a cancer progresses, its surrounding microenvironment co-evolves with it and attains an activated state through continuous paracrine communication, which creates a dynamic signaling interaction that promotes cancer initiation and growth (Pietras and Ostman 2010).

The most prominent cell types in the tumor stroma are the cancer-associated fibroblasts. CAFs are heterogeneous populations and their relative composition differs among different tumor types. Particularly, CAFs present in the stroma, which show the presence of markers such as α-smooth muscle actin (SMA), higher expression of platelet derived growth factor receptor-β (PDGFRB) and presence of fibroblast specific protein (FSP) are classified as activated CAFs and are known to promote tumor progression (Anderberg, Li et al. 2009). The mechanisms that can activate CAFs in the stroma is still not clearly understood but it is believed that tumor released factors such as tumor growth factor beta (TGF-β), platelet derived growth factor α/β (PDGFA, PDGFB), fibroblast growth factor (FGF) and interleukin-6 (IL-6) play major roles in trans-differentiation and activation of CAFs (Bronzert, Pantazis et al. 1987; Shao, Nguyen et al. 2000; Lohr, Lo et al. 2001; Giannoni, Bianchini et al. 2010).

Activated CAFs are known to contribute to tumor progression by various

methods. These cells produce and release large quantities of hormones and cytokines such as epidermal growth factors, fibroblast growth factors, IL-6 etc., that can directly stimulate cancer cells to grow rapidly (Bhowmick, Neilson et al. 2004). While CAFs are well characterized for supporting tumor progression, a few studies have also reported their cancer-initiating capacity. For example, ablation of TGFβ-II receptor in fibroblasts led to spontaneous tumors in prostate and forestomach in mice (Bhowmick, Chytil et al. 2004). In addition to providing growth cues to cancer cells, CAFs also contribute in tumors evading apoptosis by constantly providing them with survival signals like cytokines and insulin like growth factor (IGF), which can help tumors grow (Ku, Toivola et al. 2010). They are also known to produce various matrix components like collagen, which makes the ECM more cross-linked and stiff and has been shown to enhance integrin signaling in cancer cells which can activate pro-survival PI3K/AKT pathways downstream (Levental, Yu et al. 2009).

CAF secreted cytokines and chemokines also lead to the infiltration of various pro-inflammatory immune cells, which can promote angiogenesis and help tumor cells metastasize to different organs (Gerber, Hippe et al. 2009). Particularly, CAF released factors such as stromal derived factor-1 (SDF-1), vascular endothelial growth factor (VEGF), IL-8, IL-6, and IL-1β cooperate and promote new vessel formation by recruiting endothelial cells (Matsuo, Ochi et al. 2009). SDF-1 in particular is known to mobilize endothelial precursor cells from bone marrow into the tumor neo-vasculature for vessel formation (Orimo, Gupta et al. 2005). SDF-1 secretion by CAFs is driven by hypoxia-inducible factor-1 (HIF-1), which is known to promote survival of hematopoietic cells (Toullec, Gerald et al. 2010). CAFs also secrete several members of the matrix

metalloproteases (MMP) family. These enzymes can degrade ECM, which helps tumor cells invade the surrounding tissues. MMPs can also cleave membrane bound growth factors like VEGF and cytokines as well as their receptors and cell adhesion molecules like cadherins, which can lead to increased motility of cancer cells and result in epithelial to mesenchymal transition (Roy, Yang et al. 2009; Lederle, Hartenstein et al. 2010). As stroma derived factors promote initiation, growth and progression of tumor cells, they can also determine the therapeutic outcome in patients as they can act as barriers to therapy (McMillin, Negri et al. 2013).

Senescence can also affect tissue microenvironment reactivity as well as secreted factors from CAFs. Senescent fibroblasts acquire a senescence-associated secretory phenotype (SASP) which turns senescent fibroblasts into pro-inflammatory cells allowing them to increase their pro-inflammatory and pro-angiogenic cytokine and chemokine production. SASP induction in stromal fibroblasts has been positively correlated with tumor progression and it has been observed that they show this effect by inducing EMT in epithelial cells near them (Cirri and Chiarugi 2012). Along with various cytokines, senescent cells also secrete increased levels of some MMPs. The MMP family members that are consistently upregulated in senescent fibroblasts are MMP-1, MMP-3 and MMP-10 (Davalos, Coppe et al. 2010). These increased levels of secreted MMPs can degrade the components of the extracellular matrix, which can affect the physical property of the tissue structure around cells. This could help tumor cells migrate and invade through the ECM. It has also been observed that senescent cells and malignant tumors share many common repertoires of MMPs indicating the significance of senescence induction in tumor cell metastasis.

1.9 The ING family of tumor suppressors

The Inhibitor of Growth (ING) family of plant homeodomain (PHD) containing tumor suppressors is an evolutionary conserved group of proteins that affect a variety of cellular processes including chromatin remodeling, DNA damage signaling, cell cycle regulation, replicative senescence and apoptosis (Figure 3). ING1, the first member of the ING gene family, was discovered using subtractive hybridization of cDNAs between normal human breast epithelial cells and transformed breast cancer cells followed by an *in vivo* selection assay (Garkavtsev, Kazarov et al. 1996). Since their time of discovery, various aspects and characteristics of the ING group of proteins have been studied like their types; i.e. ING1-ING5 (Figure 4) (Nagashima, Shiseki et al. 2001; Feng, Hara et al. 2002; Nagashima, Shiseki et al. 2003); presence in diverse organisms (He, Helbing et al. 2005); role in apoptosis (Helbing, Veillette et al. 1997; Scott, Bonnefin et al. 2001; Vieyra, Toyama et al. 2002); deregulation in different cancer types (Campos, Chin et al. 2004; Gong, Suzuki et al. 2005); involvement in DNA damage repair (Cheung, Mitchell et al. 2001; Scott, Bonnefin et al. 2001; Berardi, Russell et al. 2004); chromatin remodeling (Loewith, Meijer et al. 2000; Kuzmichev, Zhang et al. 2002; Vieyra, Toyama et al. 2002); epigenetic regulation (Martin, Baetz et al. 2006; Pena, Davrazou et al. 2006; Shi, Hong et al. 2006); hormone responses (Toyama, Iwase et al. 2003; Wagner and Helbing 2005); regulation of brain tumor growth and angiogenesis (Garkavtsev, Kozin et al. 2004) and role in breast cancer metastasis (Thakur, Singla et al. 2014).

Involvement in this broad range of activities now seems reasonable given their stoichiometric recruitment in chromatin modifying complexes (Doyon, Cayrou et al. 2006). All of the ING proteins are believed to act as the targeting module of HAT and

HDAC complexes, by virtue of their specifically recognizing the H3K4Me3 marks (Martin, Baetz et al. 2006; Pena, Davrazou et al. 2006; Shi, Hong et al. 2006). Both ING1 and ING2 have been shown to be stoichiometric members of Sin3a HDAC complexes (that contain HDAC1 or HDAC 2). ING3 is a stoichiometric member of the NuA4/Tip60 HAT complex, whereas ING4 and ING5 can be found in the HBO1 HAT complex. ING5, which plays a role in stem cell differentiation (Mulder, Wang et al. 2012), can also be found in the MOZ/MORF HAT complex.

The human ING1 gene encodes four different isoforms, p47ING1a, p33ING1b, p24ING1c, and p27ING1d (Figure 4), among which p33ING1b is the most abundant isoform in human cells and is the best characterized so far (Vieyra, Toyama et al. 2002; He, Helbing et al. 2005). ING gene products possess distinct, but in some cases overlapping functional properties and unique expression profiles in eukaryotic systems. Ectopic overexpression of ING1 has been found to block cell cycle progression by arresting cells in G1 phase of the cell cycle, and long term expression promotes apoptosis. Consistent with a role as a tumor suppressor, inhibition of ING1 expression with antisense RNA promotes focus formation *in vitro* and tumor formation *in vivo* (Garkavtsev, Kazarov et al. 1996; Feng, Hara et al. 2002). Loss of ING1 expression has been implicated in a broad range of human cancer types, including primary breast tumors, lymphoid malignancies, testis tumors, squamous cell cancers, and head and neck cancers (Tallen, Riabowol et al. 2003; Vieyra, Senger et al. 2003; Gong, Suzuki et al. 2005), whereas mutations of ING1 genes are relatively rare, suggesting that ING1 functions as a type II tumor suppressor.

Figure 3: Diverse functions of ING1.

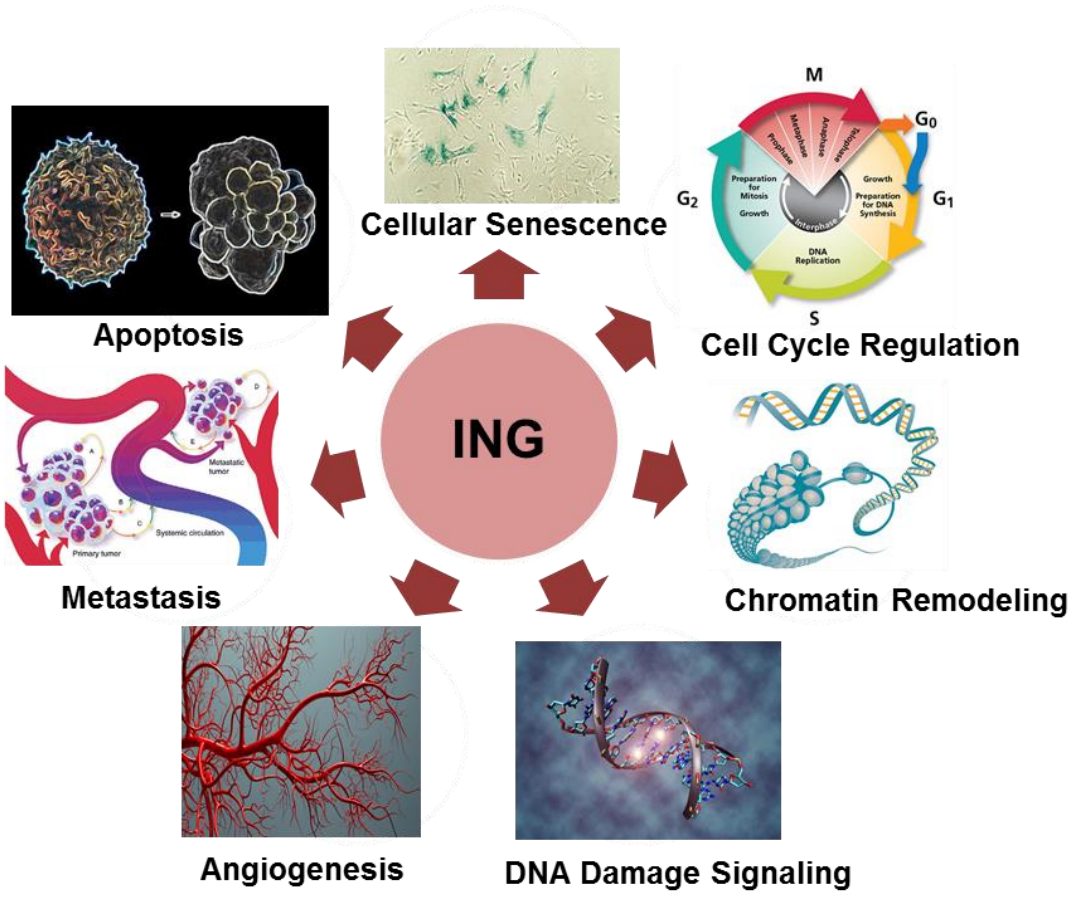

Figure 4: Domains of the ING family of proteins.

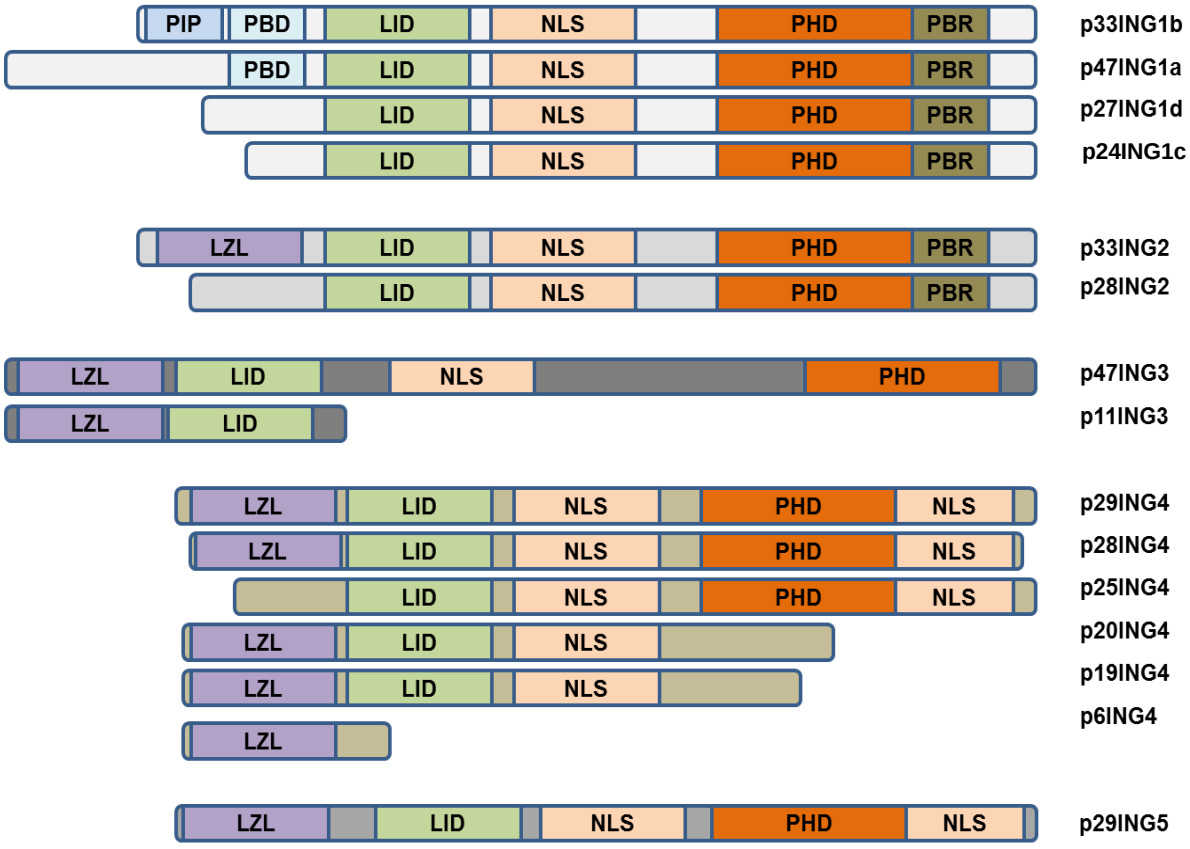

Various domains and isoforms of ING1-ING5. PIP: PCNA-interacting protein motif; PBD: Partial bromodomain; LID: Lamin interacting domain; NLS: Nuclear localization sequence; PHD: Plant homeodomain; PBR: Polybasic region; LZL: Leucine zipper like motif.

1.9.1 *Architecture of the ING family*

All ING family members share relatively similar architectural features, containing a region encoding a plant homeo domain (PHD) finger module (He, Helbing et al. 2005) which is the most highly conserved feature of the ING family and a nuclear localization signal (NLS) (Scott, Bonnefin et al. 2001; He, Helbing et al. 2005). The PHD motif is characterized by a Cys4-His-Cys3 zinc finger sequence and through this motif ING2 directly binds to di- and tri-methylated Lysine 4 residue of Histone 3 (H3K4) which is an epigenetic mark of active chromatin and gene expression (Martin, Baetz et al. 2006; Pena, Davrazou et al. 2006; Shi, Hong et al. 2006). The nuclear localization signal is located upstream of the PHD motif, and contains two functional nucleolar targeting sequences, (NTS) RRKR and KKKK, that have been shown to be individually sufficient to target p33ING1b to the nucleolus following UV irradiation in human fibroblasts. This ability of p33ING1b to translocate to the nucleolus appears to be important for the efficient promotion of apoptosis (Scott, Bonnefin et al. 2001). Recently, ING1 was also shown to translocate to the mitochondria of primary fibroblasts and established epithelial cell lines in response to apoptosis inducing stimuli, independent of the cellular p53 status (Bose, Thakur et al. 2013).

Following the PHD finger is the polybasic region (PBR), which is thought to be involved in stress-induced phosphoinositide (PI) binding (Gozani, Karuman et al. 2003; Kaadige and Ayer 2006). This interaction may indicate that INGs that target HDAC complexes (ING1 and ING2) to chromatin are strongly induced to do so by bioactive phospholipid binding in response to stress. A recent study showed that the PBR overlaps with a UIM (ubiquitin-interaction motif) in the C-terminal region of ING1b (Thalappilly,

Feng et al. 2011). This study established a link between bioactive lipid signaling and ubiquitin-mediated proteosomal degradation as it was shown that both ubiquitin and phospholipids competed for binding to this site. The UIM of ING1b was also shown to interact with mono-ubiquitinated p53 and stabilize it, by blocking polyubiquitination. A phosphorylation dependent SUMOylation motif having slight overlap with the NLS (C-terminal) at an area between this NLS and the PHD was also defined recently. Lysine 193 within this motif was shown to be SUMOylated which was dependent on phosphorylation of the Serine 199 residue (Satpathy, Guerillon et al. 2014). p33ING1b is also known to bind in a phosphorylation dependent manner with members of the 14-3-3 family and serine 199 of p33ING1b is part of the motif involved in this interaction. As a result of this interaction, a significant amount of p33ING1b is translocated out of the nucleus into the cytoplasm (Gong, Russell et al. 2006) in response to stress.

Upstream of the NLS is a conserved region, previously known as the NCR (Novel Conserved Region) which now, due to its interaction with nuclear lamins is called the LID (Lamin Interacting Domain). This domain is unique to ING proteins in the human proteome and it is through this domain that the INGs bind to and co localize with Lamin A (Han, Feng et al. 2008). The interaction between the LID and lamin A has been shown to help tether ING1 in the nucleus and regulate its functions as an epigenetic modifier. This ING1- lamin A interaction is lost in Hutchinson-Gilford progeria syndrome (HGPS) cells which show marked alterations in their chromatin structure and express a mutant form of lamin (progerin), indicating that ING1 may play a role in the transduction of the HGPS phenotype, through altering the epigenetic status of lamin A mutant cells (Satpathy, Nabbi et al. 2013).

The p33ING1b isoform is distinguished from other ING1 members by a partial bromodomain (PBD) and a specific sequence named the PCNA-Interacting-Protein (PIP) domain which are located upstream of LID in this isoform of ING1. The partial bromodomain was identified by bioinformatic analysis (He, Helbing et al. 2005). This region interacts with SAP30 of the Sin3-HDAC1 and HDAC2 complexes (Kuzmichev, Zhang et al. 2002) and thereby may help in recruitment of HAT or HDAC components for chromatin remodelling. PCNA (Proliferating Cell Nuclear Antigen) is an essential factor involved in both DNA replication and nucleotide excision repair (Maga and Hubscher 2003). There is a rapid increase in colocalization of PCNA and ING1 after UV treatment and mutations in the PIP region inhibit this interaction (Scott, Bonnefin et al. 2001). The PIP domain has also been found in other proteins that interact with PCNA that are involved in growth inhibition (p21), growth arrest after DNA damage (GADD45) and DNA replication and repair (FEN-1) (Scott, Bonnefin et al. 2001; Feng, Hara et al. 2002), among others. Figure 5 shows some of the structural features and binding partners of p33ING1b discussed above.

Figure 5: Various binding/interacting partners of p33ING1b.

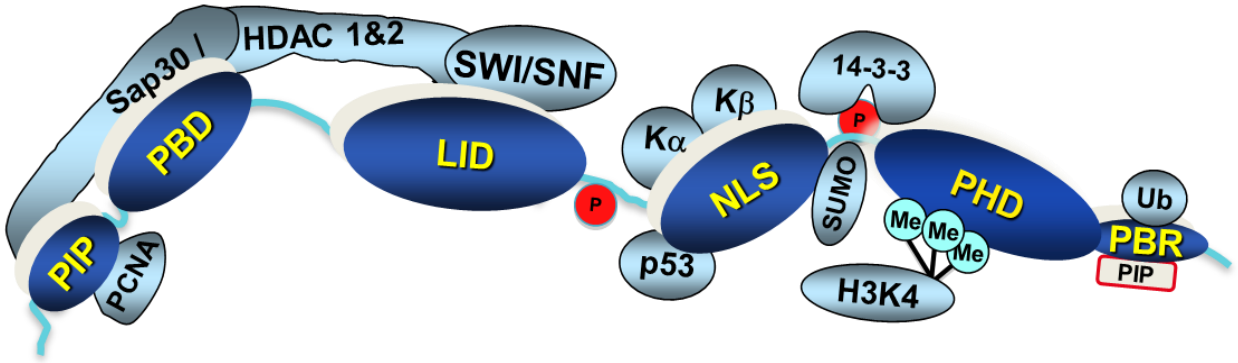

The PCNA-interacting protein motif of ING1b binds specifically to PCNA and promotes ING1b-mediated apoptosis. The partial bromodomain (PBD) binds Sap30 of the mSin3–HDAC1 complex which might target HDAC, and possibly HAT activity for some ING proteins. The lamin interacting domain (LID) binds to the lamin A protein. Mass spectrometric analysis showed that this region also interacts with the BAF170 subunit of the SWI/SNF chromatin remodeling complex. The nuclear localization signal (NLS) targets ING proteins to the nucleus through binding of the karyopherin-α and β transporter proteins. It has also been reported to mediate interaction with p53. The ING1 proteins contain a 14-3-3 recognition motif to which 14-3-3 binds when ING1 is phosphorylated on serine 199. This region also contains a PDSM and has been characterized for SUMO binding. The PHD finger has been shown to bind to core histone H3K4 in a methylation-sensitive manner. The polybasic region (PBR) of INGs 1 and 2 interacts with bioactive phosphoinositides. The PBR has also been shown to have a ubiquitin interacting motif within it.

1.9.2 *ING tumor suppressors in cancer*

All ING family members have been found to be altered in localization, sequence, or expression level in various cancer types. The level of *ING1* mRNA was found to be markedly reduced in 44% of primary breast cancer patient samples and in all breast cancer cell lines examined. However, one germ-line missense and three silent mutations in the sequence were also observed (Toyama, Iwase et al. 1999). Since this initial observation, several studies have reported decreased levels of ING1 in various cancer types including lymphoid malignancies, human gastric cancer, non-small-cell lung carcinoma, astrocytoma, neuroblastoma and sporadic colorectal cancer (Ohmori, Nagai et al. 1999; Oki, Maehara et al. 1999; Kameyama, Huang et al. 2003; Takahashi, Ozaki et al. 2004; Tallen, Kaiser et al. 2004). Reduced ING1 levels have also been correlated with increased propensity for nodal metastasis. Conversely, one study involving melanoma cell lines reported increased expression of ING1b. Silent and possible missense mutations of the *ING1* gene were also reported in the same study in human melanoma cell lines (Campos, Cheung et al. 2002).

Like ING1, decreased ING2 expression has also been reported in a various malignancies like lung cancer, hepatocellular carcinoma and head and neck squamous cell carcinoma (HNSCC) (Zhang, Pan et al. 2008; Borkosky, Gunduz et al. 2009; Ythier, Brambilla et al. 2010). ING2 has also been reported to be mislocalized in cutaneous melanomas (Lu, Dai et al. 2006). However, *ING2* expression is reportedly upregulated according to the Oncomine Database in cervical cancer, Burkitt's lymphoma and colorectal cancer (Tallen and Riabowol 2014) where it is thought to promote cancer metastasis and invasion (Kumamoto, Fujita et al. 2009).

Correlation studies involving ING3 and patient survival in different cancer types have also been reported. In head and neck cancers, ING3 was significantly downregulated and correlated with reduced overall patient survival (Gunduz, Ouchida et al. 2002; Gunduz, Beder et al. 2008). Similarly, ING3 was found to be mislocalized in malignant melanoma where decreased nuclear ING3 levels along with increased cytoplasmic ING3 levels strongly correlated with poorer 5 year Disease Specific Survival of patients with primary melanoma (Wang, Dai et al. 2007). Mutation and expression studies on the *ING3* gene concluding it to be silenced in different cancers have been reported by various groups. These include HNSCC, hepatic cancer and ovarian cancer (Tallen and Riabowol 2014).

ING4 expression is highly downregulated in gliomas. It has also been observed that ING4 expression had a strong negative correlation with tumor grade and aggressiveness (Garkavtsev, Kozin et al. 2004). In breast cancer cell lines, downregulation of ING4 also resulted in higher expression of NF-κB responsive genes, which could promote angiogenesis and tumorigenesis (Byron, Min et al. 2012). ING4 deletion and down-regulation of ING4 were also reported in HNSCC, hepatocellular carcinoma, gastric adenocarcinoma, human astrocytomas, lung cancer and breast cancer (Gunduz, Nagatsuka et al. 2005; Li, Jin et al. 2009; Klironomos, Bravou et al. 2010; Wang, Li et al. 2010).

ING5 downregulation has been reported in lung, pancreatic and ovarian cancer cell lines (Walzak, Veldhoen et al. 2008), along with primary bone marrow samples from patients with acute myeloid leukemia (AML), which may indicate the tumor suppressive role of ING5 in these malignancies (Zhang, Baumer et al. 2011). Surprisingly, in gastric

cancers, higher ING5 levels were observed in spite of ING5 being downregulated at the mRNA level (Xing, Yang et al. 2011). In HNSCC, ING5 has been reported to be mislocalized to the cytoplasm (Li, Nishida et al. 2010), with deletion of the ING5 locus in oral squamous cell carcinoma (OSCC) (Cengiz, Gunduz et al. 2007). Cytoplasmic localization of ING5 inversely correlated with nuclear ING5 levels that could predict a well-differentiated status in HNSCC. Nuclear ING5 levels also positively correlated with p21 and p300 expression, and with the apoptotic index in these cancers. In contrast to the tumor suppressive nature of ING5 in HNSCC, *ING5* gene expression is upregulated in colon cancer (Unoki, Kumamoto et al. 2009) suggesting an oncogenic function of ING5. In this study, nuclear ING5 negatively correlated, and cytoplasmic ING5 positively correlated with aggressiveness of the tumors indicating that subcellular localization of ING5 may govern its role as a tumor suppressor or as an oncogene.

Owing to their classification as tumor suppressors and their effect on cell growth and apoptosis, ING proteins have been examined for their efficacy in gene therapy or as agents in combinatorial cancer therapy. ING proteins inhibit the growth of cancer cells *in vitro* and *in vivo* when overexpressed from adenoviral vectors (Shinoura, Muramatsu et al. 1999; Shimada, Liu et al. 2002; Xie, Zhang et al. 2008). They also enhance chemosensitivity in combination with etoposide and doxorubicin (Zhang, Xu et al. 2004) and with epigenetic drugs like panobinostat and 5-azacytidine (Thakur, Feng et al. 2012). Adenovirus-mediated ING4 expression could also inhibit cell growth in various cancer models like non-small-cell lung carcinoma, hepatic cancer, breast and pancreatic carcinoma (Li, Xie et al. 2010; Xie, Sheng et al. 2011; Zhu, Lv et al. 2011). ING4 also inhibited invasion and migration in a melanoma cell model *in vitro* (Li, Martinka et al.

2008) while ING1 and ING4 were reported to inhibit angiogenesis in glioblastoma (Garkavtsev, Kozin et al. 2004; Tallen, Farhangi et al. 2009).

Since all ING proteins act as stoichiometric members of various HAT and HDAC complexes, changes in their levels could alter the epigenome of a cancer cell, which may increase the therapeutic index of many traditional cancer treatments when used in combination.

1.10 Aims and Objectives

ING proteins are type II tumor suppressors and members of various HAT/HDAC complexes. Their tumor suppressive properties have been studied previously in various types of cancers. In the first part of this study, we utilized the tumor suppressive property of ING1 in combination with various epigenetic drugs of different classes and determined if the combination could inhibit tumor growth better than when the agents were used singly. We hypothesized that targeting two distinct epigenetic phenomena in a single treatment will have greater therapeutic potential than targeting a single epigenetic pathway.

The second part of this study focusses on the anti-metastatic properties of ING1. Microarray analysis from primary fibroblasts showed that ING1 could regulate the expression of various genes implicated in cancer metastasis and cellular motility. Taking this into account, we hypothesized that modulating the levels of ING1 in highly metastatic cell lines could alter their metastatic capability. We reasoned that a part of ING1's ability to inhibit tumor growth could be by inhibiting the dispersal of cancer cells, which had not been investigated previously.

Lastly, due to ING1 being a tumor suppressor and metastasis inhibitor, that is generally downregulated in various cancers, we hypothesized that ING1 levels could predict the survival of breast cancer patients. For this, we analyzed the levels of ING1 in tumor and stromal compartments of breast cancer patient samples. Overall, this study aimed at determining the therapeutic potential of ING1 in breast cancer. We also tested the prognostic/predictive power of ING1 as a biomarker for breast cancer. This study was designed to help in developing novel ING1 based therapeutics for breast cancer treatment and prognostication.

In summary, the specific aims of this study include:

1) To determine if ING1 in combination with epigenetic drugs of different classes could inhibit breast cancer growth *in vitro* and *in vivo* more effectively than single agents.
2) To determine the effect of modulating ING1 levels on metastasis and correlation with patient survival *in vitro* and *in vivo* using an experimental metastasis mouse model.
3) To determine if ING1 expression could act as a prognostic/predictive marker for breast cancer patients.

CHAPTER 2: MATERIALS AND METHODS

2.1 Cell Culture

Established human breast cancer cell lines MCF7 (HTB22), BT20 (HTB19), MDA-MB435S (HTB129), SKBR3 (HTB30), T47D (HTB133), ZR-75-1 (CRL1500), BT474 (HTB20), Hs578T (HTB126), and MDA-MB468 (HTB132) and the immortal human mammary epithelial cell line MCF10A (CRL10317) were purchased from the ATCC. It is worth noting that MDA-MB435S cells may have been derived from a melanoma. Normal human breast epithelial cells Hs578Bst (HTB125) were a gift from Dr. Martha Stampfer. MCF10A and all breast cancer cells were cultured in high glucose Dulbecco's Modified Essential Media (H-DMEM) supplemented with 10% FBS, 0.1 mg/ml streptomycin and 100U/ml penicillin. Hs68 and Hs578Bst cells were cultured in L-DMEM supplemented with 30 ng/ml EGF and antibiotics. All cells were maintained in a humidified atmosphere at 37°C and 5% CO_2 and routinely tested negative for mycoplasma by PCR. Culture media were changed every 2-3 days.

MDA-MB231 cells from ATCC (HTB-26) and MDA-MB231 cells stably expressing an EGFP-luc2 fusion protein were cultured in H-DMEM (Lonza) supplemented with 10% FBS, 0.1 mg/ml streptomycin and 100U/ml penicillin were maintained as per ATCC guidelines. Cells were confirmed to be free of pathogenic murine viruses and mycoplasma by PCR testing at Charles River Laboratories.

Immortalized human mammary fibroblasts HMF3s (a kind gift from Dr. Parmjit Jat) were cultured in H-DMEM (Lonza) supplemented with 10% FBS, 0.1 mg/ml streptomycin and 100U/ml penicillin and maintained in a humidified atmosphere of 5% CO_2 and 95% air at 37ºC. Cells were routinely tested for mycoplasma contamination.

2.1.1 *Freezing and thawing cells*

Cells to be frozen were harvested by trypsin-EDTA (Gibco-BRL) treatment, centrifuged at 1000 rpm, and resuspended in a medium containing 10% FBS, and 5-10% sterile dimethylsulfoxide (DMSO, Sigma) to yield a concentration at approximately 1×10^6 cells/ml. One ml aliquots of cell suspension were transferred to cryovials (Nalgene) and vials were kept at -80°C overnight. Frozen cells were then stored in liquid nitrogen for long-term storage. To thaw cells, a vial of frozen cells were removed from liquid nitrogen, placed in a 37°C water bath for 2-3 minutes, the cell suspension was transferred to a fresh plate containing culture media with 10% FBS, and was incubated at 37ºC in a CO_2 incubator.

2.1.2 *Passaging of cells*

Cells upon attaining ~90% confluence were dislodged from the culture plate by using trypsin-EDTA after washing with phosphate buffer saline (PBS). An appropriate volume of media containing 10% FBS was then added to stop the trypsin activity and cells were triturated to eliminate formation of clumps. The cells were then plated in fresh tissue culture plates with uniform spreading. Primary cells such as Hs68, Hs578Bst and the breast cancer cell line SKBR3 were split at 1:2 to 1:4 ratios. All other cell lines were split at 1:4 to 1:8 ratios depending upon the experimental setup.

2.2 Preparation of adenoviral particles

For a large scale amplification of adenoviral particles, 5-10 µl of the viral stock from frozen aliquots was used to infect one 6 cm plate of HEK 293 cells. When cytopathic effects were seen in more than 50% cells (usually 1-2 days after infection), the cells with

the media were collected and subjected to 3 freeze/thaw/vortex cycles. The supernatant, crude viral lysate (CVL) was removed after spinning at 6000 rpm and was used to infect one 15 cm plate of HEK 293 cells, from which the CVL was made according to the procedure described above. Then, five 15 cm plates of cells followed by fifty 15 cm plates of cells were infected using the CVL made from above step following the protocol described above. At the final step, cells from fifty 15 cm plates were harvested and combined in 20 ml media (the rest of media was discarded) and the CVL was prepared as described (freeze/thaw/vortex). Viral titers were routinely measured to ensure accurate active viral concentrations. Adenoviral infections were optimized by titrating virus to identify multiplicities of infection (MOIs) of cells giving >95% infectivity as monitored by GFP expression and which showed minimal effects from control virus (Ad-GFP) infection. No non-specific toxicity was observed when adenoviruses were used at these MOIs.

2.2.1 *Purification of virus particles by CsCl gradient*

5 ml of the CVL was added slowly on top of a discontinuous CsCl gradient, made by layering solution A (36 g in 100 ml PBS) over solution B (62 g in 100 ml PBS) in each of four Beckman 14x89 mm ultraclear tubes. The tubes were centrifuged in a SW41 rotor (Beckman) at 35,000 rpm at 12ºC for 1 hour. The viral fraction formed a white band near the bottom of the gradient and was collected by puncturing the tube using a 23 gauge needle. Next, 8 ml of CsCl solution C (51 g in 100 ml PBS) was added into each of 2 Beckman ultraclear tubes to make a continuous gradient onto which the viral fraction from previous step was over layered. The tubes were centrifuged at the conditions mentioned above for overnight. The viral fraction containing the pure viral particles

forming a clear white band near the bottom was collected and dialyzed at 4ºC using a 10,000 MWCO dialysis cassette (Pierce) against dialysis buffer (10 mM Tris pH7.4, 150 mM NaCl, 1 mM $MgCl_2$, 3% Sucrose) for 4 hours. The purified virus was aliquoted and stored at -80ºC.

2.3 Functional Assays

2.3.1 Treatment protocol for epigenetic drugs

MDA-MB468 cells were cultured for 24 hours and then treated with LBH589 (a gift from Dr. Peter Atadja of Novartis Pharmaceuticals) or 5azaC (Sigma) at the determined IC_{50} of 100 nm for 15 hours and 40 μM for 48 hours, respectively. Cells were infected with Ad-ING1b (30 MOI) after pretreatment with the epigenetic drugs, and were harvested 24 hours post-infection. For 5azaC treatment, media containing fresh 5azaC were changed every 24 hours. LBH589 and 5azaC were prepared as 5 mM and 100 mM stocks in DMSO and PBS respectively, and stored at -80ºC until use. The time course adopted for drug treatments in combination therapies were optimized separately to attain maximum efficiency in killing cancer cells without interference in the final read out.

2.3.2 MTT assays

Approximately 5×10^4 MDA-MB468 cells were plated per well in a 96 well plate and treated with various concentrations of LBH589, 5azaC and various titres of Ad-GFP or Ad-ING1b, alone or in combinations. At the end of treatments, 50 μl of MTT (3-(4,5-dimethylthiazol-2-yl)-2,5-diphenyltetrazolium bromide) was added to each well from a 5 mg/ml stock in PBS. The plates were then incubated for 4 hours at 37ºC in the dark. The supernatant was aspirated and formazan crystals were solubilized in 100 μl DMSO at

37ºC for 10 minutes with gentle agitation. Absorbance from the plates was read at 570 nm with a Bio-Rad microplate reader. Percent growth inhibition was calculated by the formula $(OD_{control} - OD_{treated})/OD_{control} \times 100$.

2.3.3 Apoptosis and cell viability assays

Exponentially growing cells were seeded into fresh 10 cm plates at ~10% confluence 16-18 hours prior to infection. 48 hours after infection cells were harvested, washed in PBS + 5 mM EDTA and fixed in 70% ethanol at 4ºC for 30 minutes. Cells were washed twice with PBS + 5mM EDTA followed by staining in propidium iodide (PI) solution (50 μg/ml PI, 20 μg/ml RNase) (Sigma) in PBS in the dark at RT for 20-30 minutes. Samples were subsequently analyzed by flow cytometry (Flow Cytometry Facility at University of Calgary) within one hour. An Annexin V-PE/7AAD kit (BD Pharmingen) was used following the manufacturer's instructions to identify apoptotic cells by a FACScan flow cytometer in combination with BD FACSDiva Software (Becton-Dickinson). Viability of cells was assessed by trypan blue exclusion assay. The floating dead cells in the medium and cells that remained attached to the plates were collected by trypsinization and counted using a hemocytometer in the presence of 0.4% trypan blue reagent (Sigma). All experiments were done in triplicate.

2.3.4 Combination index calculations

The modes of interaction of 5azaC with LBH589 and ING1b with 5azaC or LBH589 were analyzed using CalcuSyn software (Biosoft, Cambridge, United Kingdom). The software is based on the calculations developed by Chou and Talalay (Chou and Talalay 1984), which allows the evaluation of interactions between 2 or more drugs. The

combinations of Ad-ING1b (15, 25, 35, 45 and 55 MOI) with 5azaC (20, 30, 40, 50 and 60 μM) or LBH589 (50, 75, 100, 125 and 150 nM) were tested at different ratios and inhibition of cell growth was determined by MTT assay. The software utilizes a multiple drug-effect equation derived from an enzyme kinetics model in which the output is represented as combination indices (CI) and/or isobologram analysis. Calcusyn defines synergy between two drugs when the CI value is < 1. The extent of synergism/antagonism may also be determined based on the CI value. In brief, CI values between 0.9 and 0.85 suggest a moderate synergy, whereas those in the range of 0.7 to 0.3 are indicative of clear synergistic interactions between the drugs. On the other hand, CI values in the range of 0.9 to 1.10 would suggest an additive effect while those > 1.1 suggest antagonism.

2.3.5 Cell Motility and Invasion Assays

For experiments involving ING1 knockdown, cells were transfected with an ING1 siRNA pool or scrambled siRNA and incubated for 48 hours. For experiments involving ING1 overexpression, cells were infected with Ad-ING1b + GFP or Ad-GFP at an MOI of 15. After 24 hours, cells were trypsinized and $2.5x10^4$ cells were added to 8 μm pore size inserts (BD Biosciences) to perform transwell migration assay as per manufacturer's instructions. For invasion assays, cells were treated as described, but $3.5x10^4$ were placed in 8 μm pore size Matrigel coated invasion chamber inserts (BD BioCoat) and incubated for 24 hours.

2.3.6 Multiplex Assay for Cytokine and Chemokine screening

Media from transfected/infected cells were collected and screened for released cytokines

and chemokines using an ELISA based assay (Eve Technologies, Calgary Alberta). Cells (MDA-MB231 or HMF3s) were inoculated overnight in 6 well dishes and were infected with Ad-ING1 or Ad-GFP virus at 15 MOI and allowed to grow for 48 hours with media changed 12 hours post infection. After 48 hours, cell media were carefully collected in sterile centrifuge tubes without disturbing the cells. The media were then centrifuged at 4ºC for 10 minutes at 13,000 rpm. After centrifugation, the media supernatant were transferred into fresh sterile tubes and stored at -80ºC unless analyzed immediately.

2.3.7 Three-dimensional cell culture

Three-dimensional culture of HMF3s and MCF7 cells were performed in ultra-low attachment 96-well plates (BD Biosciences). HMF3s cells were infected with Ad-ING1a or Ad-GFP at 15 MOI for 48 hrs. The plates were firstly coated with 50 µl of 30% growth factor reduced Matrigel (3 mg/ml) (BD Bioscience) in complete medium (DMEM-containing 10% FEBS, penicillin, streptomycin and amphotericin B (Lonza) and were incubated for 1 hour in a CO_2 incubator at 37°C to form a layer. Cell suspensions of HMF3s and MCF7 cells were then made (100 cells/50 µl) in 30% Matrigel and were carefully layered without formation of bubbles on the solidified layer in the wells. For co-culture experiments, a 1:1 ratio of HMF3s cells and MCF7 cells was used. Fresh media were supplemented every three days and images were taken after 2 weeks using a Zeiss Axiovert 200M microscope.

2.3.8 Zymography

To determine the activity of matrix metalloproteases MMP-1 and MMP-2, gelatin and casein zymography were performed, respectively. HMF3s cells were grown in 6 well

dishes and infected with Ad-ING1a or Ad-GFP for 48 hours at 15 MOI and the media was centrifuged at 4ºC for 10 minutes at 13,000 rpm. The collected media supernatants were then mixed with 2X sample buffer (65.8 mM Tris-HCl pH 6.8, 25% (w/v) glycerol, 2% SDS, 0.1% bromophenol blue) and incubated at room temperature for 10-15 minutes. The samples were then subjected to zymography by resolving on 10% SDS-polyacrylamide gels containing 1 mg/ml porcine skin-derived gelatin (Sigma) or casein (Sigma). After electrophoresis, the gels were incubated for 30 minutes at room temperature with gentle agitation in renaturation buffer (2.5% Triton X-100) to remove SDS. The gels were then incubated in developing buffer (50mM Tris-HCl, 0.2M NaCl, 5mM $CaCl_2$ and 0.02% Brij 35) at 37ºC overnight with gentle agitation. After incubation in the developing buffer, gels were stained with 0.5% (w/v) Coomassie Blue R-250 for 30 minutes and destained with destaining solution methanol : acetic acid : water (50:10:40). For casein zymography, gels were pre-run for 30 minutes at 100 V before loading samples to remove excess casein.

2.4 Western blotting

Cells were washed with PBS, lysed in SDS loading buffer, sonicated on ice and following PAGE, samples were transferred to nitrocellulose membranes (Millipore) by electrophoresis. Membranes were blocked with 5% non-fat milk in a solution of 0.1% Tween-20 in PBS (PBST) for 1h at room temperature and blotted with α-ING1 monoclonal (SACRI Antibody Services), α-PARP (Santa Cruz), α-γH2AX (Millipore), α-caspase-3 or α-β actin (Cell Signaling) antibodies. Membranes were then washed 3 times for 10 minutes each in PBST followed by incubation with secondary antibodies conjugated to horse radish peroxidase in PBST containing 5% non-fat milk for 30-45

minutes. After washing with PBST, signals were detected by enhanced chemiluminescence reagent (Millipore) on X-ray films (Kodak).

2.5 Transfection

siRNA transfections were done using Lipofectamine 2000 (InVitrogen) according to the manufacturer's guidelines. ING1 siRNA smartpool and scrambled siRNA (Thermoscientific) were transfected into cells at a final concentration of 100 nM.

2.6 RNA isolation and quantitative real time PCR

Total RNA from cells was isolated using RNeasy Kits (Qiagen) according to the manufacturer's guidelines and reverse transcribed using an ABI reverse transcription kit (Applied Biosystems). Real time PCR was carried out in triplicate using SYBR Select Mastermix (Invitrogen) on an Applied Biosystems 7900HT fast real-time PCR system using a standard protocol. GAPDH expression was used as a normalization control. The ΔCT method was used for analysis of real time PCR products.

2.7 Primer sequences

Primers used were as follows: N-cadherin (CDH2), 5'agccaaccttaactgaggagt3' (forward) and 5'ggcaagttgattggagggatg3' (reverse); Platelet-derived growth factor alpha polypeptide (PDGFA), 5'gcaagaccaggacggtcattt3' (forward) and 5'ggcacttgacactgctcgt3' (reverse); Platelet-derived growth factor receptor, alpha polypeptide (PDGFRA), 5'tggcagtaccccatgtctgaa3' (forward) and 5'ccaagaccgtcacaaaaaggc3' (reverse); Platelet-derived growth factor receptor, beta polypeptide (PDGFRB), 5'agcaccttcgttctgacctg3' (forward) and 5'tattctcccgtgtctagccca3' (reverse); Hyaluronan synthase 2 (HAS2),

5’ctcttttggactgtatggtgcc3’ (forward) and 5’agggtaggttagccttttcaca3’ (reverse); Programmed cell death 4 (PDCD4), 5’acaggtgtatgatgtggagga3’ (forward) and 5’ttctcaaatgccctttcatccaa3’ (reverse); Glyceraldehyde 3-phosphate dehydrogenase (GAPDH), 5’gtcagtggtggacctgacct3’ (forward) and 5’aggggtctacatggcaactg3’ (reverse).

2.8 Patient Cohort

The Calgary Tamoxifen Cohort contains demographic, clinical and pathology data for 819 breast cancer patients diagnosed between 1985 and 2000 at the Tom Baker Cancer Centre in Calgary, Canada. Inclusion criteria were a confirmed diagnosis of invasive breast carcinoma, primary surgical intervention, and adjuvant tamoxifen therapy (20 mg p.o./day). Exclusion criteria were the absence of available surgical formalin-fixed paraffin-embedded (FFPE) tissue, prior cancer diagnosis (except non-melanoma skin cancer), or treatment with primary or adjuvant chemotherapy. 532 subjects, with a median follow-up time of 82.1 months, met the criteria and had triplicate 0.6 mm FFPE cores built into tissue microarrays (TMAs). While ER and PR ligand binding assays (LBA) were routinely performed during the diagnosis period for this cohort, all patients were treated with tamoxifen, as definitive evidence that ER poor patients did not respond to tamoxifen, was lacking at that time. Retrospective ER, PR and HER2 status was established using the Dako PharmDx ER and PR immunohistochemistry assays and the Herceptest immunohistochemistry assay, as per the manufacturer’s instructions. ER+ or PR+ or Her2+ status was defined as maximum ER or PR Allred score <3 across triplicate cores, or an average Her2 ASCO score >2 across triplicate cores. All tissues were fixed and embedded using a standard protocol.

2.9 Fluorescence Immunohistochemistry

After tissue microarray construction, 4 μm thick sections were cut from the TMA block and deparaffinized in xylene, rinsed in ethanol, and rehydrated. Heat-induced epitope retrieval was performed by heating slides to 121°C in a citrate-based buffer (pH 6.0) target retrieval solution (Dako, Mississauga, ON, Canada) for 6 minutes, in a decloaking chamber (Biocare Medical, Concord, CA, USA). Slides were stained using a Dako Autostainer. Endogenous peroxidase activity was quenched with a 10 minute incubation of peroxidase block (Dako) followed by a 15 minute protein block (Signal Stain, Cell Signaling, Danvers, MA, USA) to eliminate non-specific antibody binding. Slides were washed with TBST wash buffer (Dako) and then incubated at room temperature for 60 minutes with Signal Stain protein block (Cell Signaling) containing a 1:500 dilution of mouse anti-ING1 mAb, clone CAb5 (SACRI Antibody Facility, University of Calgary, Calgary, AB, Canada). Additional antibodies including anti-pan-cytokeratin guinea pig monoclonal (Acris, San Diego, CA, USA), anti-vimentin rabbit mAb, clone EPR3776 (Epitomics, Burlingame, CA, USA) and Alexa-488 conjugated goat anti-guinea pig antibody (Invitrogen, Burlington, ON, Canada) were used as suggested by suppliers.

2.9.1 *Automated image acquisition and analysis*

Automated image acquisition was performed using an Aperio Scanscope FL (Aperio Inc., Vista, CA, USA). High-resolution slide images were acquired using the Scanscope FL 8/10-bit monochrome TDI line-image capture camera using filters specific for DAPI to define the nuclear compartment, FITC to define cytokeratin positive cells and the tumor cytosolic compartment, Cy3 to define the target biomarker ING1, and Cy5 to define

vimentin positive non-malignant stromal cells.

Images were analysed using the AQUAnalysis® program, version 2.3.4.1. A tumor-specific mask was generated to distinguish breast cancer cells from surrounding stromal tissue by thresholding the pan-cytokeratin images. Threshold levels were verified and adjusted by spot-checking a small sample of images to determine an optimal threshold value. All images were then processed using this optimal threshold value and all subsequent image manipulations involved only image information from the masked area. Images were validated according to the following: 1) >10% of the tissue area is pan-cytokeratin positive, 2) >50% of the image was usable (i.e. not compromised due to overlapping or out of focus tissue). Unusable areas within each image were manually cropped and excluded from the final analysis.

2.9.2 *Assessment of ING1 Expression*

The average intensity of target ING1 signal in the tumor mask was tabulated and used to generate tumor specific AQUA scores, which reflect the average signal intensity per tumor area. The ING1 expression score was defined as the mean ING1 malignant cell-specific AQUA score from triplicate cores for each patient sample. Patients were dichotomized at the lowest or highest tertiles of ING1 expression within the entire cohort, to define Low ING1 and High ING1 expression categories.

2.9.3 *Statistical Analysis for patient data*

Statistical analyses were performed using Stata 12 (StataCorp LP). Histogram distributions were used to compare the distributions of tumor ING1 expression scores to those from normal breast epithelium (n=7). For survival analysis, the events under study

were disease free survival (DFS), defined as the time of diagnosis to recurrence, metastatic disease, or death from breast cancer; distant metastasis free survival (DMFS), defined as the time of diagnosis to recurrent metastatic disease; and disease specific overall survival (DSOS), defined as the time of diagnosis to death from breast cancer. Patients were censored at the time a patient died from another cause, or the follow-up period ended. Kaplan Meier survival analysis was performed to estimate the probability of 5-year DFS, 5-year DMFS, or 7.5-year DSOS. Cox proportional hazards analyses were conducted to assess the impact of clinical covariates in multivariate analysis.

2.10 Animal Studies

2.10.1 Subcutaneous xenograft model

To establish subcutaneous tumors, actively growing MDA-MB468 breast cancer cells were harvested and $7x10^6$ cells in 100 µl PBS were injected into the mammary fat pads of mice. The lesions were allowed to grow until their average sizes were approximately 5 mm x 5 mm (about 2 weeks). The mice were then randomized into 6 groups for various treatments including PBS vehicle control, Ad-GFP control, Ad-ING1b, 5azaC, Ad-GFP plus 5azaC, and Ad-ING1b plus 5azaC combination groups. Treatment started at day 1, $2x10^8$ PFU of Ad-GFP or Ad-ING1 were given intratumorally (it) twice a week for a total of 10 treatments. 5azaC was administered intraperitoneally (ip) every other day (3 times a week) at 5 mg/kg for a total of 15 injections (5 weeks). Tumors were then re-challenged ($2x10^9$ pfu) for another 3 weeks in the same pattern from day 57 to 77 when the tumors in the combination group showed signs of rapid growth. Tumor size and body weight were recorded twice weekly. Tumor cross-sectional area was calculated by

multiplying the length x width and tumor volume was calculated by cubing the mean value of length and width. Dose of 5azaC to be used was determined in preliminary trials testing different doses of 5azaC versus tumor size and total animal body weight. 5 mg/kg dose was optimal for having no effect on body weight but an effect on inhibiting tumor growth.

2.10.2 Breast cancer experimental metastasis model

To generate metastases, 6-week old female (16-18 g) NIH-III (*nu/nu; beige/beige*) female mice were anesthetized by intraperitoneal (i.p) injection of ketamine (100 mg/kg) and xylazine (10 mg/kg), and then given 150 mg/kg D-luciferin (Gold Biotechnology, St. Louis, MO). Mice were then inoculated with $2x10^5$ MDA-MB231-luc2 cells suspended in 100uL of PBS, by intra-cardiac (i.c.) injection in the left ventricle of the heart. Metastases were monitored by bioluminescence imaging on day 7, 10, 14, 17, 21, 28 and 35 post-injection. To visualize and to quantify metastatic growth, bioluminescence imaging (Xenogen/Caliper) was used, and anatomical sites of soft tissue metastasis were confirmed by *ex vivo* bioluminescence of organs at necropsy. Image analysis was performed using Living Image® 4.1 software from Caliper Life Sciences. The bioluminescence signal intensity was quantified with the Living Image 4.2 software, as total photon flux (photons/second) in a uniform region of interest (ROI) or flux from the whole body. For *ex vivo* imaging, organs were placed in 24-well cell culture plates along with 200 µl of D-luciferin (15 mg/ml) and imaged for 2 minutes.

2.10.2.1 *Micro-computed tomography (µCT)*

Knee bone loss induced by bone metastases was assessed by µCT. Hind limbs were

dissected and cleaned of muscle tissue before fixation in 4% PFA for 7 days and scanned in a µCT scanner (vivaCT 40, Scanco Medical, Switzerland). For scanning, the bones were placed in a special sample holder with 6 upright cylinders that fit one mouse hind limb each. The holder was placed in the µCT scanner (vivaCT 40, Scanco Medical, Switzerland) and a region of interest, in this case the whole limb, was selected following a scout-view of the samples in the holder. Approximately, 1000 tomographic images per stack were acquired in a period of 3 hours at 70 kVp (applied peak, 114 µA, and 200 ms integration time). The scan generated 555 cross-sectional slices that were used to reconstruct a three-dimensional (3D) image of the sample. For the analysis, a region of proximal tibia was used to determine the bone morphometric parameters bone volume/total volume (BV/TV), cortical bone volume/total volume (Ct BV/TV) and bone mineral density (BMD) that were used to analyze the magnitude of tumor induced osteolysis.

2.10.2.2 *Histology*

Fresh hind limbs with bone metastasis from control and ING1b overexpressing groups of mice were fixed in 4% PFA and decalcified for 2 weeks in 14% EDTA at pH 8.0 with change of solutions every 24 hours. Tissues were embedded in paraffin (Paraplast-Plus, -X-tra (50), McCormick Scientific), and 4-8 µm sections were cut. A tri-chrome stain was performed for histological examination of knee sections.

CHAPTER 3: RESULTS

3.1 ING1 and 5-Azacytidine Act Synergistically to Block Breast Cancer Cell Growth

3.1.1 ING1b and ING2 act independent of p53 status

ING1 expression is reduced in breast tumors and breast cancer cell lines (Garkavtsev, Kazarov et al. 1996; Toyama, Iwase et al. 1999; Tokunaga, Maehara et al. 2000; Liu, Wu et al. 2003; Nouman, Anderson et al. 2003) but few studies have tested the effects of increasing ING1b in breast cancer cells. In contrast, induction of apoptosis by other INGs has been reported in many cancer types (Helbing, Veillette et al. 1997; Nagashima, Shiseki et al. 2001; Cheung and Li 2002; Nagashima, Shiseki et al. 2003; Zhu, Lin et al. 2005; Li, Xie et al. 2010) and in normal diploid fibroblasts (Scott, Bonnefin et al. 2001; Vieyra, Toyama et al. 2002) and some reports suggest that ING1 requires p53 activity to induce apoptosis (Garkavtsev, Grigorian et al. 1998; Cheung and Li 2002). To further test this idea, nine breast cancer cell lines and two non-tumorigenic breast epithelial cell strains with different growth rates and with varying ER, p53 and HER2/neu status (Table 3) were infected with GFP, GFP-ING1b or GFP-ING2 to see if ING proteins affected breast cancer cells in a p53-sensitive or growth rate-dependent manner. MDA-MB468 and SKBR3 cells were most susceptible to both ING1b and ING2 compared to other cell lines (Figure 6) suggesting that neither growth rate nor p53 status strongly affected the ability of ING1 to induce apoptosis. Levels of ING1 and ING2 expressions in these cell lines did not affect the infection capacity of adenovirus particles as all the cell lines had same amount of infection ability, irrespective of different levels of ING1 and ING2 expressed at endogenous levels.

A previous study reported a positive association between ING1b and ER levels in breast cancer tissues (Nouman, Anderson et al. 2003), and ING1b stimulates the

transcriptional activity of ERα (Toyama, Iwase et al. 2003; Toyama and Iwase 2004). Thus, we asked if ER negative breast cancer cell lines that are at a more advanced stage would be more sensitive to exogenous ING1 than ER positive cells. Our results support this idea since both SKBR3 and MDA-MB468 are ER negative and they exhibited the greatest sensitivity to both ING1b and ING2. ING1 most effectively induced apoptosis and cell death in cells with mutant, rather than wild type p53 (SKBR3 and MDA-MB468), but was also able to induce cell death in MCF10A and ZR-75-1 that encode wild type p53. Thus, no clear association between ING1 killing efficiency and p53 status was seen, nor was any association between killing efficacy and HER2/neu overexpression noted.

Table 3: Characteristics of breast epithelial cell lines examined

Cell Lines	Cell Source	Tumorigenic (Nude Mice)	ER Status	p53 Status	HER2/neu overexpression
Bst578	Normal Tissue	No	+	Wild Type	No
MCF10A	Fibrocystic disease (immortalized)	No	+	Wild Type	No
MCF7	Adenocarcinoma (pleural effusion)	Yes	+	Wild Type	No
BT20	Adenocarcinoma (pleural effusion)	Yes	−	Mutant	Yes
MDAMB435	Ductal carcinoma (pericardial effusion)	No	−	Mutant	No
SKBR3	Adenocarcinoma (pleural effusion)	Yes	−	Mutant	Yes
T47D	Ductal carcinoma (pleural effusion)	Yes	+	Mutant	No
ZR-75-1	Ductal carcinoma (ascites)	Yes	+	Wild Type	No
BT474	Ductal carcinoma	Yes	+	Mutant	Yes
Hs578T	Ductal carcinoma	No	−	Mutant	No
MDAMB468	Adenocarcinoma (pleural effusion)	Yes	−	Mutant	No

Bst578 is a normal primary epithelial cell strain and MCF10A is an established, but phenotypically normal cell line. MCF7 is also known to harbor a caspase 3 mutation that makes it relatively resistant to apoptosis. MDA-MB-435S cells may be a melanoma cell line.

Figure 6: Cell Death and Apoptosis in response to ING1 and ING2.

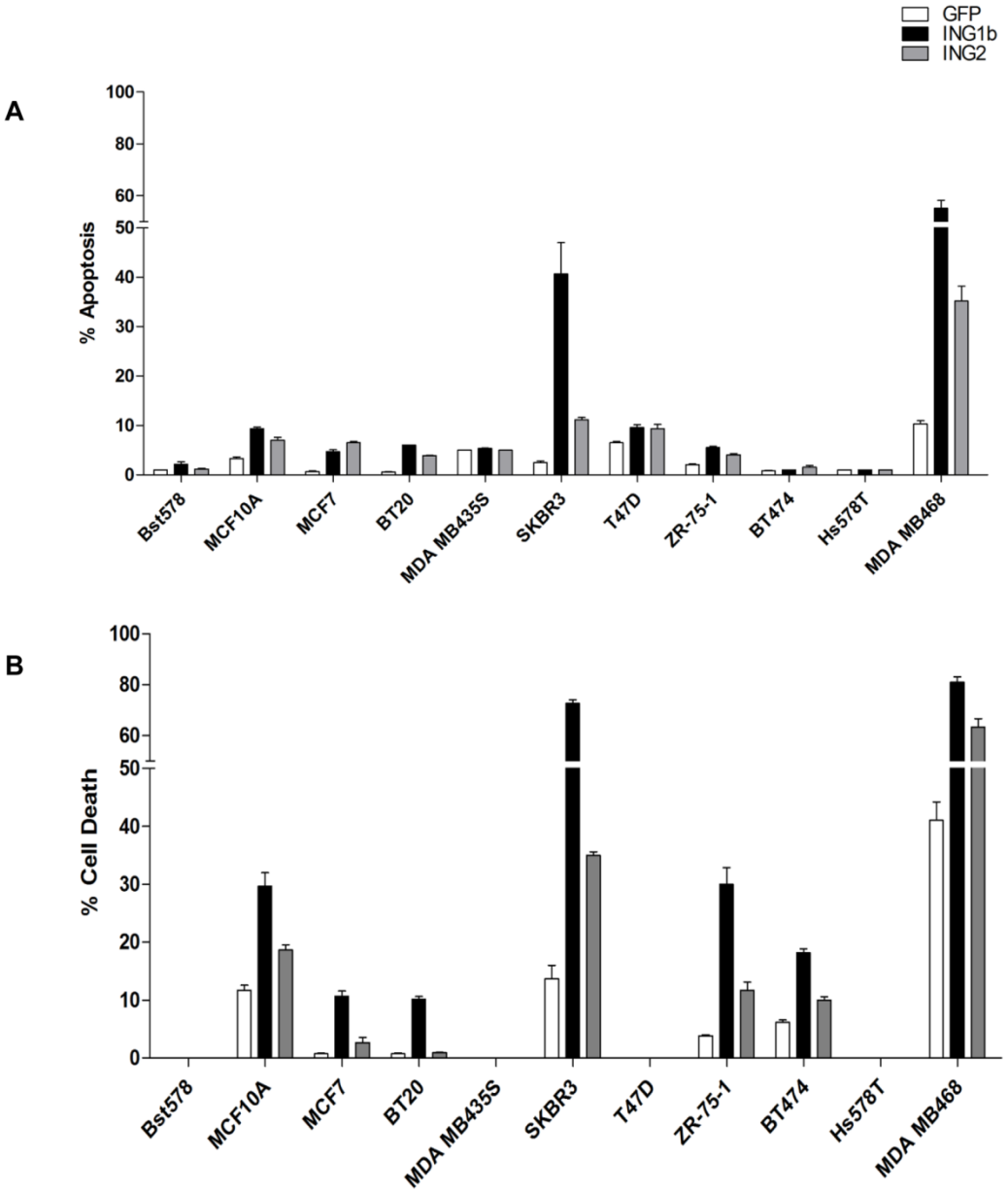

The indicated breast cancer cell lines were grown and tested for the ability of adenoviral constructs encoding GFP, GFP plus ING1b or GFP plus ING2 expressed from separate promoters to A) induce apoptosis as estimated by propidium iodide staining for sub-G1 DNA content, or B) induce cell death as estimated by cell survival (Coulter counting). Results were obtained using an MOI of 10, 48 hours after infection. The MDA-MB468 and SKBR3 lines were most susceptible to ING at this MOI and other lines showed increased susceptibility at higher MOIs (data not shown). Normal Bst578 cells were fully resistant to this concentration of virus. Uninfected cells were used as controls to normalize other cell numbers against.

3.1.2 ING1b enhances the efficiency of cell killing by epigenetic drugs

Cancer cells frequently show altered DNA methylation and histone modifications such as histone acetylation, resulting in deregulation of gene transcription (Ropero and Esteller 2007). To test whether targeting these two epigenetic pathways simultaneously would induce synergistic cell killing, MDA-MB468 cells that are sensitive to ING1 were treated with LBH589 and 5azaC independently and in combination. As shown in Figure 7A, a weak additive effect was noted. Since ING1 enhanced paclitaxel and etoposide induced apoptosis in osteosarcoma cells (Garkavtsev and Boucher 2005), we asked if ING1b could also enhance toxicity of 5azaC and the third generation HDAC inhibitor LBH589. ING1b enhanced the ability of both LBH589 and 5azaC to induce cell death better than when combining LBH589 with 5azaC and ING1b was more effective in combination with 5azaC. This was not a result of using a relatively more effective dose of 5azaC, since 5azaC and LBH589 were used at concentrations that had similar effects upon survival individually. To determine if this relationship held in another cell line, T47D cells, which are very resistant to ING1-induced cell death, were tested using the same protocol. As seen in Figure 8, although viral titers used were significantly higher and were tested through an even larger range, the combination of 5AzaC and ING1b was again, most effective in killing cells. These results indicate that targeting two different epigenetic mechanisms using a biological agent in combination with a chemical agent is more effective that using two chemical agents in inducing cell death in breast cancer cells, but the absolute effects are greatest in cells more sensitive to ING1.

Figure 7: Cell death in MDA-MB468 cells in response to ING1b and epigenetic chemotherapeutics.

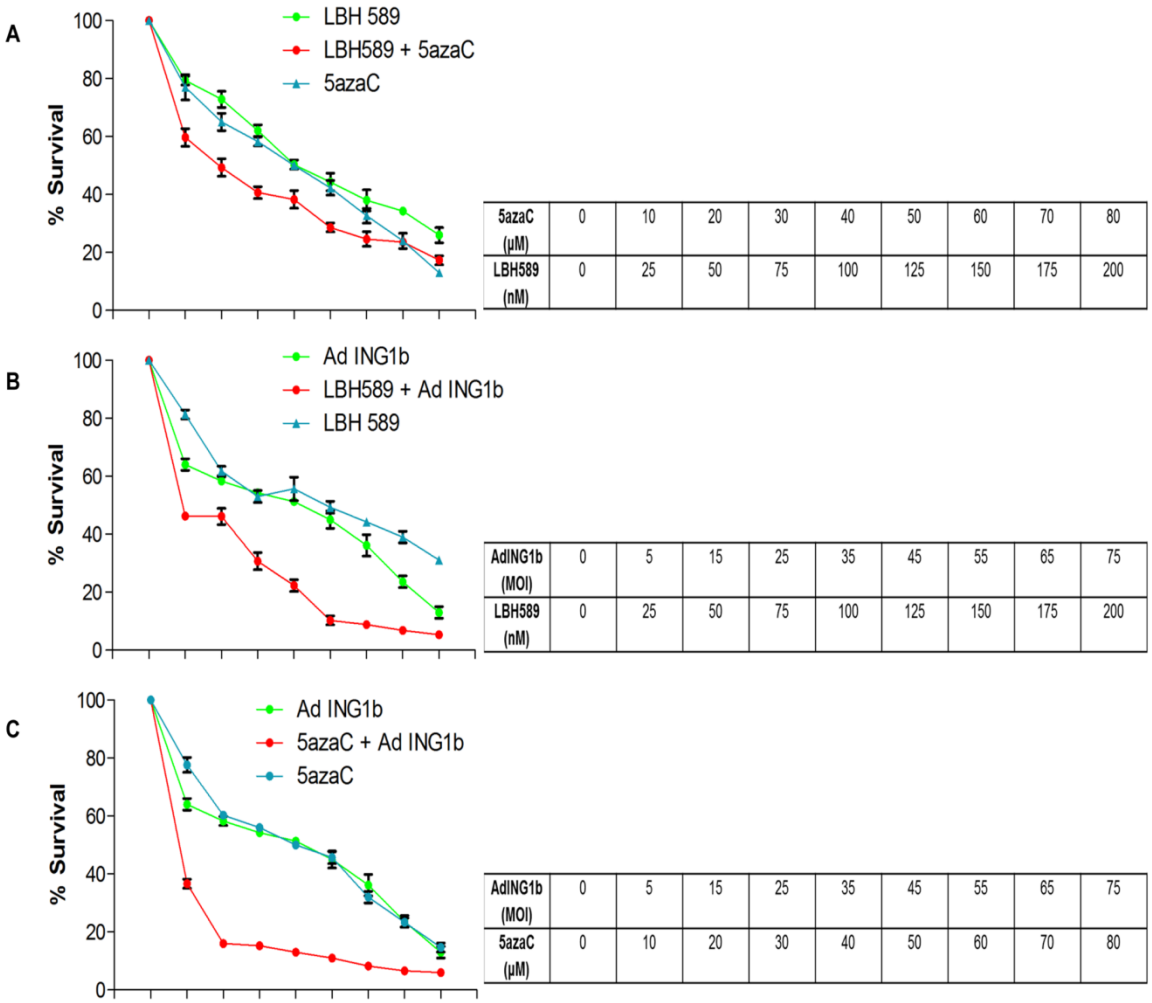

MDA-MB468 cells were grown and treated with various concentrations of **A**) LBH589 and 5azaC alone or in combination, or **B, C**) in combination with adenoviral constructs expressing GFP plus ING1b at various MOIs. In combination treatments, cells were pretreated with LBH589 for 15 hours or 5azaC for 48 hours and then infected with adenoviral constructs and analyzed after 24 hours. The levels of cell death induced by these treatments were estimated by MTT assay. The combination of 5azaC with ING1b shown in panel C was more effective in inducing cell death in MDA-MB468 cells at all concentrations compared to other agents tested singly or in combination. Two way ANOVA with Bonferroni's multiple comparison test was used for calculating P values ($P<0.001$ for both combination treatments shown in panels B&C compared to single agents).

Figure 8: Cell death in T47D cells in response to ING1b and epigenetic chemotherapeutics.

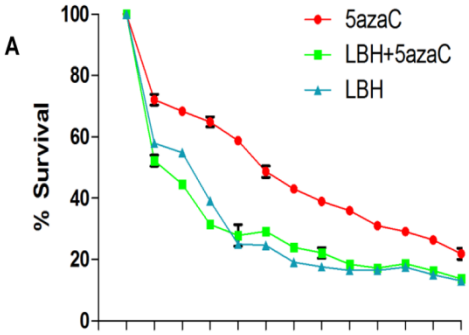

5azaC (μM)	10	20	30	40	50	60	70	80	90	100	110	120
LBH589 (nM)	25	50	75	100	125	150	175	200	225	250	275	300

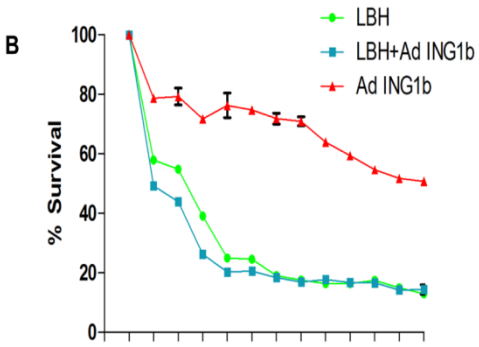

Ad-ING1b (MOI)	10	20	30	40	50	60	70	80	90	100	110	120
LBH589 (nM)	25	50	75	100	125	150	175	200	225	250	275	300

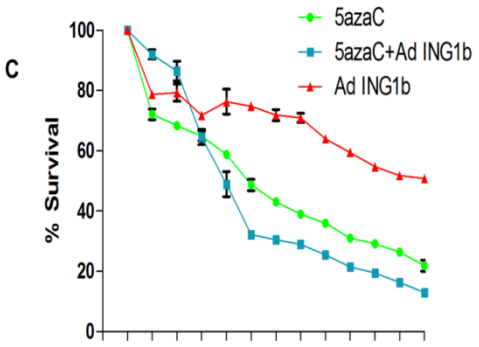

Ad-ING1b (MOI)	10	20	30	40	50	60	70	80	90	100	110	120
5azaC (μM)	10	20	30	40	50	60	70	80	90	100	110	120

T47D cells were grown and treated with various concentrations of **A**) LBH589 and 5azaC alone or in combination, or **B, C**) in combination with adenoviral constructs expressing GFP plus ING1b at various MOIs. MOIs used were greater than for MDA-MB468. The levels of cell death induced by these treatments were estimated by MTT assay. The combination of 5azaC with ING1b shown in panel C was more effective in inducing cell death in T47D cells compared to other agents tested singly or in combination. Two way ANOVA with Bonferroni's multiple comparison test was used for calculating P values ($P<0.001$ for both combination treatments shown in panels B&C compared to single agents).

3.1.3 ING1b acts in synergy with 5azaC to induce cell death

To quantitatively determine how much more effective targeting two separate, versus a single epigenetic pathway was, we assessed interactions using Normalized Isobolograms and Combination Index (CI) values generated using CalcuSyn software. Cells were pretreated with various doses of 5azaC or LBH589 and then treated with the other chemotherapeutic or infected with ING1b adenovirus. Intensities of interactions were determined based upon the CI value generated by the software with particular combinations of drugs and ING1b. Treating with both epigenetic drug agents gave a less than additive effect (Figure 9A). In contrast, the combination of ING1b with LBH589 ranged from non-synergistic to synergistic (CI 0.9-0.5) when both ING1b and LBH589 were used at higher doses (Figure 9B). The combination of ING1b with 5azaC showed clear synergy (CI 0.4-0.2) at all concentrations tested (Figure 9C). Plotting of isobolograms with data generated from ING1-resistant T47D cells (Figure 10A–C) confirmed that the most synergy in T47D cell killing was seen between ING1b and 5AzaC (Figure 10C) as previously noted for cells of the MDA-MB468 line, indicating that this effect was not dependent upon the absolute sensitivity of cells to ING1-induced death.

To further test this using an independent assay, cells were pretreated with 5azaC or LBH589 at IC_{50} concentrations and subsequently infected with adenovirus (30 MOI) expressing GFP or GFP plus ING1b. The treatment groups with combinations of ING1b with 5azaC and ING1b with LBH589 showed significant decreases in the number of viable cells ($P<0.0001$) 48 hr after infection as estimated by trypan blue staining (Figure 11). Again, the combination of ING1b plus 5azaC was most efficacious and virtually

eliminating viable cells. This is consistent with the idea that targeting two pathways eliminates cancer cells more effectively than targeting one pathway with two agents, and demonstrates that adenoviral infection does not induce cell death at these MOIs alone, or when combined with 5azaC or LBH589.

Figure 9: Combination Indices of ING1b with epigenetic chemotherapeutics.

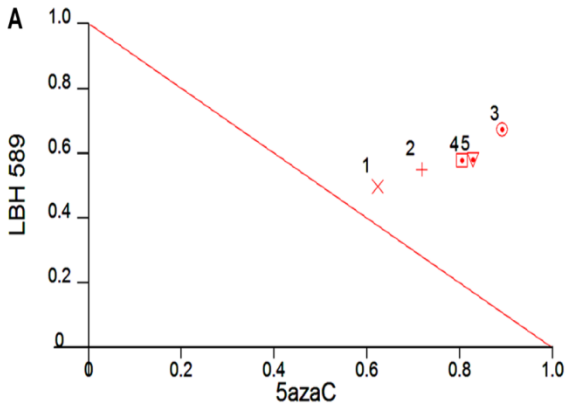

Combination no.	LBH589 (nM)	5azaC (μM)	CI
1	50	20	1.120
2	75	30	1.269
3	100	40	1.566
4	125	50	1.382
5	150	60	1.409

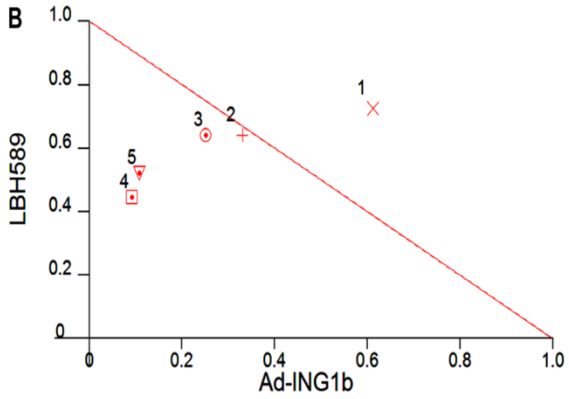

Combination no.	LBH589 (nM)	Ad ING1b (MOI)	CI
1	50	15	1.338
2	75	25	0.972
3	100	35	0.893
4	125	45	0.537
5	150	55	0.629

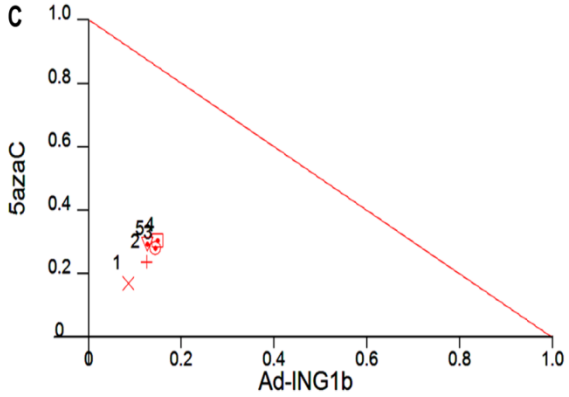

Combination no.	5azaC (μM)	Ad ING1b (MOI)	CI
1	20	15	0.257
2	30	25	0.364
3	40	35	0.425
4	50	45	0.454
5	60	55	0.421

MDA-MB468 cells were treated with combinations of A) LBH589 plus 5azaC, B) adenoviral vector expressing GFP plus ING1b and LBH589 or C) adenoviral vector expressing GFP plus ING1b plus 5azaC at various concentrations. Combination indexes were determined using CalcuSyn software. Isobologram analysis showed that 5azaC plus Ad-ING1b showed the highest degree of synergy in inducing cell death of the combinations tested.

Figure 10: Combination Indices of ING1b with epigenetic chemotherapeutics.

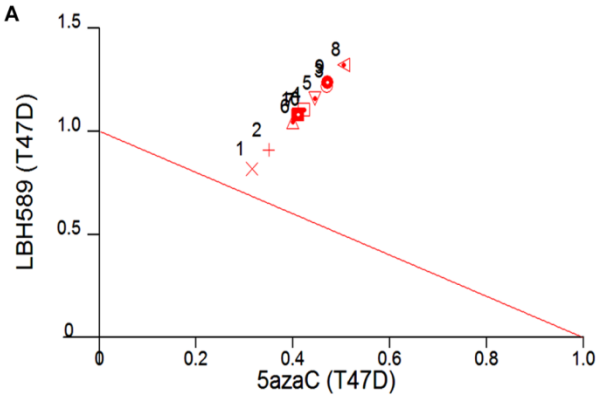

Combination No.	LBH589 (nM)	5azaC (μM)	CI
1	75	30	1.133
2	100	40	1.259
3	125	50	1.688
4	150	60	1.527
5	175	70	1.607
6	200	80	1.446
7	225	90	1.484
8	250	100	1.829
9	275	110	1.710
10	300	120	1.494

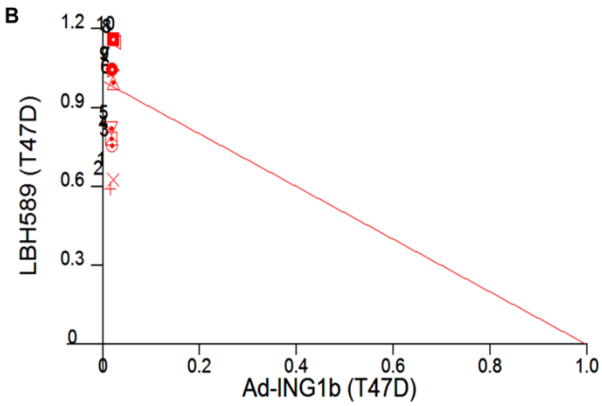

Combination No.	LBH589 (nM)	Ad-ING1b (MOI)	CI
1	75	30	.648
2	100	40	.609
3	125	50	.775
4	150	60	.801
5	175	70	.839
6	200	80	1.017
7	225	90	1.065
8	250	100	1.174
9	275	110	1.064
10	300	120	1.180

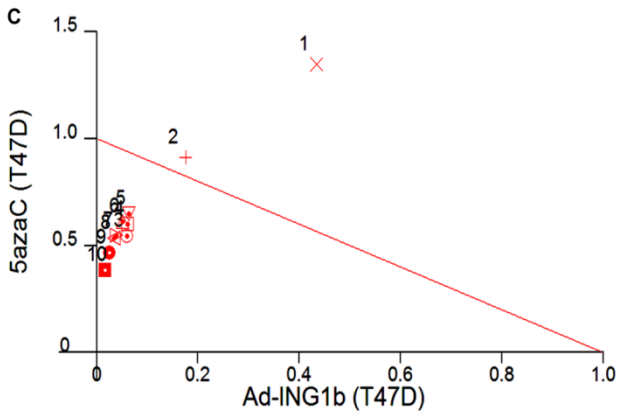

Combination No.	5azaC (μM)	Ad-ING1b (MOI)	CI
1	30	30	1.783
2	40	40	1.090
3	50	50	.604
4	60	60	.661
5	70	70	.714
6	80	80	.666
7	90	90	.587
8	100	100	.568
9	110	110	.494
10	120	120	.403

T47D cells were treated with combinations of **A**) LBH589 plus 5azaC, **B**) adenoviral vector expressing GFP plus ING1b and LBH589 or **C**) adenoviral vector expressing GFP plus ING1b plus 5azaC at various concentrations and Combination Indexes were determined using CalcuSyn software. The Isobologram analysis showed that 5azaC plus Ad-ING1b showed the highest degree of synergy in inducing cell death of the combinations tested.

Figure 11: Effects of ING1b in combination with epigenetic chemotherapeutics.

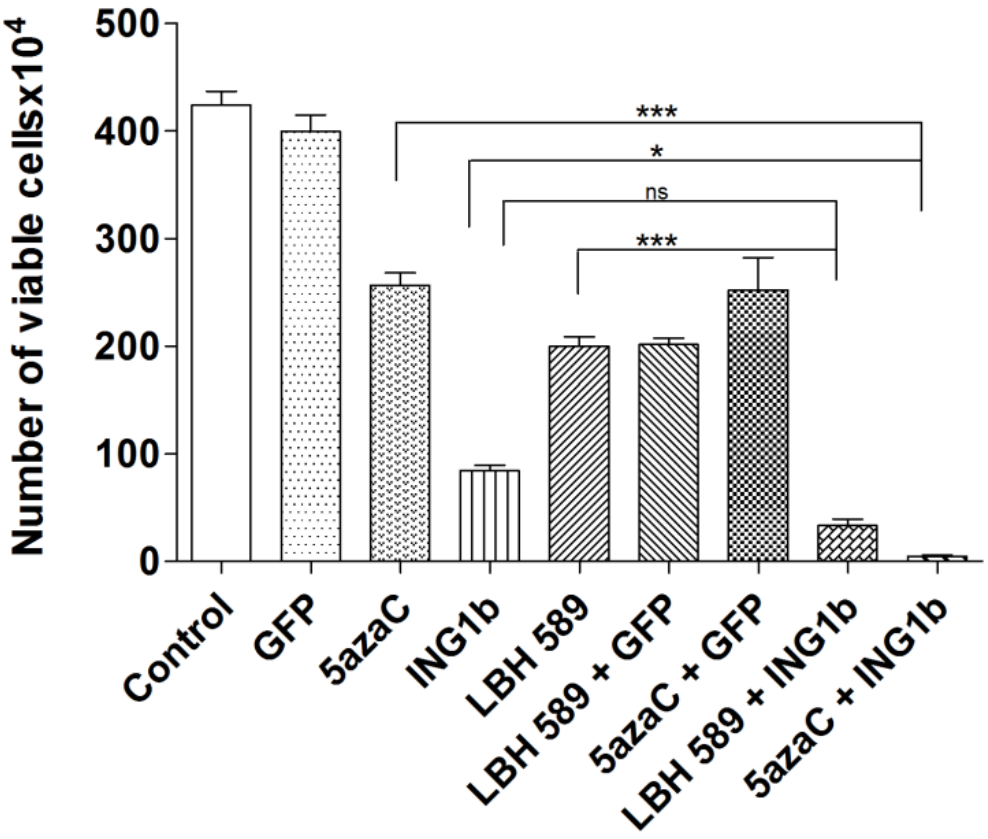

MDA-MB468 cells were treated alone or with the combinations of virus (30 MOI) and 5azaC (48 hours, 40 µM) or LBH589 (15 hours, 100 nM) indicated. Untreated cells and cells infected with Ad-GFP (30 MOI) alone served as controls. Cells were harvested 48 hours after infection and stained with Trypan Blue. Cell number was determined by counting the number of unstained cells using a haemocytometer. One-way ANOVA and Tukey's multiple comparison post-tests were performed to calculate P values (*** indicates $P<0.0001$ compared to the control).

3.1.4 ING1b plus 5azaC induces DNA damage and apoptosis

Cells treated with combinations of 5azaC, control and ING1 adenovirus were analyzed for Annexin V binding as a marker of early apoptosis (Figure 12A). 5azaC and ING1b caused significantly higher percentages of apoptotic cells in comparison to the 5azaC only, ING1b only and the GFP controls (Figure 10A; $P<0.0001$), and this effect was reflected by reduced numbers of cells showing cell morphology consistent with apoptosis (Figure 12B). MDA-MB468 cells appeared to be very sensitive to ING1b-induced early apoptosis events as estimated by annexin V binding, which may explain an apparently additive, rather than synergistic effect when combined with 5azaC in this experiment. If analysis of the entire population of cells is done in the flow cytometry analysis, rather than omitting cells that have been killed by the treatment, the combination of 5azaC and ING1b again shows clear synergy. Most cells treated with Ad-ING1b showed morphology reminiscent of apoptosis, but cells survived longer than those treated with 5azaC plus ING1b. Fewer cells were present on plates treated with 5azaC due to inhibition of cell cycle progression (Sanchez-Abarca, Gutierrez-Cosio et al. 2010).

Apoptosis involves initiation, effector and execution phases (Eastman and Rigas 1999). To better determine the progression of the apoptotic process in response to these agents, we evaluated the status of caspase-3 and PARP, which act at later stages of apoptosis. A significant increase in the amount of cleaved caspase-3 was noted in cells treated with the combination of ING1b and 5azaC compared to treatment with single agents (Figure 12C). A similar trend was seen in the ratio of cleaved:uncleaved PARP. 5azaC is also known to induce DNA double strand breaks in cells (Kiziltepe, Hideshima et al. 2007), which can be estimated by evaluating levels of phosphorylated histone

variant γH2AX. A massive increase in the level of γH2AX was observed in response to 5azaC plus ING1b compared to 5azaC or ING1b alone. This may be due to the fact that 5azaC has been shown to act synergistically with Bortezomib, a proteasome inhibitor and with Doxorubicin in inducing DNA damage (Kiziltepe, Hideshima et al. 2007). ING1b was reported to be able to affect proteasomal degradation of several proteins including p53 (Thalappilly, Feng et al. 2011) and Doxorubicin specifically affects ubiquitination of a subset of proteins (Mandili, Khadjavi et al. 2012). Thus, it is tempting to speculate that convergent effects of 5azaC and ING1b in blocking proteasomal degradation may result in increased DNA damage, through a currently undefined mechanism that may or may not involve the reactivation of major tumor suppressor genes such as p53 (Nagashima, Shiseki et al. 2001), or Rb (Han, Feng et al. 2008). These data provide the first evidence that ING1b exacerbates 5azaC-induced DNA damage.

Figure 12: Apoptosis in response to 5azaC and ING1b in MDA-MB468 cells.

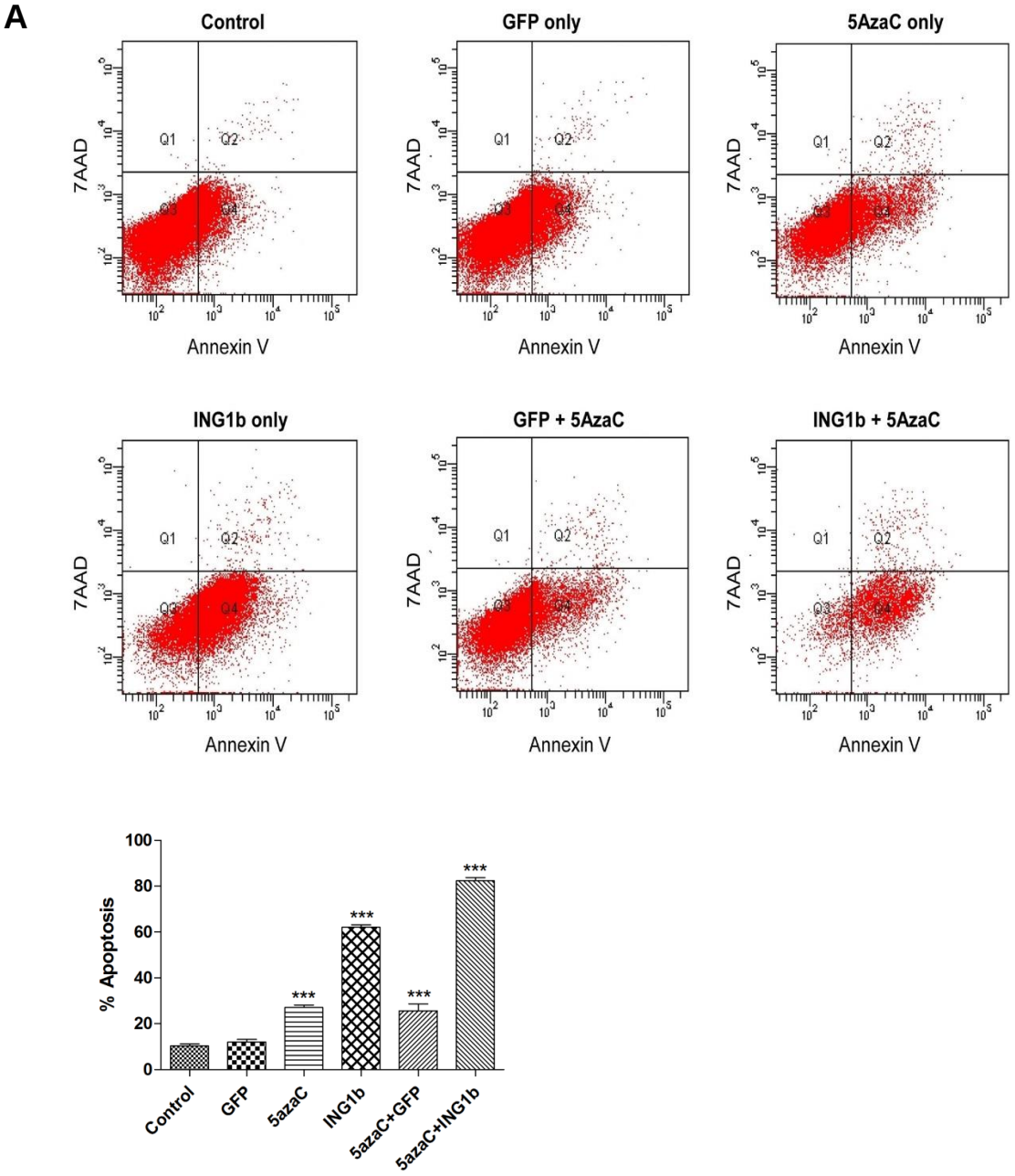

Cells were pretreated with 40 µM 5azaC for 48 hours and then infected with adenoviral constructs expressing GFP or ING1b plus GFP (30 MOI). Untreated cells and cells infected with only Ad-GFP or Ad-ING1b plus GFP served as controls. Cells were harvested 24 hours later, stained for annexin V and the percentage of the cell population undergoing apoptosis was estimated by determining the percentage of annexin V positive cells by flow cytometry. Cells treated with a combination of 5azaC and Ad-ING1b plus GFP showed a higher amount of apoptosis induced in comparison to controls. One way ANOVA and Tukey's multiple comparison post-test were performed to calculate P values comparing treated to untreated control cells (*** indicates P<0.0001).

Apoptosis in response to 5azaC and ING1b in MDA-MB468 cells (contd.)

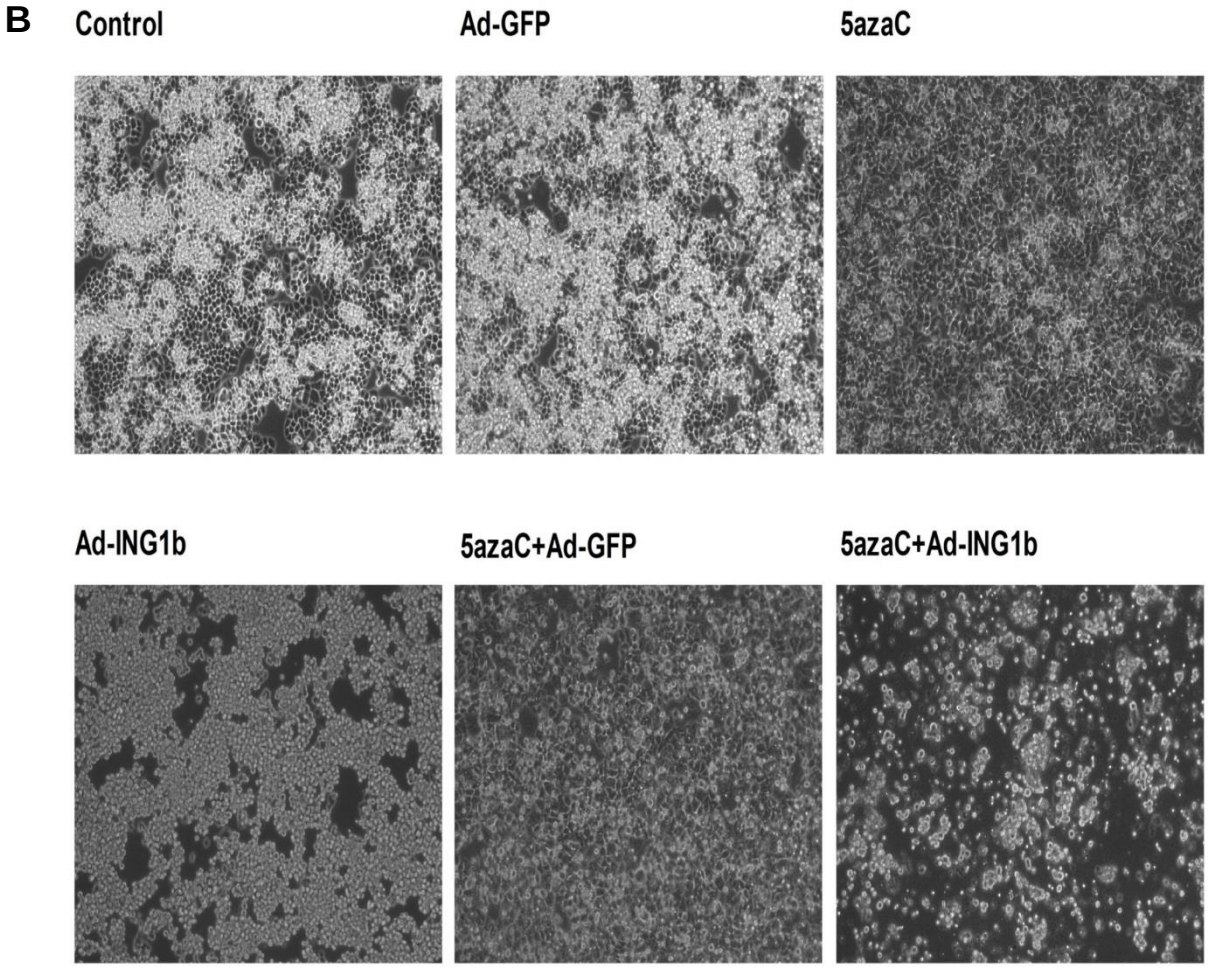

Clear morphological changes were noted in cells 24 hours after treatment with Ad-ING1b alone, or in combination with 5azaC. The combination blocked cell growth and induced morphological changes consistent with apoptosis in the great majority (99% +) of cells examined. Infection with Ad-GFP had little effect upon cell number or shape while 5azaC inhibited cell growth but was not effective in inducing an apoptotic phenotype in the majority of cells.

Apoptosis in response to 5azaC and ING1b in MDA-MB468 cells (contd.)

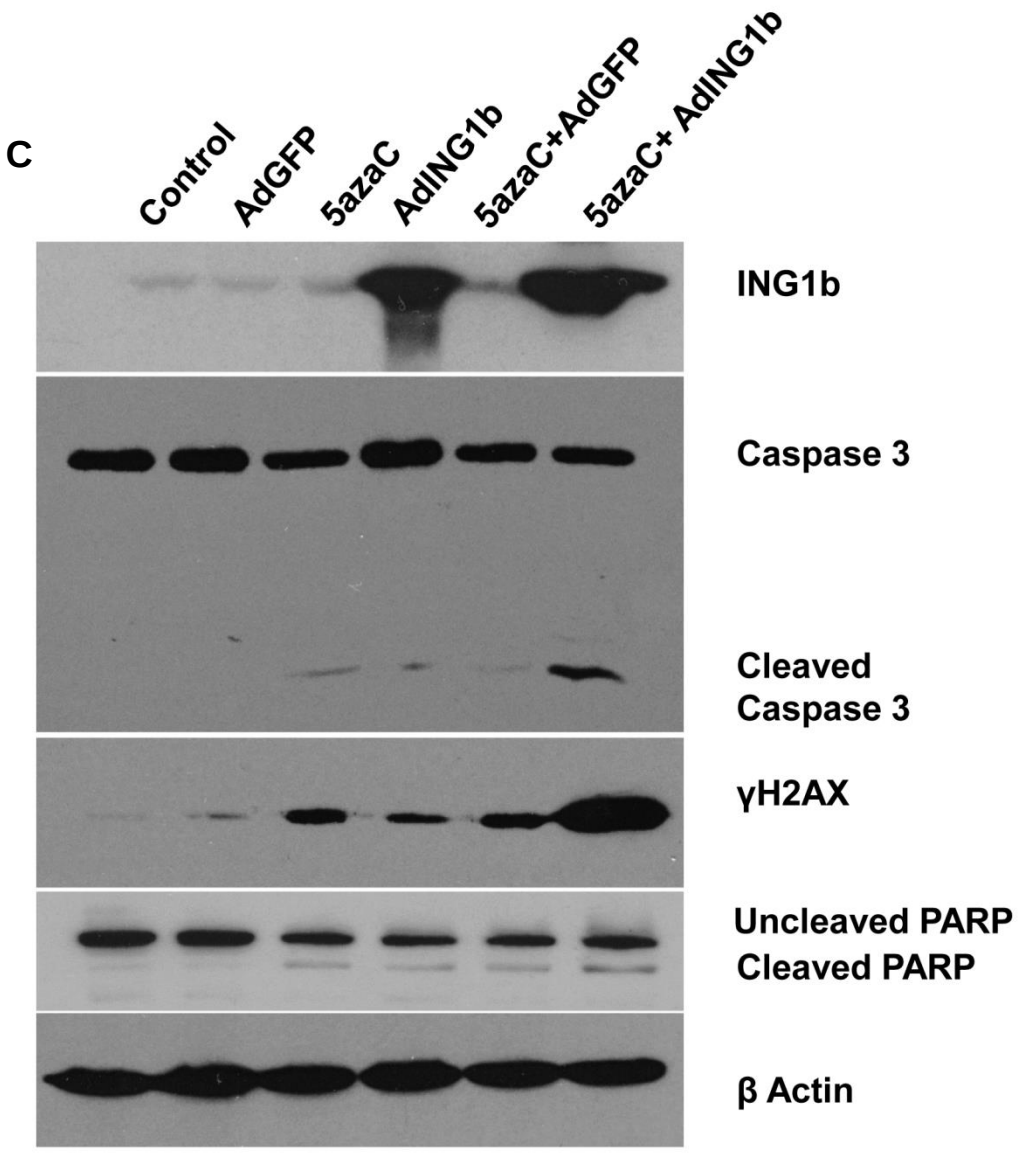

Cells treated with the indicated agents for 48 hours were harvested in Laemmli sample buffer, lysates were boiled and equal amounts of protein from each sample were electrophoresed and blotted with the indicated antibodies.

3.1.5 Ad-ING1b plus 5azaC significantly reduce tumor size in a mouse xenograft model

We next tested for ING1b-5azaC synergy using an *in vivo* xenograft tumor model. Pilot experiments determined that treatment with 5 mg/kg of 5azaC affected tumor growth but not animal body weight. MDA-MB468 cells were injected into SCID mice to generate tumors and when tumors reached 125 mm^3, treatments with combinations of 5azaC and ING1b were started. Animals were treated from day 1 through 33, monitored in the absence of treatment from day 33 through 57, and were then treated from day 57 through 77 with 10-fold more virus (a 3-fold increase in MOI due to larger starting volume of tumor) to see if tumors acquired resistance as often seen in response to other agents (Raguz and Yague 2008). As shown in Figure 13, the combination of 5azaC and ING1b was the most effective in inhibiting tumor growth at the lower MOI of Ad-ING1b and tumors decreased in size in response to injection at the higher MOI used. Injected animals showed no adverse side effects at the higher level of virus. The growth of the tumors was monitored until day 105 at which point animals were sacrificed according to animal care guidelines. These data indicates that synergy between ING1b and 5azaC was maintained *in vivo*, that cells did not acquire resistance to virally expressed ING1b, and that higher viral titers were effective in reducing tumor volume. The latter observation underscores the importance of optimizing viral dosage *in vivo* versus *in vitro*, where much more effective killing was observed at relatively lower MOI.

Figure 13: AdING1b plus 5azaC significantly reduce tumor volume *in vivo* in a mouse xenograft model.

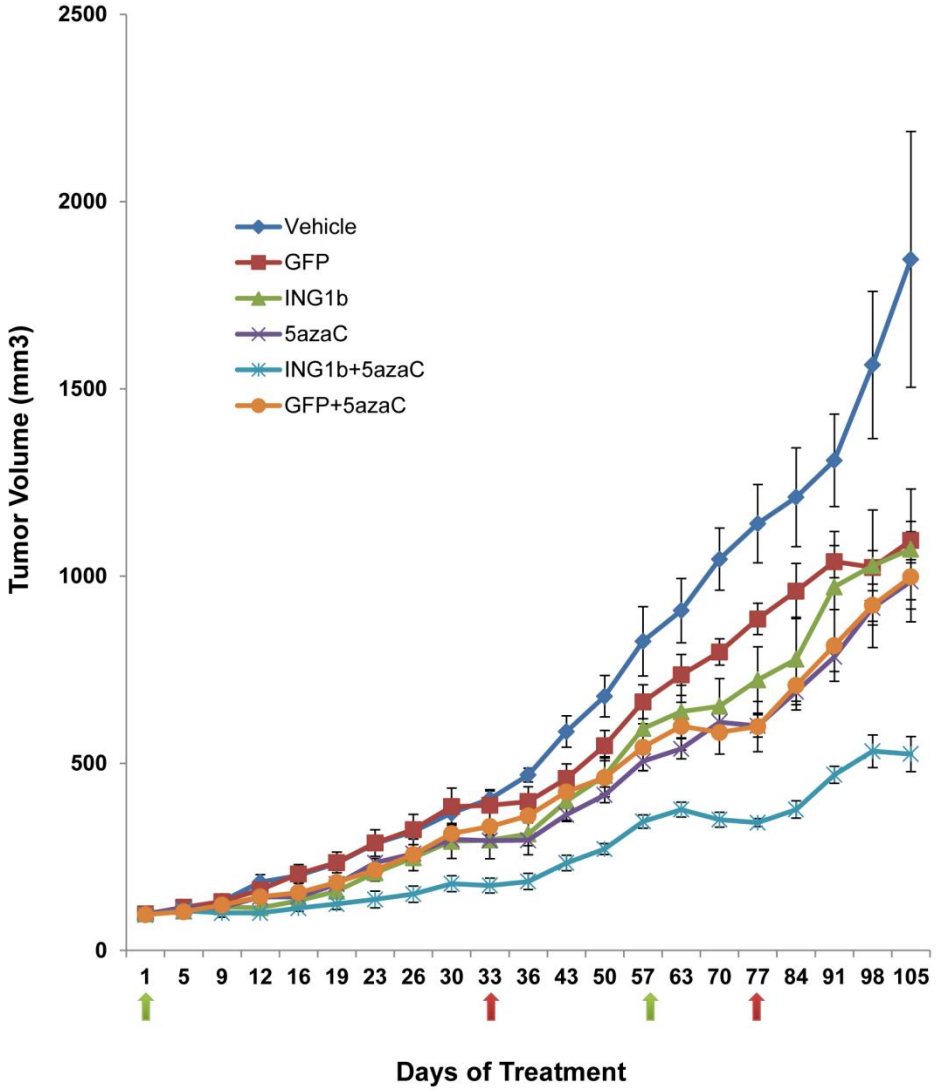

7×10^6 MDA-MB468 cells/animal were injected into the mammary fat pads of mice and in two weeks when tumors reached a size of 5 mm × 5 mm × 5 mm, treatment was begun (green arrow at day one). Viral constructs (2×10^8 PFU, calculated to provide an MOI of 1–5) were injected intratumorally twice a week for 5 weeks (10 injections) and 5azaC was injected intraperitoneally three times a week for 5 weeks (15 injections). Treatments were halted at day 33 (first red arrow on the abscissa) and resumed at day 57 with 2×10^9 PFU of virus and the same concentration of 5azaC. Given the larger tumor volume, this was calculated to increase the MOI by ~3-fold over the initial MOI. As noted by the decrease in tumor volume over days 57–77, tumors had not developed resistance to the combination treatment and regressed in response to higher viral titers. No adverse reactions were noted to this concentration of virus. Each time point represents the average value of five animals per group. Two way ANOVA with Bonferroni's multiple comparison test was used for determining significance.

3.2 Reduced ING1 levels in breast cancer promotes metastasis

3.2.1 ING1 regulates genes related to breast cancer

Previous studies have shown that ING1 overexpression selectively kills breast cancer cells *in vitro* and in a mouse mammary model (Thakur, Feng et al. 2012) while reduced ING1 expression was seen in >40% of primary breast tumors (Toyama, Iwase et al. 1999). To examine how ING1 might limit cancer cell growth and survival, we identified genes that were regulated by ING1 using a Nimblegen microarray-based platform (MSc thesis work of Uyen Tran). The analysis identified 844 genes that were reproducibly induced, and 1500 that were repressed at least two-fold in response to ING1b overexpression (Figure 14). The analysis identified 14-3-3 sigma (SFN), a gene frequently repressed in breast cancer (Umbricht, Evron et al. 2001) as the gene most highly induced by ING1, while a PDGF receptor gene (PDGFRA) was most highly repressed. Pathway analysis of ING1-repressed genes showed that breast cancer had the strongest association (p=0.0008; kappa similarity score=1.0 where 0.75-1.0=very high; 0.5-0.75=high, 0.25-0.5=moderate and below 0.25=low) followed by colorectal cancer (Figure 14B-C), while genes transcriptionally activated had less clear links to cancer pathways (data not shown).

Figure 14: ING1b regulated genes.

A

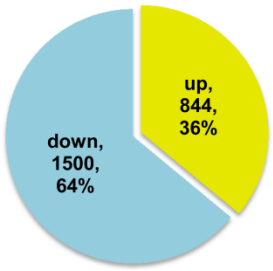

B

Term	P-Value
Breast cancer	8.0E-4
Colorectal cancer; Tourette syndrome; Bone density; Pregnancy loss, recurrent; Cleft lip without cleft palate; Juvenile polyposis; Cleft palate	8.7E-4
Diabetes, type 2; Nephropathy in other diseases	1.1E-3
Ovarian cancer	3.0E-3
Colon cancer	6.4E-3
Colorectal cancer	1.2E-2
Stomach cancer	2.3E-2
Atopy beta-lactam allergy	2.4E-2
Prostate cancer	4.4E-2
Colorectal cancer; Endometrial cancer	4.7E-2

C

#	Category	Term	Kappa
1	GENETIC_ASSOCIATION_DB_DISEASE	Breast cancer	1.00
2	GENETIC_ASSOCIATION_DB_DISEASE	Colorectal cancer	0.60
3	GENETIC_ASSOCIATION_DB_DISEASE	Lung cancer	0.42
4	GENETIC_ASSOCIATION_DB_DISEASE	Prostate cancer	0.41
5	GENETIC_ASSOCIATION_DB_DISEASE	Stomach cancer	0.34
6	GENETIC_ASSOCIATION_DB_DISEASE	Ovarian cancer	0.33
7	GENETIC_ASSOCIATION_DB_DISEASE	Bladder cancer	0.32
8	GOTERM_BP_FAT	Regulation of cell cycle	0.32
9	GENETIC_ASSOCIATION_DB_DISEASE	Esophageal cancer	0.30

(**A**) Ectopic expression of ING1 reproducibly induced 844 and repressed 1,500 genes by >2-fold in three separate trials. (**B**) Analysis of the 1,500 repressed genes using the Genetic_Association_DB_Disease and analysis using DAVID. Pathways with $p<0.05$ are shown. (**C**) Disease profiling of the 1,500 repressed genes by similarity score gave values of Kappa between 1.0 and 0.3 where 0.75-1.0 is very high, 0.5-0.75 is high, 0.25-0.5 is moderate and < 0.25 is a low score. Pathways showing scores above low are shown.

3.2.2 ING1 levels are reduced in breast cancer cells

Our study using the retrospective Calgary Tamoxifen Breast Cancer Cohort, included 532 patients diagnosed with invasive breast cancer, treated at the Tom Baker Cancer Centre (TBCC) between 1985 and 2000. Selection criteria are outlined in Materials and Methods and clinico-pathologic characteristics are shown in Table 4. Median follow-up time for the cohort was 82.1 months. Mean age was 66 years and the majority of patients (85%; n=451) were postmenopausal women when age was dichotomized around the median age of menopause in Canada (52 years). Patients were distributed between stages (1997), with 44% (n=233) stage I, 31% stage II (n=163), 8.0% stage III (n=40), and 1% stage IV (n=7). 79% of patients had a low-grade tumor (n=419, tumor grade 1 or 2), 51% (n=271) had a tumor size of less than 2 cm, and 64.0% (n=342) were lymph node negative. A minority of patients had disease progression within 5 years of diagnosis (18%, n=95), and the majority of these patients also developed distant metastatic disease within this timeframe (14%, n=74). ER, PR, and Her2 status were not systematically performed at the time of diagnosis for many of the patients in this cohort; retrospective IHC-based analysis of the TMAs was performed to determine the status of each of these biomarkers.

ING1 protein level was measured using quantitative fluorescence immunohistochemistry on the HistoRx AQUA® platform (Camp, Chung et al. 2002). The specificity of the ING1 monoclonal antibody used for fluorescence IHC was assessed using control transfected 293 cells and ING1 overexpressing 293 cells (Suzuki, Boland et al. 2011). Endogenous ING1 expression was weak and nuclear in the control 293 cells, whereas overexpressed ING1 was strong and present in both the nuclear and cytoplasmic compartments (Figure 15A, left panels). The specificity of the ING1 fluorescence IHC

assay was confirmed by comparing Cy3 signal detection in placenta treated with or without the ING1 antibody (Figure 15A, right panels). ING1 staining in normal breast tissue was weak and predominantly nuclear. ING1 levels were similar in ductal epithelium, myoepithelium, and stromal cells (Figure 15B, top panels). In breast cancers with low ING levels, staining was weaker than in surrounding non-malignant stromal cells (Figure 15B, mid panels). In tumors expressing high levels of ING1, ING1 staining was strongly nuclear with clearly detectable cytoplasmic protein compared with the weaker nuclear and diffused cytoplasmic ING1 staining in surrounding non-malignant stromal cells (Figure 15B, lower panels).

To determine whether ING1 expression was altered in breast cancer cells compared to normal breast epithelial cells we compared ING1 expression within our Tamoxifen-treated breast cancer cohort to a 95% confidence interval (C.I.) around the median results obtained from normal breast epithelium (Figure 15C). Median tumor ING1 expression was 267 (red line) and fell at the lower end of the normal breast 95% C.I. (ING1=254-660, thin blue lines) indicating that ING1 expression tends to be lost in breast cancer cells as compared to the normal epithelium from which they are derived.

Table 4: Association of clinico-pathological characteristics of breast cancer patients with expression levels of ING1.

Characteristic	# of Cases (%)	ER+/Her2-			ER- or Her2+		
		Low Ing1	High Ing1	χ^2 p-value	Low Ing1	High Ing1	Fisher's Exact p-value
Age							
Range	35.8-95.5						
Median	66						
< 53	81 (15)	18	49	0.298	1	2	1.000
≥ 53	451 (85)	121	242		11	18	
Body Mass Index							
Normal	136 (26)	36	74	0.869	5	7	0.747
Underweight	8 (1)	2	2		0	0	
Overweight	136 (26)	38	71		5	7	
Obese	107 (20)	29	62		2	1	
Unknown	145 (27)						
Stage							
I	233 (44)	54	134	0.345	1	7	0.239
II	163 (31)	48	86		7	6	
III	40 (8)	10	19		2	4	
IV	7 (1)	0	3		1	1	
Unknown	89 (17)						
Tumor Grade							
Low (1/2)	419 (79)	117	229	0.466	4	13	0.119
High (3)	68 (13)	14	35		7	5	
Unknown	45 (8)						
Tumor Size							
< 2cm	271 (51)	70	154	0.629	1	10	0.019*
≥ 2cm	221 (42)	59	117		10	8	
Unknown	40 (7)						
Lymph Node Status							
Negative	342 (64)	81	192	0.085	3	13	0.205
Positive	117 (22)	38	59		4	5	
Unknown	73 (14)						
ER status							
No	16 (3)	0	0	nd	6	9	1.000
Yes	473 (89)	139	291		6	11	
Unknown	43 (8)						
PR status							
No	56 (11)	12	24	0.937	4	10	0.466
Yes	416 (78)	118	243		7	9	
Unknown	60 (11)						
Her2 status							
No	505 (95)	139	291	nd	5	8	1.000
Yes	22 (4)	0	0		7	12	
Unknown	5 (1)						
Any Recurrence							
No	437 (82)	114	234	0.692	6	18	0.030*
Yes	95 (18)	25	57		6	2	
Distant Recurrence							
No	458 (86)	117	248	0.776	6	20	0.001*
Yes	74 (14)	22	43		6	0	
Radiation Therapy							
No	199 (37)	45	117	0.079	7	8	0.710
Yes	319 (60)	93	165		5	10	
Unknown	14 (3)						

The listed clinico-pathological characteristics were analyzed for their correlation with low/high levels of ING1. High levels of ING1 show a negative correlation with tumor size, recurrence and distant recurrence of cancer in the ER- or Her2+ group of patients in the cohort.

Figure 15: Immunohistochemical staining and quantitation of ING1 using the HistoRx AQUA platform.

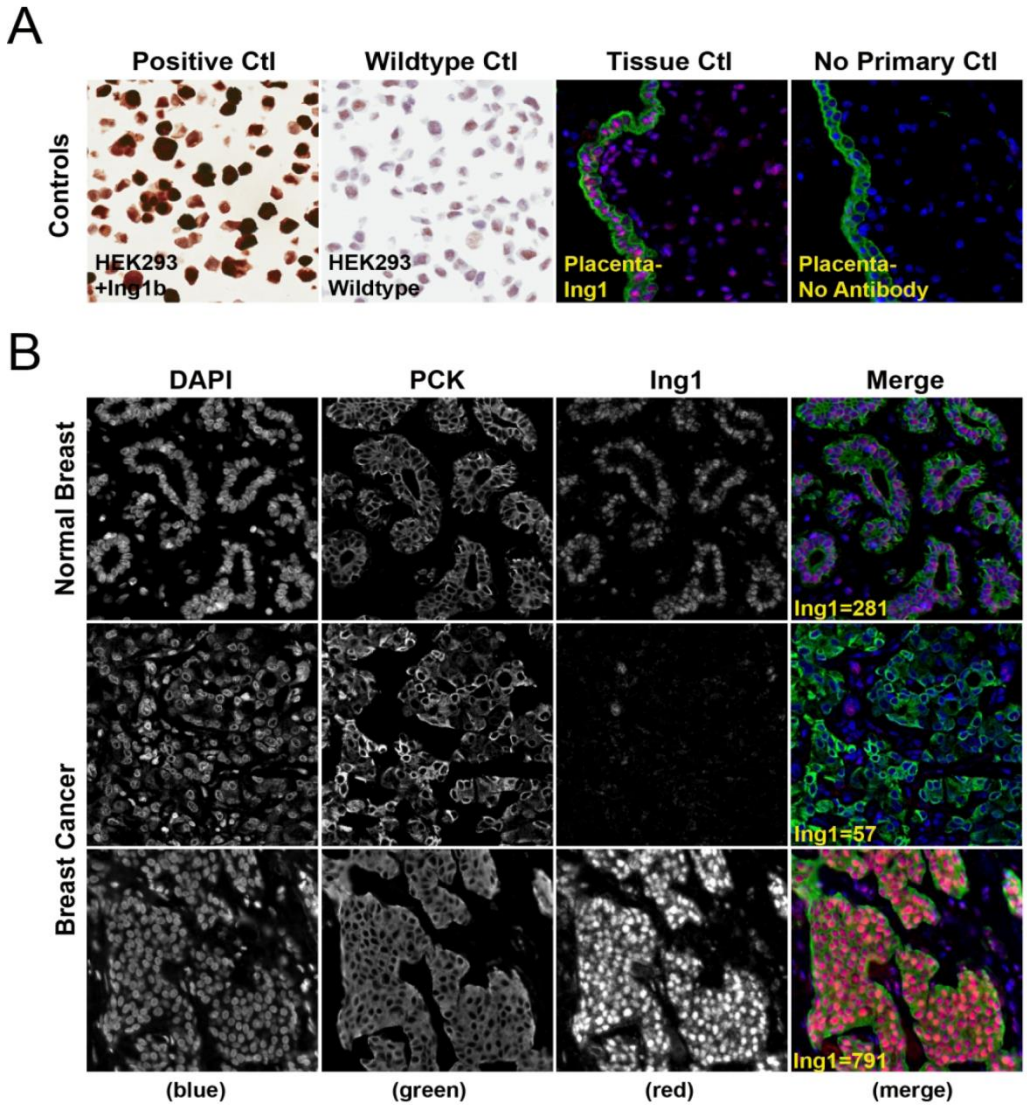

(**A**) Representative images showing specificity of the ING1 monoclonal antibody in HEK293 cells and HEK293 cells overexpressing ING1 (left panels) and in placenta treated with or without the ING1 antibody (right panels). (**B**) Representative examples of quantitative fluorescent IHC images for ING1 expression in normal breast tissue (top row of panels) and breast cancer tissue (two bottom rows of panels). AQUA scores represent the expression level of ING1 within the pan-cytokeratin defined epithelial/tumor compartment. DAPI-stained nuclei are depicted in blue, pan-cytokeratin-stained epithelial/tumor cells are depicted in green, and ING1 protein expression is depicted in red.

Immunohistochemical staining and quantitation of ING1 using the HistoRx AQUA platform. (contd.)

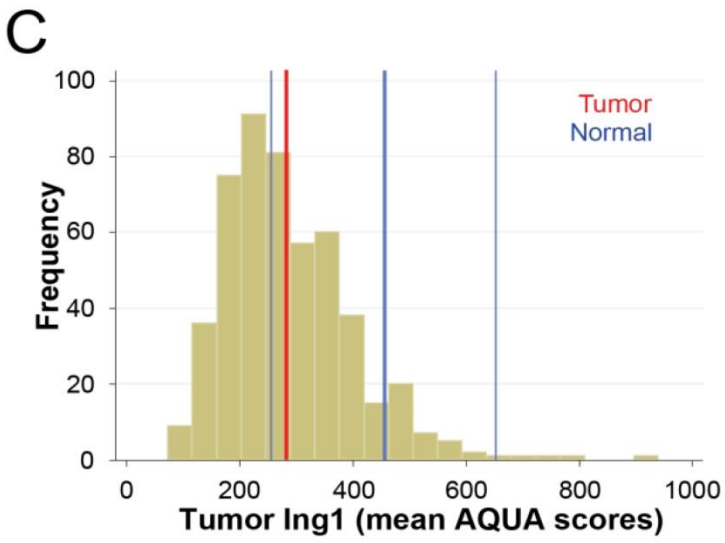

(**C**) Histogram distribution representing ING1 expression within breast cancer patient samples. The solid blue line represents median ING1 expression in normal breast tissue, the broken blue lines represent 95% CI from median ING1 expression in normal breast tissue, and the solid red line represents median ING1 expression in breast cancer patient samples.

3.2.3 Prognostic value of ING1 protein expression

As the Calgary Tamoxifen Breast Cancer Cohort is not defined by a particular subtype of breast cancer and the different subtypes are known to have distinct biology, we classified patients for which there was corresponding ING1 expression data into luminal breast cancer (ER positive and Her2 negative, n=430) and non-luminal breast cancer (ER negative or Her2 positive, n=32) groups for analysis. Breast cancer patients were further dichotomized at the lowest tertile of ING1 expression (ING1< 226), as assessed in all patients for which there was an ING1 score (n=501), to identify low and high ING1 expressing tumors within the luminal and non-luminal subtypes. This cutpoint was selected as, unlike median ING1 expression (ING1=267), the lowest tertile falls below the 95% confidence interval for ING1 expression in normal breast epithelium (ING1=254-660), identifying a population of tumors that have substantial loss of ING1 expression compared to normal tissue. Loss of ING1 did not correlate with any clinico-pathological variables in the luminal group, whereas low ING1 expression correlated with tumor size greater than 2 cm (p=0.019) as well as recurrence (p=0.030) and distant recurrence (p=0.001) in the non-luminal group (Table 4). No differences in survival outcomes were seen by Kaplan Meier analysis in the luminal group dichotomized by ING1 expression (Figure 16A-C). However, in the non-luminal group low ING1 levels correlated with survival outcomes, including: disease free survival (Figure 16D, logrank p=0.013), disease specific overall survival (Figure 16E, logrank p=0.0071), and distant metastasis free survival (Figure 16F, logrank p=0.0003).

Figure 16: Kaplan-Meier survival analysis.

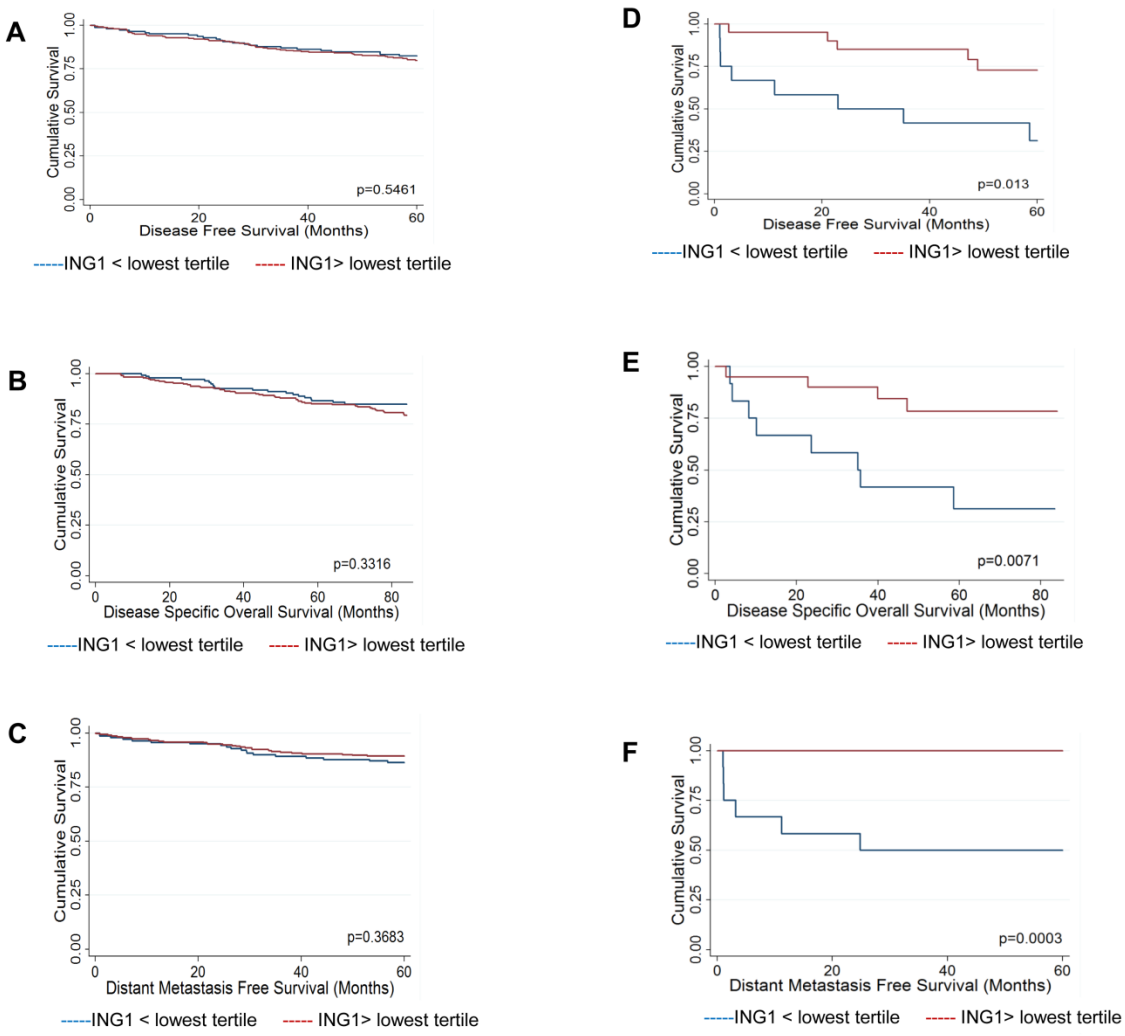

(**A-C**) **Survival of patients in the ER+/Her2- group**. Kaplan-Meier survival curves for (**A**) disease free survival (**B**) disease specific overall survival and (**C**) distant metastasis free survival. No difference was noted between breast cancer patients with below lowest tertile or above lowest tertile of ING1levels. (**D-F**) **Survival of patients in the ER- or Her2+ group**. Kaplan-Meier survival curves for (**D**) disease free survival (**E**) disease specific overall survival and (**F**) distant metastasis free survival. ING1 levels positively correlate with the three categories of survival in ER- or Her2+ breast cancer patients.

3.2.4 ING1 protein levels regulate migration and invasion of MDA-MB231 cells

We next evaluated the ability of ING1 to regulate migratory and invasive behavior of the MDA-MB231 triple negative breast cancer cell line. Ectopic expression of ING1 did not appear to block growth or induce cell death in MDA-MB231 cells as reported previously for INGs in other cell types (Figure 17A). Consistent with this, and with ING1 inhibiting migratory behavior, initial scratch tests suggested that expression of ING1 by infection with adenovirus inhibited the ability of MDA-MB231 cells to migrate to fill in wounds in cell monolayers (Figure 17A). We then checked the migratory properties of these cells upon ING1 overexpression and knockdown using a transwell migration assay. ING1 inhibited migration to the lower chamber by ~3.5 fold (Figure 17B) whereas ING1 knockdown increased the number of migratory cells by 1.3 fold, compared to controls. These reciprocal results corroborate results from the scratch tests and are consistent with ING1 negatively regulating cell migration.

Metastatic cancer cells actively penetrate the basement membrane to migrate and form tumors at distant sites. Given the link between low ING1 levels and lymph node involvement, we asked if ING1 could play a role in breast cancer cell invasion. As shown in figure 17C, ING1 overexpression reduced the ability of MDA-MB231 cells to invade through the matrigel membrane. Similarly, ING1 knockdown had a reciprocal effect as cells with reduced levels of ING1 showed increased invasive capacity compared to control cells. Similar results were obtained when ING1 levels were modulated in normal mesenchymal human foreskin fibroblasts (HS68) as ING1 also regulated the invasive capacity of these cells *in vitro* (Figure 18).

Figure 17: ING1 protein levels regulate migration and invasion of MDA-MB231 cells *in vitro*.

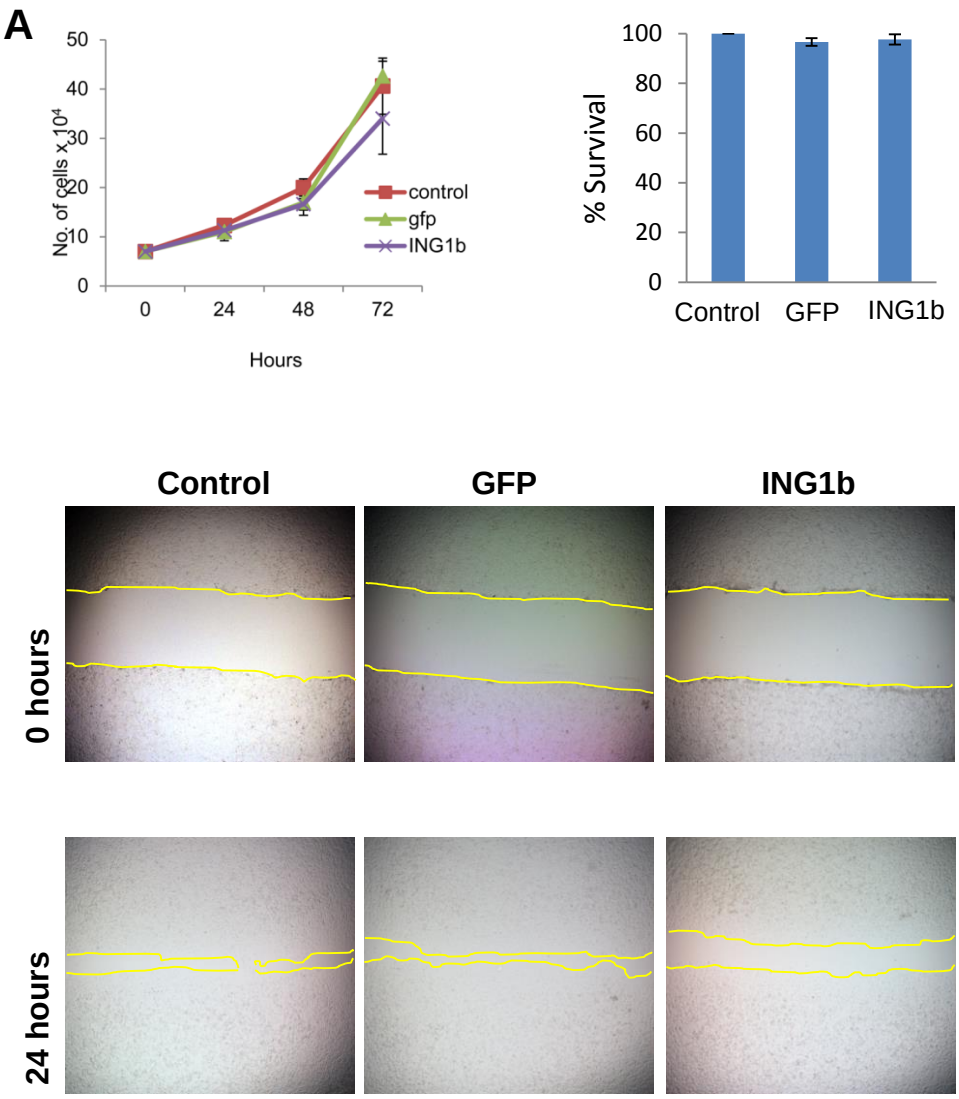

(**A**) Change in number/survival of MDA-MB231 cells upon infection with adenovirus expressing GFP or GFP + ING1 determined by cell count (top left) and MTT assay (top right). Scratch assay using MDA-MB231 cells upon infection with Ad-GFP or ING1b (bottom).

ING1 protein levels regulate migration and invasion of MDA-MB231 cells *in vitro*. (contd.)

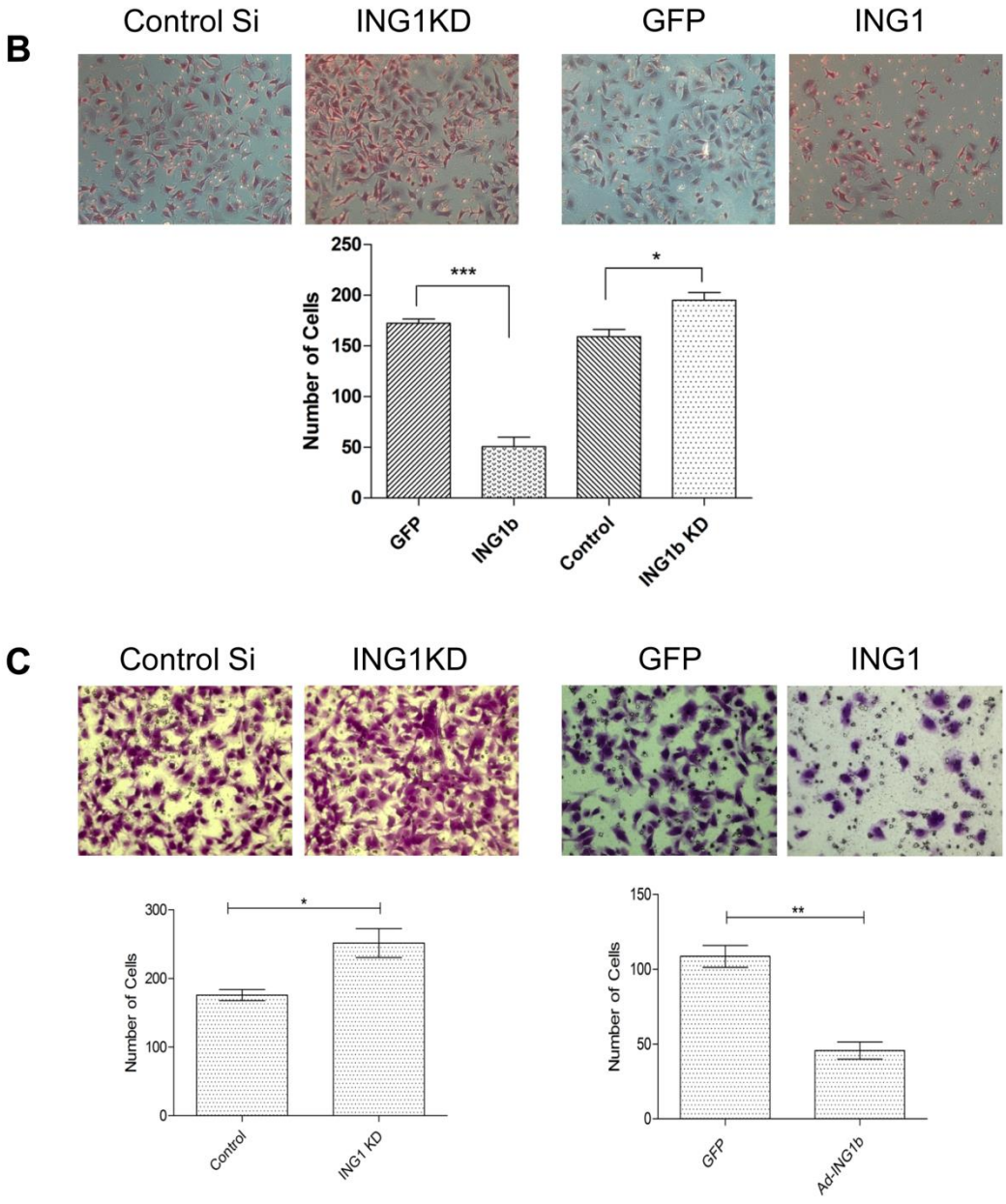

(**B**) Representative images and quantification from transwell migration assays (n=3) and (**C**) matrigel invasion assays upon ING1 overexpression or knockdown in MDA-MB231 cells (n=3; *p<0.05, ***p<0.001).

Figure 18: ING1 inhibits invasion of HS68 fibroblasts.

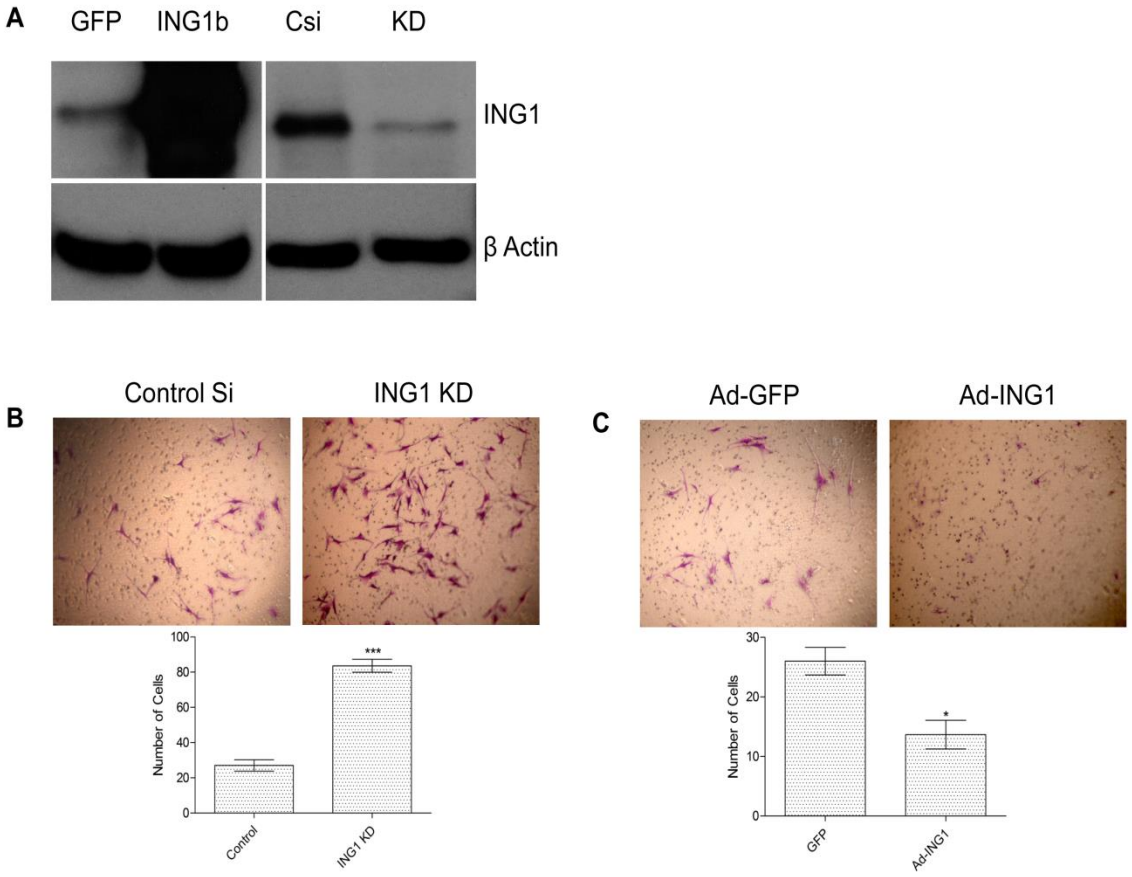

(**A**) Western blot analysis of extent of ING1 expression or knockdown in HS68 cells. (**B**)Representative images of matrigel invasion assays upon ING1 overexpression or knockdown in HS68 cells.

3.2.5 Mechanism of metastasis inhibition by ING1

To identify mechanisms potentially responsible for altered invasive ability of MDA-MB231 cells upon changing ING1 protein levels, we quantified expression of various EMT related genes that were also regulated by ING1 (Yang *et al*, manuscript in preparation). The PDGF/PDGFR pathway was of particular interest because of its established role in promoting metastasis in various types of cancers (Jechlinger, Sommer et al. 2006; Schito, Rey et al. 2012) and our initial microarray results showed that PDGFRA was the most highly downregulated gene. To test the effects of ING1 on PDGF signaling, ING1 was overexpressed or knocked down to levels seen in figure 19A. Both PDGF A and PDGFR B mRNA were upregulated by knockdown of ING1 as assessed by quantitative real time PCR (Figure 19B). It was also observed that PDGF-AA/AB protein levels were increased in the conditioned media of the ING1 knockdown cells as compared to control cells (Figure 19C). These data indicate that ING1 knockdown activates the PDGF/PDGFR pathway, which increases motility and invasiveness (Schito, Rey et al. 2012).

Figure 20 shows the results of examining the expression of other genes implicated in metastasis. We noted that these all show insignificant changes in expression upon modulating ING1 levels in MDA-MB231 cells, highlighting the magnitude of ING1 regulation of PDGFA and PDGFRB.

Figure 19: ING1 affects the PDGF/PDGFR pathway.

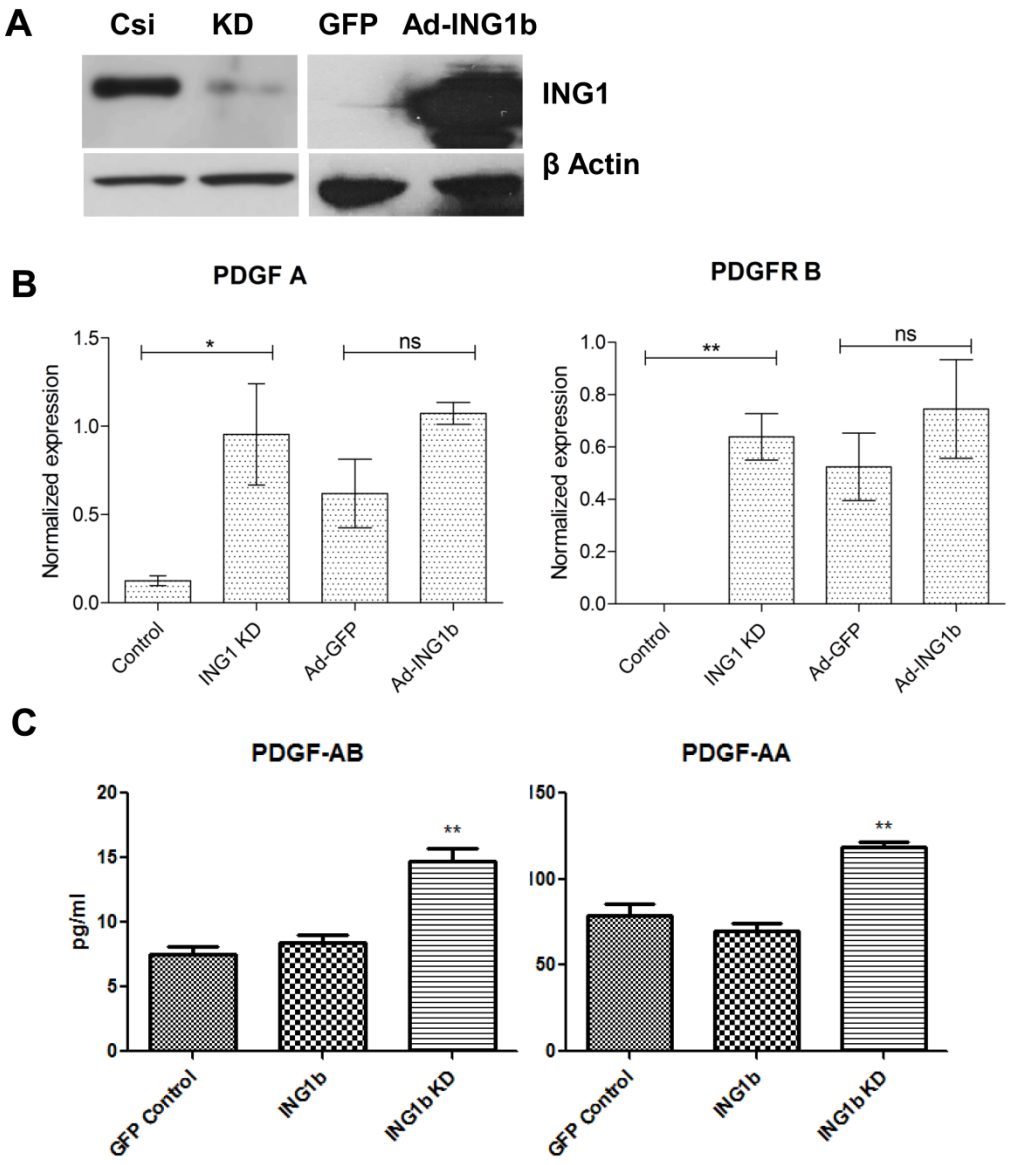

(**A**) Representative western blot image showing levels of ING1 protein upon knockdown using siRNA and overexpression using an adenoviral construct encoding GFP and ING1 under separate promoters. (**B**) Expression of PDGF-A and PDGFR-B in MDA-MB231 cells upon ING1 overexpression or knockdown as determined by Q-RT PCR (n=3; *$p<0.05$, **$p<0.001$). (**C**) Amount of PDGF AB/AA protein present in the media supernatant of ING1 overexpressing or knockdown MDA-MB231 cells determined by ELISA (**$p<0.001$).

Figure 20: Other genes tested for change in expression upon modulating ING1 expression in MDA-MB231 cells.

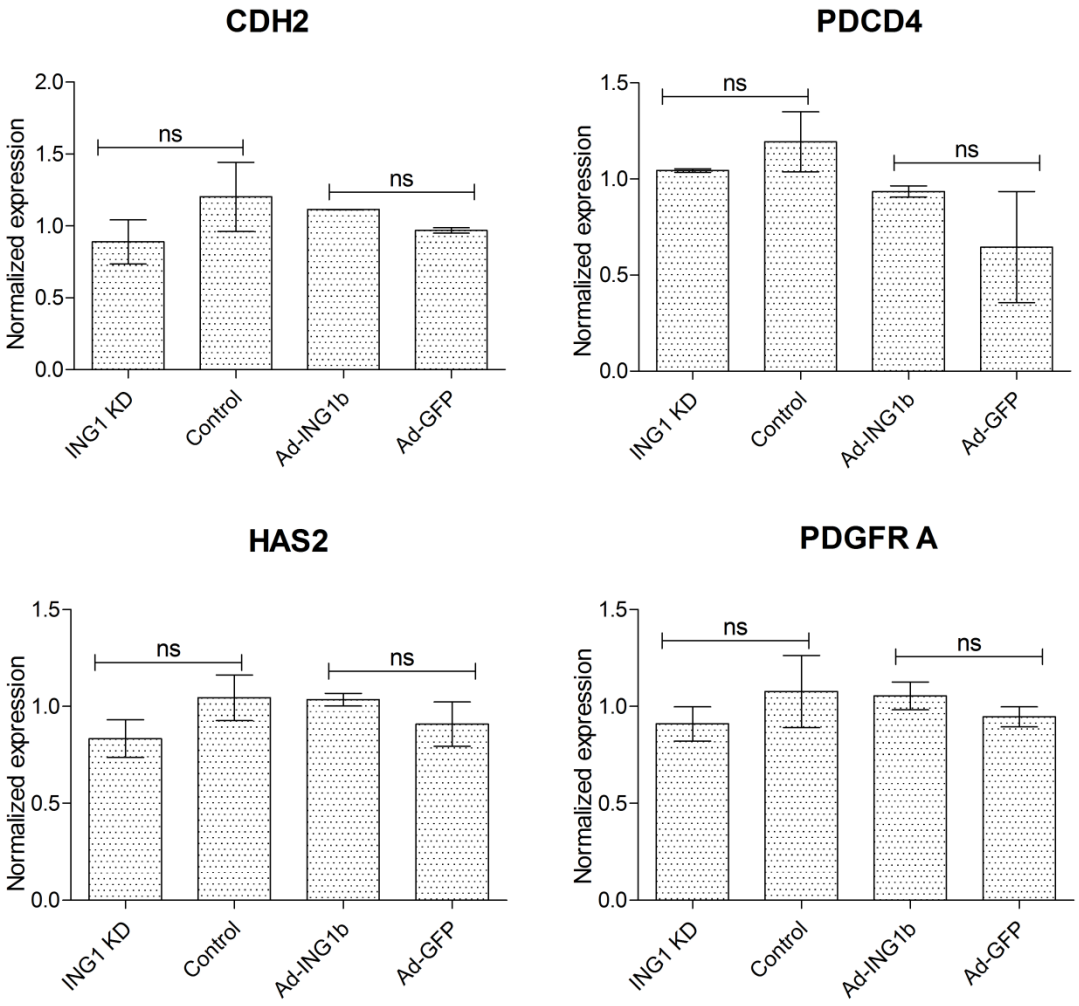

3.2.6 ING1b overexpression inhibits the development of metastases and improves survival

Given the results of the *in vitro* experiments, ING1b overexpression in highly metastatic MDA-MB231-luc2 cells might also reduce the development and progression of MDA-MB231 metastasis *in vivo*. To test this, MDA-MB231-luc2 cells were infected with adeno-ING1b GFP or adeno-GFP for 24 hours at the same MOI. The cells were then injected into the arterial circulation of NIH-III (*nu/nu; beige/beige*) mice. To monitor location and growth of metastatic tumors, bioluminescence imaging (BLI) was carried out at 7, 14, 21 and 28 days post-tumor cell inoculation in both control and ING1b overexpressing groups (Figure 21A-B). While metastatic burden as estimated by bioluminescence increased in the control group of mice from day 7 (1.3×10^6) to 28 (2.2×10^9) by ~1700-fold, the ING1b mice showed dramatically reduced bioluminescence levels with bioluminescence increasing ~24-fold (3×10^6 to 7.3×10^7) in the same time frame for an overall ~70-fold reduction ($p<0.001$). ING1b overexpressing mice also had fewer metastatic sites when compared to controls (Figure 21C; $p=0.0001$). Notably, only 3 out of 12 mice in the ING1b overexpressing group developed a single metastatic site per mouse whereas 2-5 metastatic sites per mouse were found in the control group. ING1b overexpressing mice also showed enhanced survival compared to the control mice (Figure 21D; $p<0.0001$).

Figure 21: ING1b overexpression inhibits metastasis *in vivo* and improves survival.

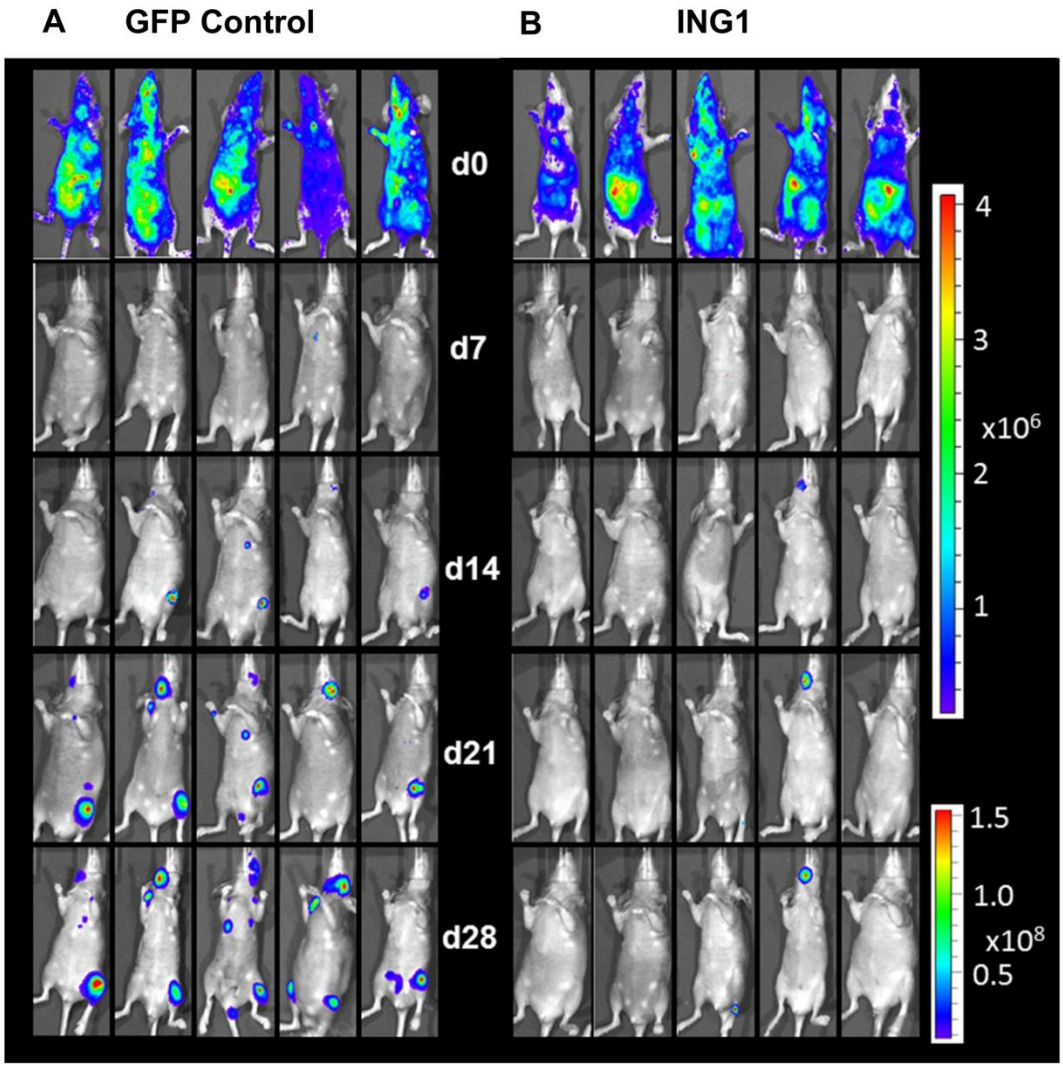

Representative ventral bioluminescence images (BLI) taken on days 0, 7, 14, 21 and 28 from mice injected with control MDA-MB-231-luc2 cells (**A**) or ING1b overexpressing MDA-MB-231-luc2 cells (**B**). Subsets of mice were sacrificed between days 28-35 due to ethics guidelines for permissible tumour burden.

ING1b overexpression inhibits metastasis *in vivo* and improves survival. (contd.)

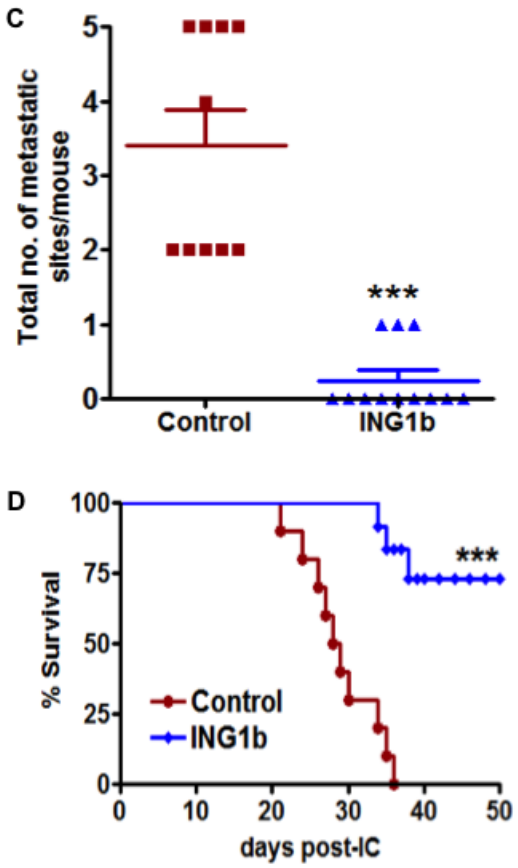

(**C**) Scatter dot plot showing total number of metastatic sites per mouse in ING1b overexpressing group (n=12) compared to controls (n=10; p=0.0001). (**D**) Kaplan–Meier survival curve showing overall survival for ING1b overexpressing group of mice (n=12) compared to GFP controls (n=10, log-rank test ***p<0.001).

3.2.7 ING1b overexpression completely blocks the development of knee metastases

MDA-MB231-luc2 cells used in this study have a strong propensity to generate knee osteolytic metastases (Bondareva, Downey et al. 2009). Bioluminescence imaging (BLI) of these mice show that unilateral or bilateral knee metastases develop within 2-3 weeks (Figure 21A). Representative knee regions of interest (ROI) from control and ING1b overexpressing mice are shown in figure 22A. BLI quantification of knee ROI revealed that there was no increase in photon emission in the ING1b overexpressing mice for the entire duration of the experiment, which sharply differed from control mice (Figure 22B; $p<0.001$). 3D μCT imaging of knees from the control group confirmed extensive bone osteolytic damage from metastases compared to the ING1b overexpressing group of animals (Figure 22C). Similarly, trichrome staining of control knee bones showed the presence of large tumors, while no tumors were apparent in the knee bones of ING1b mice (Figure 22D). ING1b overexpression resulted in the complete inhibition of tumor-induced bone osteolysis and a consistent preservation of bone integrity as assessed by bone parameters, bone volume divided by total volume (BV/TV), cortical bone volume divided by total volume (Ct BV/TV) and bone mineral density (BMD) (Figure 22E).

Figure 22: ING1b completely blocks the initiation and progression of knee metastasis.

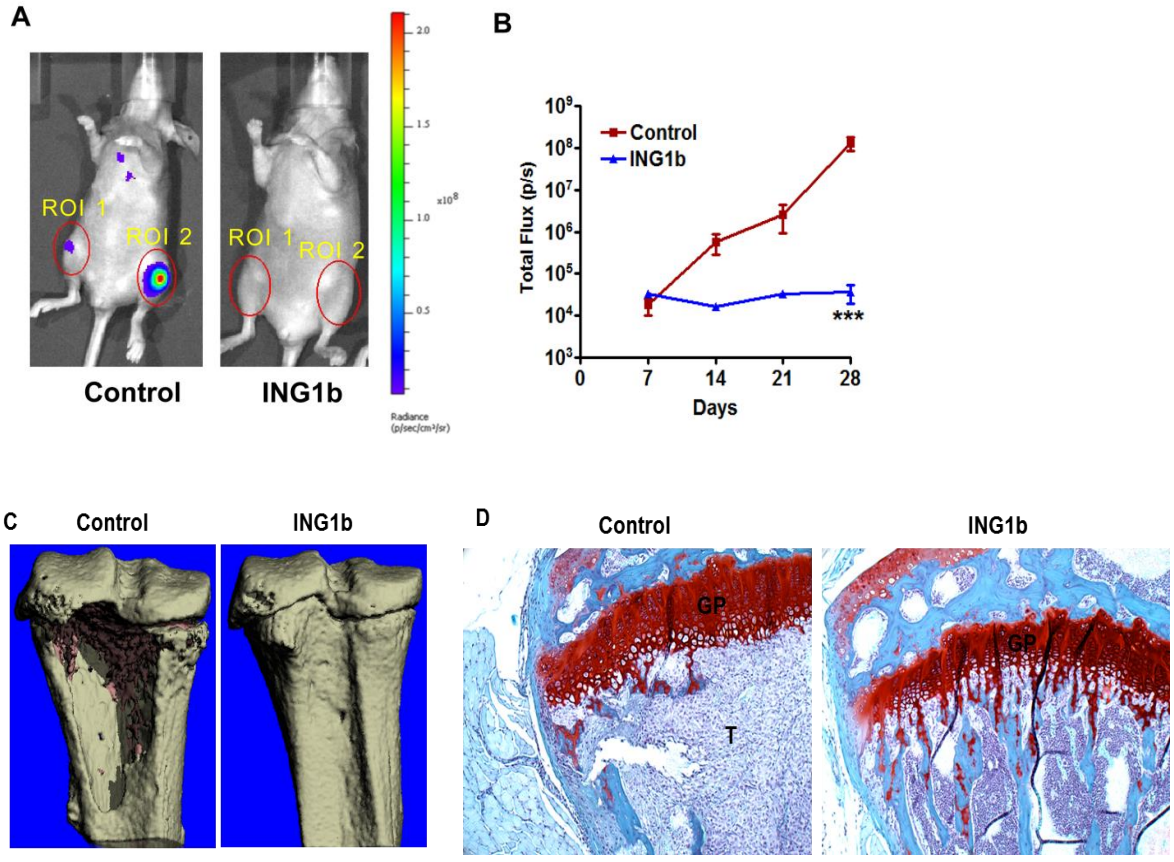

(**A**) Representative ventral BLI are shown from control and ING1b overexpressing mice to visualize differences in knee metastasis between these groups. Combined regions of interest (ROI 1+ ROI 2) are shown with red circles over the knees. (**B**) A line graph showing combined knee bone metastatic growth comparison between control and the ING1b overexpressing group showing complete inhibition of knee metastasis progression in the ING1b group of mice (***$p<0.001$). (**C**) Representative μCT images from the proximal tibia of control and ING1b overexpressing mice. Extensive tumor-induced cortical bone loss is seen in the control group of mice compared to ING1b overexpressing mice where no bone loss was observed. (**D**) Histology of knee bone stained with trichrome. Control bone displays a large tumor (T=tumor area) whereas bone from an ING1b overexpressing mouse shows no tumor (GP=growth plate).

ING1b completely blocks the initiation and progression of knee metastasis. (contd.)

E

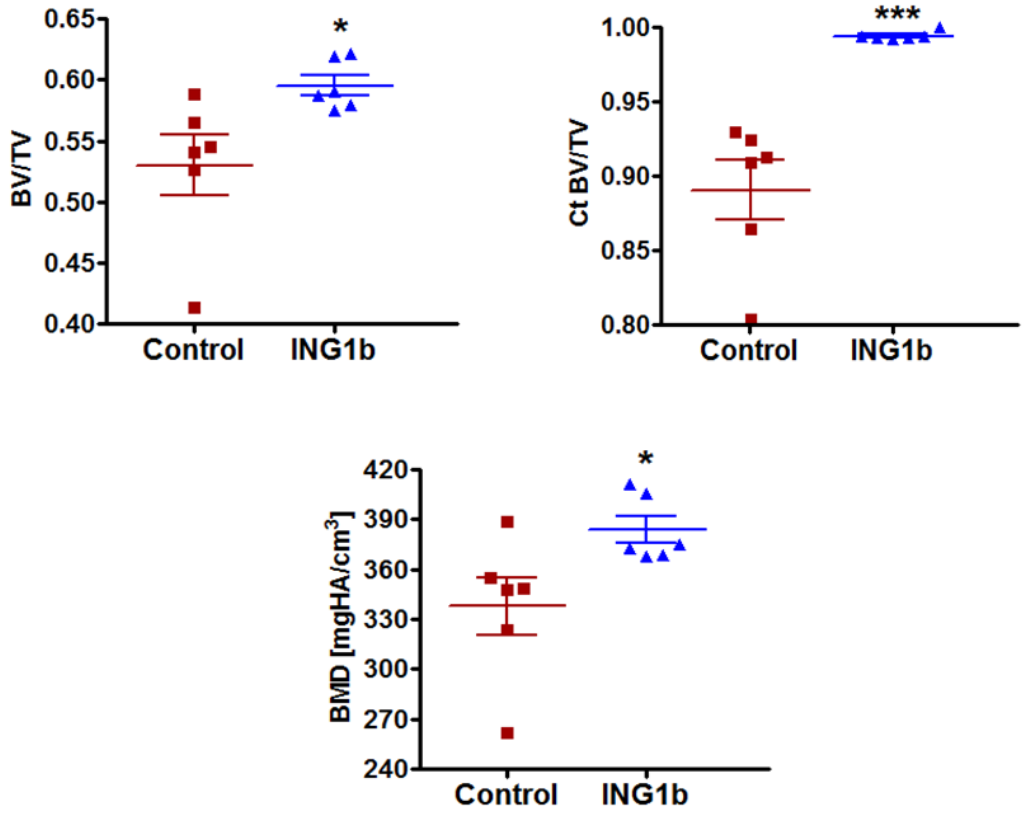

(**E**) µCT bone parameter analysis of control and ING1b overexpressing groups of mice showing data on bone volume/total volume (BV/TV), Cortical bone volume/total volume (Ct BV/TV) and bone mineral density (BMD) (n=6 per group; * $p<0.05$; *** $p<0.001$).

3.3 Stromal expression of ING1 correlates with of breast cancer patient survival

3.3.1 Stromal ING1 expression in breast cancer patient samples

ING1 protein level was measured using quantitative fluorescence immunohistochemistry on the HistoRx AQUA® platform in breast cancer patient samples from the Calgary Tamoxifen cohort as described previously. The specificity of the ING1 monoclonal antibody used for fluorescence IHC was assessed in HEK293 cells and placental tissue (Figure 15 A and duplicated in Figure 23A top panel). The patient samples were also stained with anti-pan cytokeratin and anti-vimentin antibodies to specifically demarcate the tumor region from the stromal region respectively. As our focus was on the expression of ING1 protein in the stromal region of breast cancer patients, we used the expression of ING1 in the vimentin positive region of normal breast tissue sample as our baseline control (Figure 23B top panel). The ING1 localization was found to be primarily nuclear in these regions with a mean AQUA score of 109 which was used as a cut point to dichotomize patients. In breast cancer patient samples, varying levels of ING1 expression were found in the stromal (vimentin positive) regions which were quantified and then used for classifying patients with low stromal or high stromal ING1 expressing tumors.

Figure 23B middle panels shows a representative images of a sample with low stromal ING1 expression (AQUA score 25.6) and the bottom row of panels show representative images of a patient sample with high stromal ING1 expression (AQUA score 291).

Figure 23: Immunohistochemical staining and quantitation of stromal ING1 using the HistoRx AQUA platform.

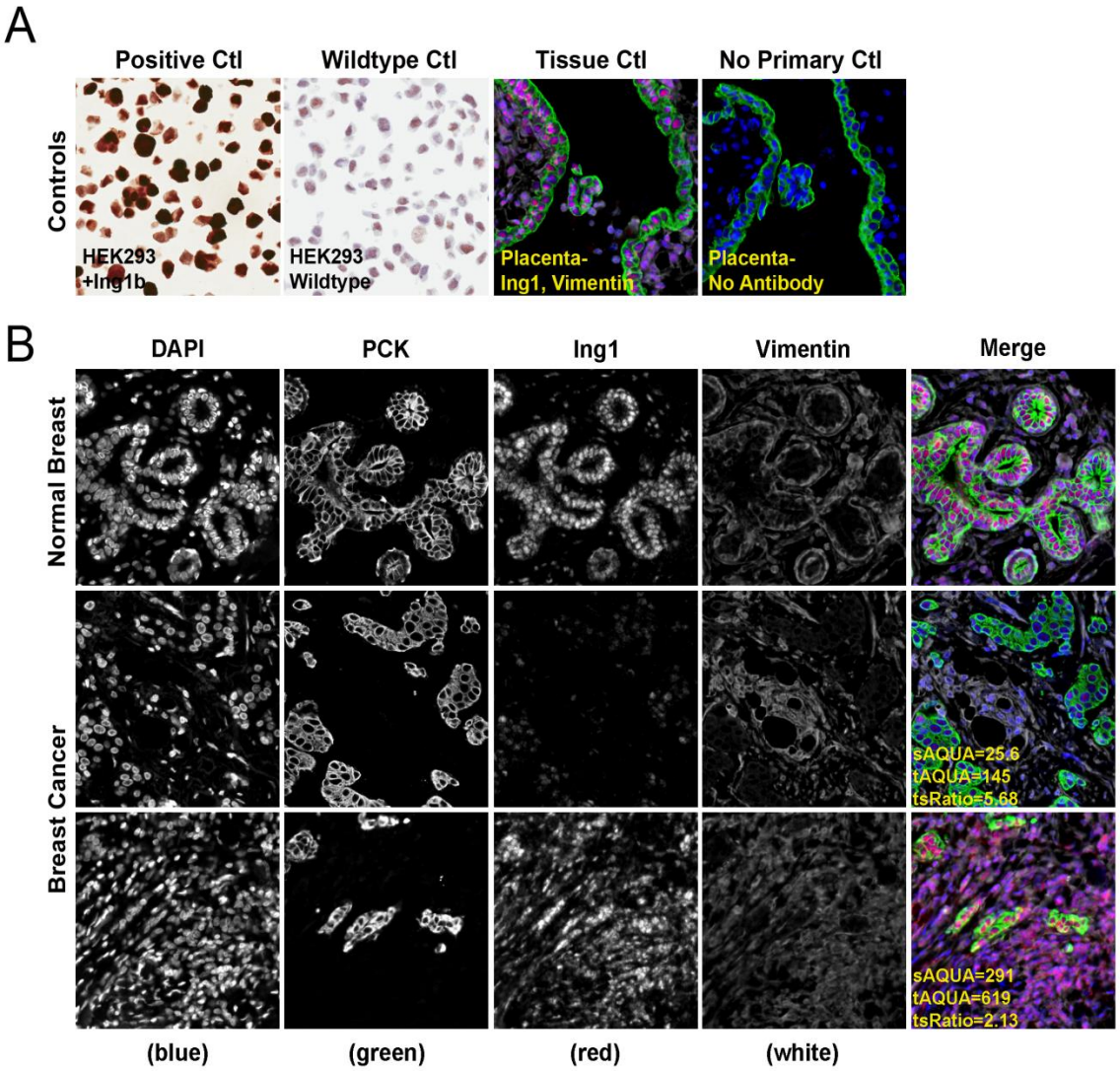

(A) Representative images showing specificity of the ING1 monoclonal antibody in HEK293 cells and HEK293 cells overexpressing ING1 (left panels) and in placenta treated with or without the ING1 antibody (right panels). (**B**) Representative examples of quantitative fluorescent IHC images for ING1 expression in normal breast tissue (top row of panels) and breast cancer tissue (two bottom rows of panels). tAQUA scores represent the expression level of ING1 within the pan-cytokeratin defined epithelial/tumor compartment; sAQUA scores represent expression level of ING1 in the vimentin defined mesenchymal/stromal compartment. DAPI-stained nuclei are depicted in blue, pan-cytokeratin stained epithelial/tumor cells are depicted in green, ING1 protein expression is depicted in red and vimentin stained mesenchymal/stromal cells in white.

3.3.2 Prognostic value of stromal ING1 expression in breast cancer patients

As described previously, the cohort tested in this study has patients classified into luminal breast cancer (ER positive and Her2 negative, n=430) and non-luminal breast cancer (ER negative or Her2 positive, n=32) groups for analysis. We tested the prognostic value of stromal ING1 expression in both the above mentioned populations. ING1 levels in the vimentin positive normal breast tissue (ING1=109) was used as a cutoff to further dichotomize the populations into low stromal (ING1<109) and high stromal (ING1>109) ING1 expressers.

Contrary to the observations made with ING1 expression in the tumor compartment, significant results were obtained in the luminal group. In this group, stromal ING1 expression correlated with clinico-pathological characteristics like tumor grade (p=0.001) and tumor size (p=0.020) whereas the non-luminal group did not show correlation to any of the clinic-pathological characteristics listed in table 5. High stromal ING1 expression in the luminal group also correlated to poor survival outcomes in patients as indicated by Kaplan Meier analysis. This observation was made in both survival outcomes, including disease free survival (Figure 24B, p=0.0001) and disease specific overall survival (Figure 24E, p=0.0076). Interestingly, no differences in survival outcomes were seen in this analysis in the non-luminal group dichotomized by ING1 expression (Figure 24C, 24F) which previously has shown that higher ING1 expression in the tumor compartment could predict better survival outcome for breast cancer patients. This observation suggests that ING1 expression level in tumor and stromal regions could specifically predict survival of patients having different types of breast cancers.

Next, a Cox proportional hazards model was used to assess the independent prognostic value of stromal ING1 in the cohort. This analysis was performed to determine if any of the clinically relevant biomarkers along with stromal ING1 levels has a strong prognostic/predictive ability regarding disease free survival in the cohort. Established biomarkers such as tumor grade, tumor size, lymph node status, ER levels and HER2 status were included in the multivariate model along with stromal ING1 levels since these variables are routinely used by physicians when making treatment decisions in the clinic. The variables included in the analysis were compared for their hazard ratio (HR) which indicates the prognostic power of a given biomarker. In the analysis, tumor grade [HR 2.741, p=0.002], lymph node status [HR 3.505, p<0.001] and stromal ING1 [HR 2.320, p=0.002], were significantly and independently associated with disease free survival in ER+/HER2- population (Table 6). This suggests that stromal ING1 levels are equal in predictive power to the established variables of tumor grade and lymph node status.

Table 5: Association of clinico-pathological characteristics of ER+/HER2- breast cancer patients with levels of ING1 in the stroma.

Characteristic	# of Cases (%)	ER+/Her2-		
		Low Ing1	High Ing1	p-value
Age				
< 53	72 (16.25)	56	16	0.880
≥ 53	371 (83.75)	284	87	
Menopausal Status				
Pre-Menopausal	26 (5.90)	17	9	
Peri-Menopausal	21 (4.70)	18	3	
Post-Menopausal	321 (72.50)	242	79	0.231
n/a (male)	1 (0.20)	1	0	
Unknown	74 (16.70)	62	12	
Stage				
I	188 (42.40)	148	40	
II	138 (31.20)	105	33	
III	36 (8.20)	24	12	0.365
IV	5 (1.10)	3	2	
Unknown	76 (17.20)	60	16	
Tumor Grade				
1	103 (25.40)	88	15	
2	247 (60.80)	195	52	0.001*
3	56 (13.80)	31	25	
Tumor Size				
< 2cm	223 (53.86)	179	44	0.020*
≥ 2cm	191 (46.14)	137	54	
Lymph Node Status				
Negative	278 (72.77)	220	58	0.103
Positive	104 (27.23)	74	30	
Rx Tamoxifen				
No	161 (37.44)	118	43	0.196
Yes	269 (62.56)	212	57	

The listed clinico-pathological characteristics were analyzed for their correlation with low/high levels of stromal ING1. Stromal ING1 shows a correlation with tumor grade and size in the ER+/ Her2- group of patients in the cohort.

Figure 24: Kaplan-Meier survival analysis (stromal ING1).

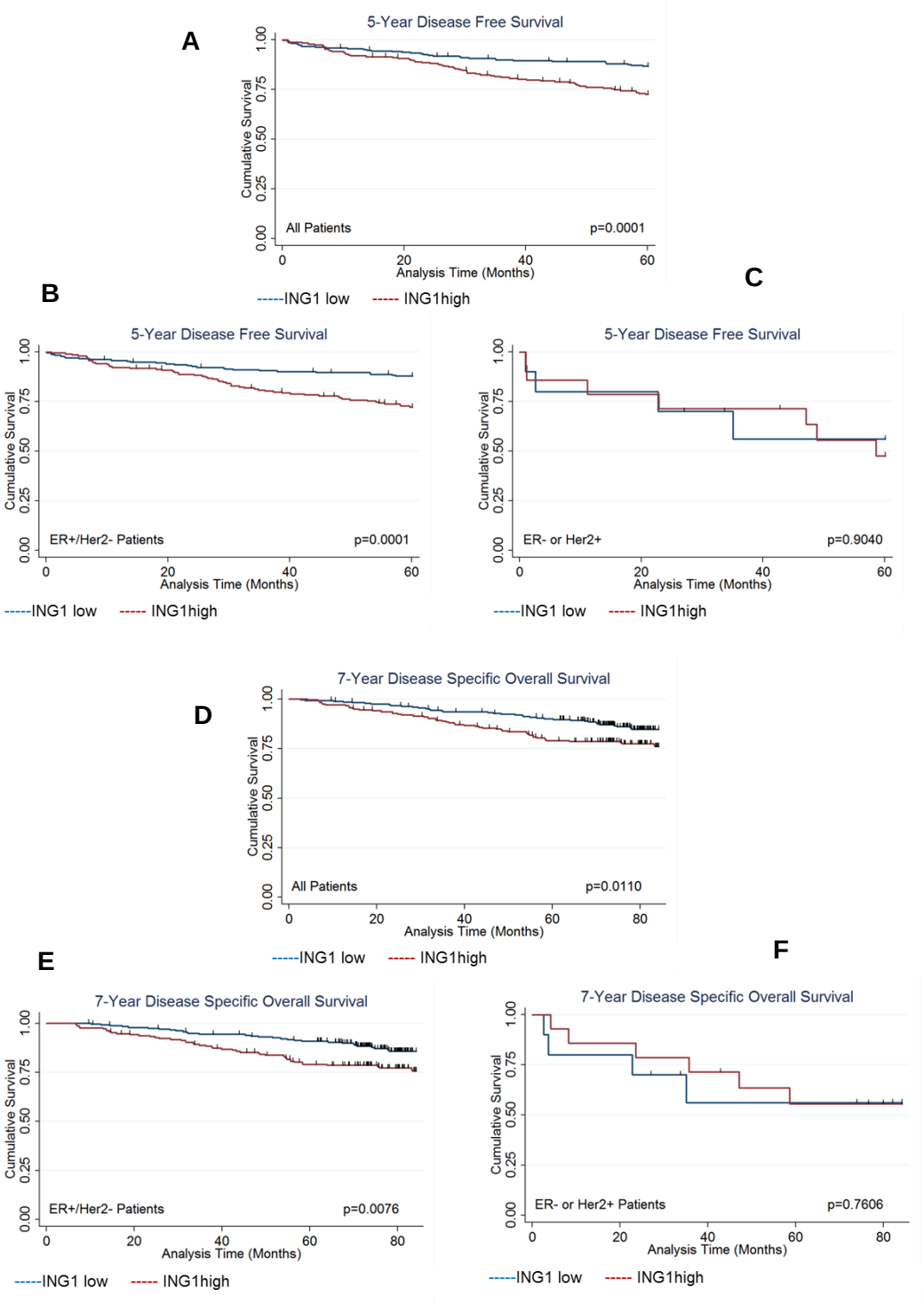

(**A-C**) Kaplan-Meier survival curves for Disease free survival (**A**) in total population (**B**) ER+/HER2- group (**C**) ER- or HER2+ group. (**D-F**) Kaplan-Meier survival curves for Disease specific overall survival (**D**) in total population (**E**) ER+/HER2- group (**F**) ER- or HER2+ group.

Table 6: Multivariate analysis of Disease free survival.

All Patients

Variable	Hazard ratio	Std. error	p value	95% CI
Tumor Grade	2.741	0.738	<0.001	1.618 – 4.647
Tumor Size	1.431	0.389	0.188	0.840 – 2.437
Lymph node Status	3.505	0.881	<0.001	2.142 – 5.737
ER	0.360	0.143	0.010	0.165 – 0.785
HER2	1.669	0.997	0.391	0.518 – 5.383
Stromal ING1	2.125	0.558	0.004	1.270 – 3.557

ER+/HER2- Patients

Variable	Hazard ratio	Std. error	p value	95% CI
Tumor Grade	2.447	0.721	0.002	1.374 – 4.358
Tumor Size	1.401	0.398	0.236	0.802 – 2.446
Lymph node Status	3.429	0.931	<0.001	2.014 – 5.839
Stromal ING1	2.320	0.636	0.002	1.356 – 3.969

Multivariate analysis of clinically relevant biomarkers along with stromal ING1. Stromal ING1 level is a significant and independent biomarker in the total population and ER+/HER2- sub-population in the Calgary Tamoxifen Cohort.

3.3.3 ING1 regulates levels of cytokines produced in mammary fibroblasts

In the stroma, fibroblasts are the most abundant cell type and are the most active cellular component of cancer associated stroma (Olsen, Moreira et al. 2010). They are believed to play active roles in the promotion of processes like angiogenesis, metastasis and overall tumor growth through expressing various paracrine factors. As high stromal ING1 expression significantly correlated with poor patient survival in the breast cancer cohort tested in this study, we next wanted to determine what cytokines might be regulated by ING1 in the stroma. In order to determine this, ING1a was overexpressed using adenoviral vectors in the human mammary fibroblast cells (HMF3s) and the conditioned media from these cells was collected and analyzed for various cytokines/chemokines using an ELISA based assay. ING1a was chosen since it is believed that senescing stromal cells contribute to the induction of cancers *in vivo* and we here found that of the ING1 isoforms, ING1a is most effective in inducing cellular senescence (Soliman, Berardi et al. 2008). Figure 25A shows several cytokines that showed a significant decrease in levels upon ING1a overexpression compared to GFP overexpressing HMF3s cells. In contrast, some cytokines in the panel were upregulated upon ING1a overexpression (Figure 25B) leaving interpretation of ING1a effects unclear.

Tumor associated stroma is also known to produce a plethora of matrix metalloproteases (MMPs), which act on the cell surface of cells and help tumor cells to invade surrounding tissue and metastasize to distant regions to form secondary tumors. Taking this into consideration, we tested for changes in the levels of various MMPs and their inhibitors, tissue inhibitors of metalloproteases (TIMPs). There were significant changes in the amount of all MMPs examined in HMF3s cells overexpressing ING1a,

with simultaneous decrease in the levels of inhibitory TIMPs. Figure 26 shows the MMPs and TIMPs which show a significant change in levels with respect to ING1 overexpression in HMF3s cells. With the exception of MMP-2, all other MMPs increased in levels while TIMPs decreased in cells overexpressing ING1a, consistent with ING1 playing an active role in invasion and metastasis.

Figure 25: Cytokine profile of HMF3s upon ING1a overexpression.

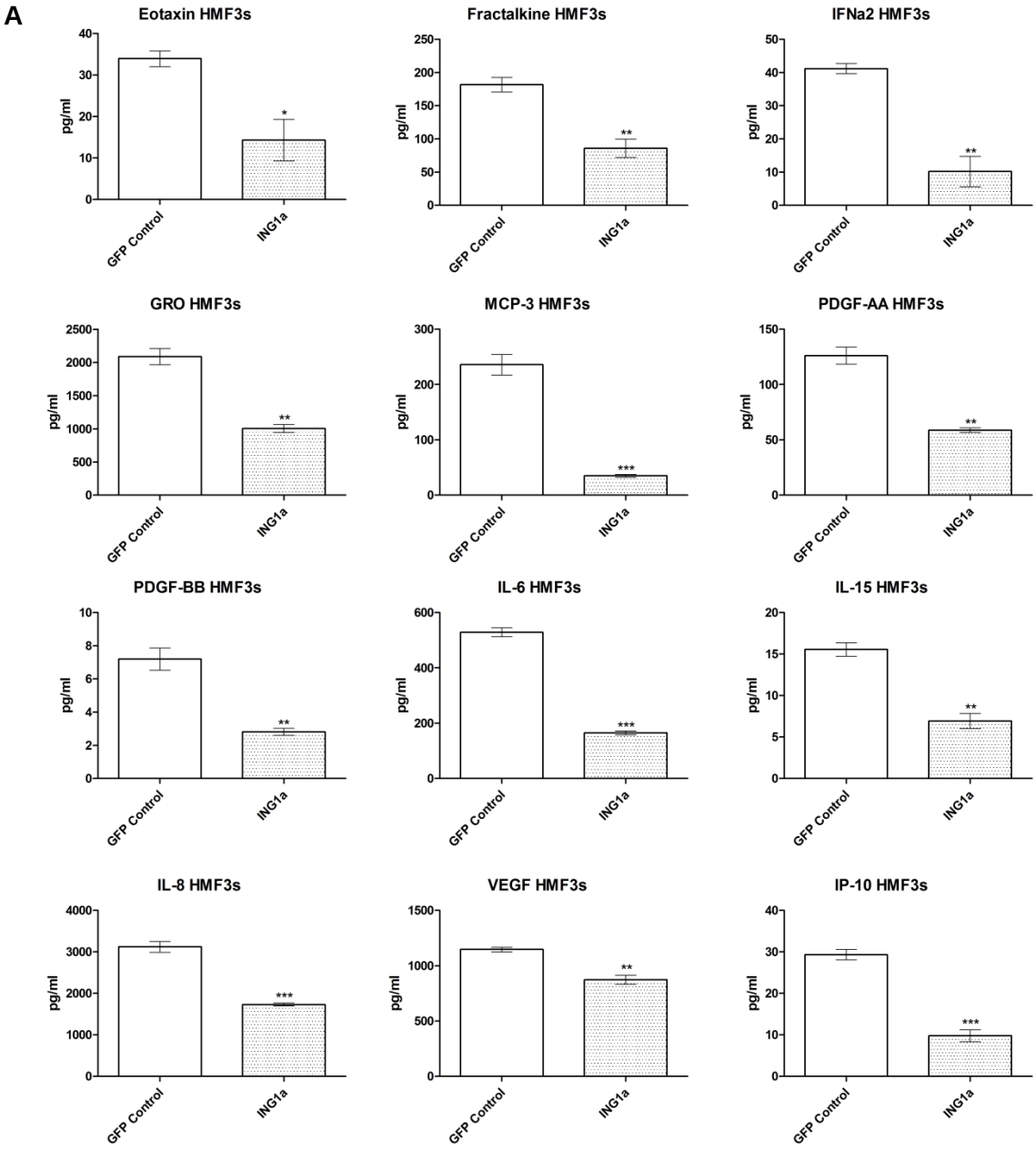

(**A**) Cytokines showing decrease in concentration upon ING1a overexpression in HMF3s cells as compared to GFP control (n=3; * $p<0.05$; ** $p<0.001$; *** $p<0.0001$).

Cytokine profile of HMF3s upon ING1a overexpression. (contd.)

B

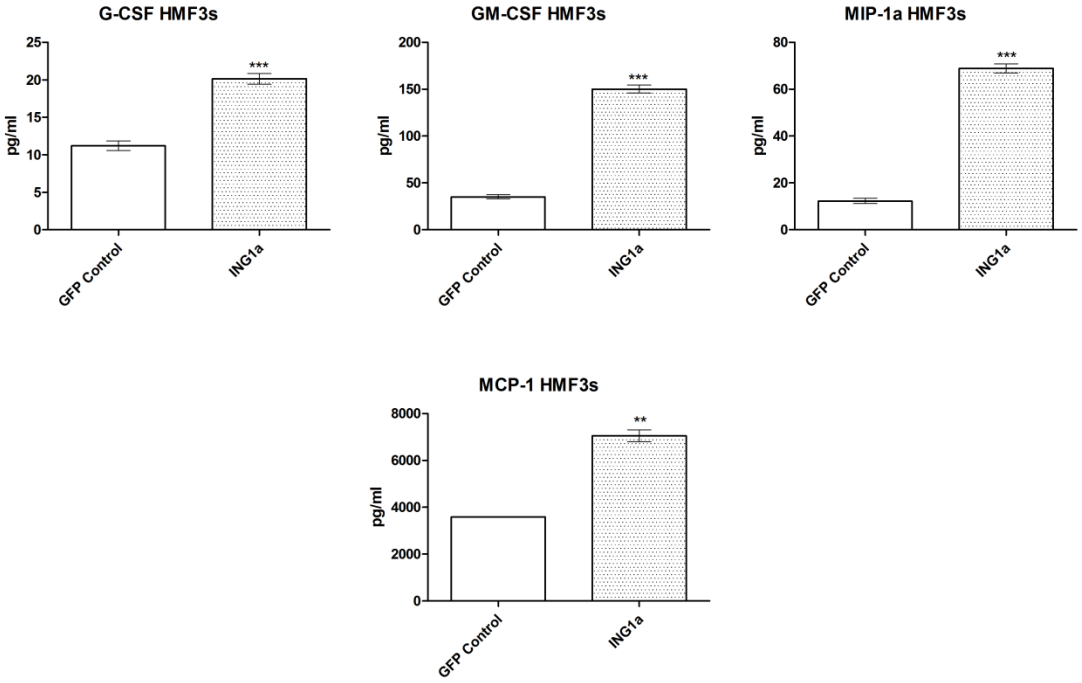

(**B**) Cytokines showing increase in concentration upon ING1a overexpression in HMF3s cells as compared to GFP control (n=3; ** $p<0.001$; *** $p<0.0001$).

Figure 26: MMPs/TIMPs regulated by ING1a in HMF3s cells.

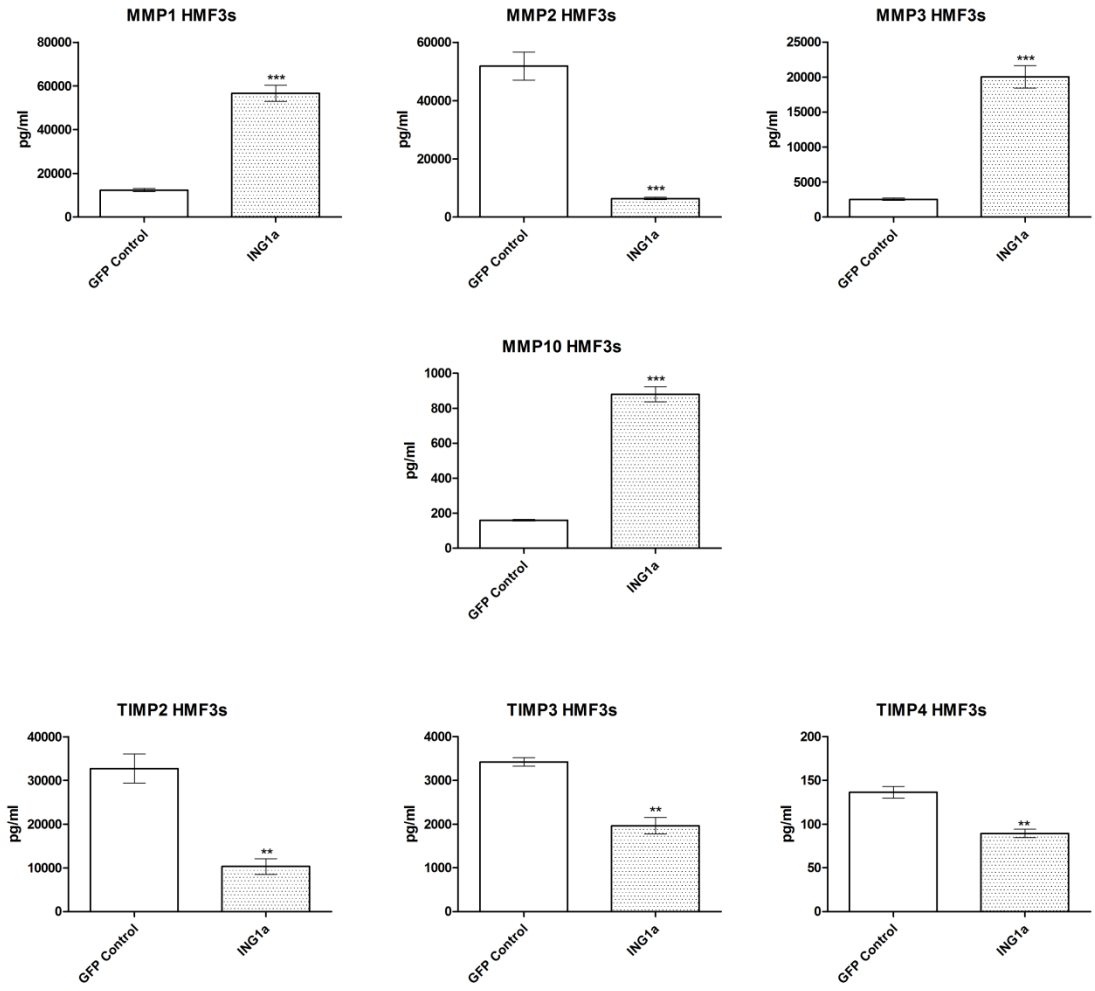

MMPs and TIMPs showing significant change upon ING1a overexpression in HMF3s cells (n=3; ** $p<0.001$; *** $p<0.0001$).

3.3.4 Functional assay for MMPs regulated by ING1a in HMF3s cells

Since we saw a significant change in the levels of MMPs released by HMF3s cells upon ING1a overexpression, our next experiment was to determine the functional activity of the MMPs produced. The activation of MMPs is believed to be a key feature in inducing tumor invasiveness and metastasis both *in vitro* and *in vivo* and both *MMP-1* and *MMP-2* have been identified as genes associated with the ability of human breast cancer cells to metastasize spontaneously to the lungs in immune deficient mice (Minn, Gupta et al. 2005). In another study involving a mammary fat pad rat xenograft model, expression of MMP-1 in stromal fibroblasts was shown to confer high invasion potential to breast carcinoma cells (Boire, Covic et al. 2005).

Using zymography analysis, we determined the caseinolytic and gelatinolytic activity of MMP-1 and MMP-2 respectively in cells expressing ING1a. Results obtained from this experiment were in line with the results from ELISA based analysis as conditioned media from HMF3s cells overexpressing ING1a had greater MMP-1 activity compared to media from untreated cells and GFP only expressing cells (Figure 27). Similar to our previous observations, the activity of pro-MMP-2 was reduced in the conditioned media from ING1a overexpressing HMF3s cells in comparison to control and GFP expressing cells.

Figure 27: Zymography for MMP-1 and MMP-2.

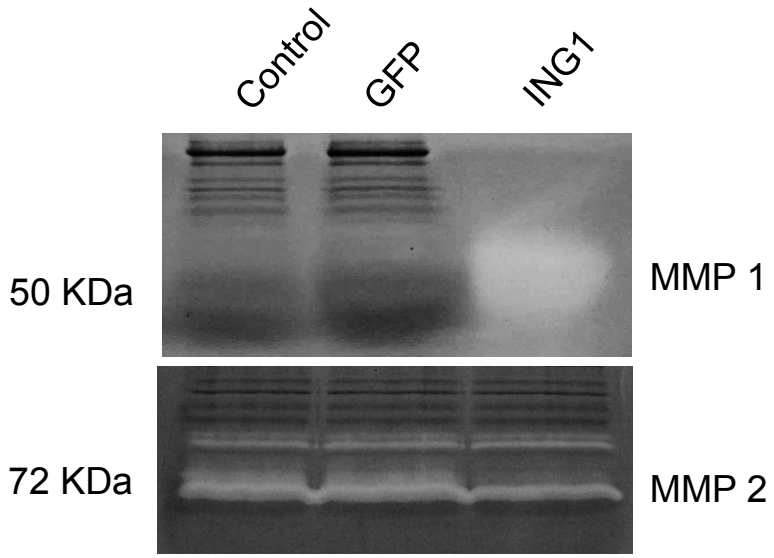

Zymographs depicting caseinolytic and gelatinolytic activity of MMP-1 and MMP-2 respectively in HMF3s cells.

3.3.5 ING1a overexpressing HMF3s cells induce disorganization of breast cancer cell derived organoids

In a physiological setting, cancer associated fibroblasts in the stroma are believed to release factors that help tumor cells to invade surrounding tissue, metastasize or divide more rapidly. In order to recapitulate this physiological phenomenon *in vitro* we employed a three dimensional culture system in which cells from an ER+ breast cancer cell line MCF7, and HMF3s fibroblast cells expressing ING1a, were grown separately in the context of matrix support to provide an environment that more closely reflects an *in vivo* setting. We then co-cultured MCF7 and HMF3s expressing ING1a in order to test whether paracrine factors released by HMF3s upon ING1a overexpression could affect organoids formed by MCF7.

The organoids derived from both MCF7 and HMF3s cells were monitored at distinct time intervals by phase contrast microscopy. Non-transformed mammary epithelial cells are known to form spheres with lumens in three-dimensional cultures, that mimic mammary gland tissue (Debnath and Brugge 2005). We found that both MCF7 as well as control HMF3s cells expressing GFP formed filled spheres (Figure 28A-B) in culture. This observation is expected with MCF7 being a breast cancer cell line derived from a metastatic site and the HMF3s fibroblast cell line being of mesenchymal origin. HMF3s cells overexpressing ING1a cultured alone also formed filled spheroids which were considerably smaller in size than those formed by MCF7 and GFP expressing HMF3s cells when cultured alone (Figure 28C).

Three dimensional culture assays allow phenotypic discrimination between nonmalignant and malignant mammary cells. Nonmalignant cells grown in a three dimensional context form growth arrested acinus-like colonies, whereas malignant cells form disorganized colonies that continue to proliferate (Petersen, Ronnov-Jessen et al. 1992). Similar results were obtained when HMF3s cells overexpressing ING1a were co-cultured with MCF7 cells (Figure 28E). The colonies formed in this combination were more disorganized and distorted as compared to individual controls and when MCF7 cells co-cultured with GFP expressing HMF3s cells (Figure 28D). Taken together these data suggest that ING1a expression in mesenchymal fibroblasts induces release of certain paracrine factors which may further induce epithelial breast cancer cells to attain a more aggressive phenotype.

Figure 28: Three dimensional co-culture of MCF7 and HMF3s cells.

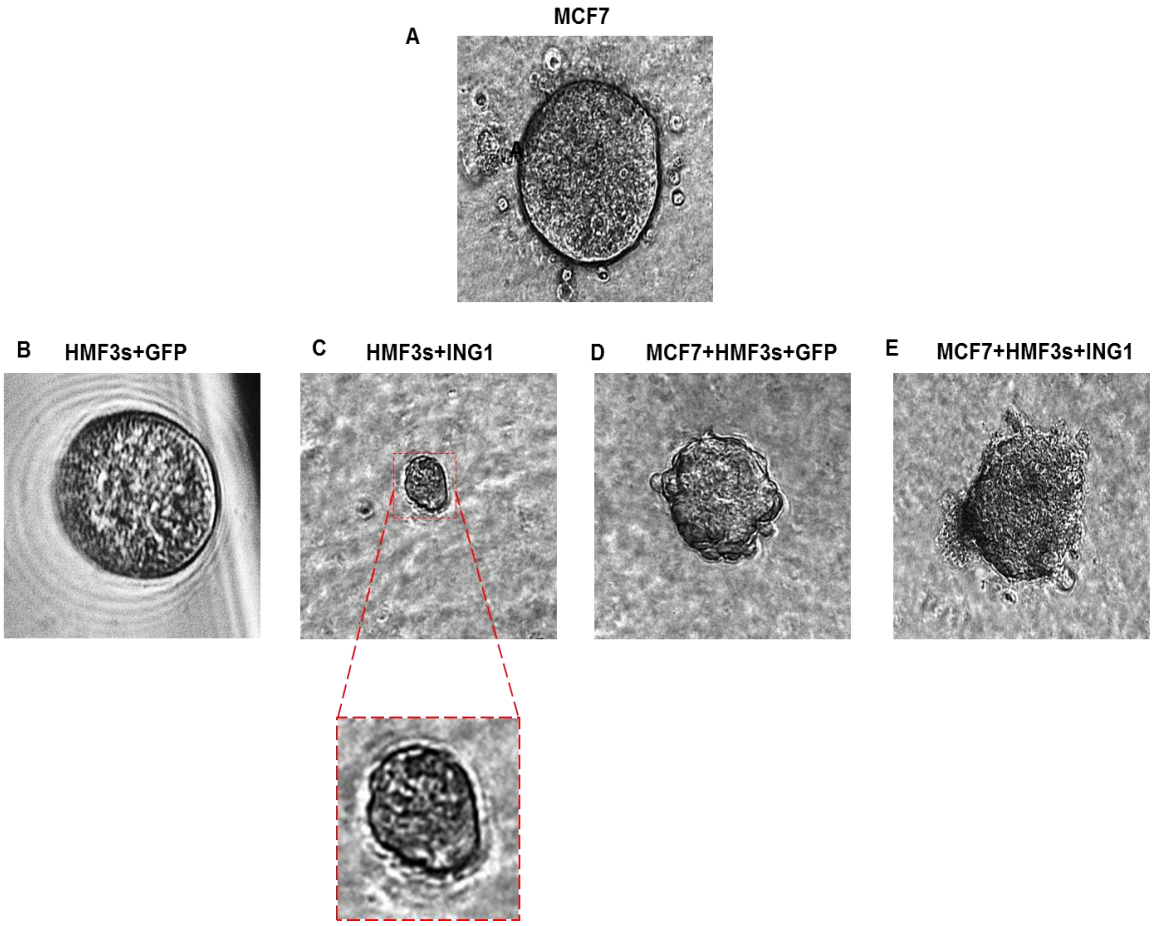

ING1a induces disorganization of MCF7 breast cancer cell-derived organoids. MCF7 or HMF3s cells were grown individually or co-cultured in Matrigel in three-dimensional cultures in ultralow attachment 96-well plates. Representative images of day 14 (**A**) MCF7 cells alone (**B**) HMF3s cells expressing GFP (**C**) HMF3s cells expressing ING1a; inset magnified spheroid (**D**) MCF7 cells co-cultured with GFP expressing HMF3s cells (**E**) MCF7 cells co-cultured with HMF3s cells expressing ING1a captured by digital camera phase contrast microscopy.

CHAPTER 4: DISCUSSION

4.1 ING1 and 5-Azacytidine Act Synergistically to Block Breast Cancer Cell Growth

In this study we have found that ING1b and ING2 proteins differentially induce cell death and apoptosis in breast cancer cell lines compared to normal breast epithelial cells. This activity does not depend upon the status of p53 or HER2/neu levels, but increased efficiency was seen in cells that were ER negative. In contrast to the lack of synergy and even antagonism seen when using the chemical agents 5azaC and LBH589 to target two distinct epigenetic pathways in cancer cells, the efficiency of ING1b mediated cell death increased significantly when it was used in combination with both LBH589 and 5azaC. However, synergy was significantly greater with 5azaC, which targets a distinct epigenetic mechanism compared to ING1. Treatment with ING1b plus 5azaC induced apoptosis by several criteria, and also acted together to induce DNA damage as estimated by increased levels of γH2AX. This combination also inhibited tumor growth in subcutaneous xenograft tumors in mice. The MOI that was optimal for elimination of cells *in vitro* when used with 5azaC (MOI = 30; Figure 11) was insufficient to completely block tumor growth *in vivo*, although an MOI of 90 was able to cause tumor regression with no obvious side effects. Based upon this logic of targeting different pathways, we speculate that, when used with viral constructs encoding proteins that affect DNA methylation, LBH589 would synergize better than 5azaC. Such combinations may act more effectively since both increasing histone acetylation and demethylating promoters may be needed to reactivate the expression of genes inactivated in cancer cells such as tumor suppressors involved with growth arrest and apoptosis as suggested previously (Herman and Baylin 2003).

We identified two breast cancer cell lines, SKBR3 and MDA-MB468 that are unusually sensitive to ING1-induced cell death. Both lines have mutant p53 and negative ER status, features that are characteristic of more advanced stages of breast cancer. This suggests that ING1 may preferentially target more aggressive tumors. However, other breast cancer cell lines which have p53 and ER status similar to SKBR3 and MDA-MB468, exhibited a more limited degree of apoptosis upon ING1b and ING2 overexpression indicating that other factors in the two susceptible lines contribute to their extreme sensitivity to ING-induced apoptosis. It is worth noting that the two most susceptible lines also expressed relatively higher levels of ING1 compared to other cancer lines (data not shown), but how this might be related to sensitivity is currently unknown. Future experiments to compare the gene expression profiles in response to ING1 expression in susceptible versus resistant breast cancer lines will help determine apoptotic pathways impinged upon by the ING1 protein. It may also be informative to examine other components of known ING complexes such as the members of the HDAC complexes that INGs 1 and 2 participate in (Doyon, Cayrou et al. 2006) to understand the differential sensitivity of the lines to overexpression of the INGs.

When used together, treatment of cells with 5azaC and LBH589 showed an effect greater than when each compound was used individually, but effects were less than additive suggesting antagonism, an idea borne out by high CI values on the isobologram shown in Figure 7A. In contrast, ING1b showed synergy with 5azaC and with LBH589, but significantly greater synergy was seen with 5azaC as depicted by lower CI values (compare Figures 7B&C). While the most likely explanation for this difference is that targeting two different epigenetic pathways is more effective than targeting one pathway

with two agents, this does not explain why ING1b plus 5azaC is so much more effective that 5azaC and LBH589 in inducing apoptosis. One explanation may be that the mechanism of ING1 synergy with 5azaC may go beyond effects by ING1 upon histone acetylation, consistent with our preliminary results in a separate study showing that INGs also have extranuclear effects upon apoptosis, particularly at the mitochondria (Bose, Thakur et al. 2013). It should also be noted that possible "off target" cytopathic effects resulting from usage of higher doses of 5azaC may contribute to enhanced cell death upon expressing ING1 in these cells.

To further address the underlying mechanism of this enhanced apoptosis and cell death, the expression and processing of caspase-3 and PARP were examined. Both caspase-3 and PARP are cleaved in the late "execution" apoptotic phase and the combination of ING1b and 5azaC together induced cleavage of caspase-3. ING1b also enhanced the ability of 5azaC to induce DNA damage which, when added together with activation of effectors of apoptosis, may explain the enhanced apoptosis and cell death induction by the combination of ING1b and 5azaC.

In our *in vivo* experiments, we demonstrate that a combination of ING1b plus 5azaC could suppress the growth of subcutaneous xenograft tumors in SCID mice without any significant toxicity as determined by maintenance of body weight. Moreover, the tumors did not develop any resistance when the treatment was stopped and responded well on the reintroduction of the combination, particularly when Ad-ING1 virus was used at a concentration optimized *in vivo*. This suggests the potential for using ING1 as a novel therapeutic agent since it enhances the efficacy of chemotherapeutic drugs when used in combination in breast cancer patients. It is also worth mentioning that MDA-

MB468 is a breast cancer cell line that is triple negative (ER-/PR-/HER2-), which would typically be derived from an advanced, aggressive and metastasized clinical stage tumor. Such tumors are insensitive to treatments such as hormone therapy or Herceptin targeted therapy and if they become resistant to chemotherapy, there are no known treatments that are able to ameliorate this disease. Given the effective nature of targeting the two epigenetic pathways shown in this study, we propose that this strategy may provide an effective therapeutic approach for cancer patients who have exhausted other modes of treatment.

4.2 Reduced ING1 levels in breast cancer promotes metastasis

In this study we show that altering the levels of ING1 affects the expression of genes known to be altered in breast cancer, consistent with ING1 being initially identified as a gene repressed in breast cancer cell lines (Garkavtsev, Kazarov et al. 1996) that can regulate gene expression (Feng, Bonni et al. 2006). AQUA analysis of samples from 532 breast cancer patients extends previous studies that have used limited numbers of samples and were lacking internal controls and show that reduction of ING1 levels frequently occurs in primary breast tumors. The technique that we have used i.e. automated quantitative IHC, eliminates observer bias in the measurement of protein expression. Also, using this technique one can quantitatively measure protein expression within different sub-cellular (nucleus/cytoplasm) and tissue (tumor/stroma) compartments, therefore possibly improving the clinical applicability of this technique. Despite the advantages of the AQUA technique that was used to determine ING1 expression in our experiments, this technique is not widely available in routine laboratory diagnostics which limits its current clinical utility.

Similar to previous observations made, ING1 was generally downregulated in a majority of breast cancer patients compared to expression in normal breast epithelial tissue, which further strengthens the idea of ING1 being a type-II tumor suppressor. Here we also show that higher levels of tumor ING1 correlate strongly with disease free survival (logrank p=0.013), disease specific overall survival (logrank p=0.0071), and distant metastasis free survival (logrank p=0.0003) in non-luminal, but not in luminal breast cancers. These data suggest that ING1 plays a role in curbing metastasis, and indeed, knockdown of ING1 promoted, and overexpression of ING1 inhibited cell migration and invasion by several experimental measures. These included scratch and transwell migration assays and a matrigel membrane invasion assay. By examination of genes that were found previously to be associated with the epithelial-mesenchymal transition (Taube, Herschkowitz et al. 2010) and that were also found to be regulated by ING1 (Yang *et al*., in preparation), we identified platelet-derived growth factor A (PDGF A) and the platelet-derived growth factor receptor B (PDGFR B) as genes that were regulated by ING1 in a similar manner in the MDA-MB231 human breast adenocarcinoma cell line that is used widely for invasion assays. Knockdown of ING1 by ~90% caused very robust increases in both PDGF-A and PDGFR-B, as might be expected if the usual function of ING1 was to repress these genes whose products are associated with invasion and metastasis (Carvalho, Milanezi et al. 2005; Schito, Rey et al. 2012). Although a logical expectation might be to see a decrease in these gene transcripts in response to ING1 overexpression, we did not find this to be the case. Overexpression of ING1 caused no significant changes in transcript levels of either of these genes, suggesting that overexpression of ING1 did not increase the activity of the Sin3A HDAC

complex that contains ING1 as a stoichiometric member (Doyon, Cayrou et al. 2006). This should also be noted that efficiency of the primers for RT-PCR analysis was not determined which may have possible caveats, but is unlikely, as corroborative results showing increase in PDGFA protein level were obtained from an independent experiment upon ING1 knockdown (Figure 19B). Both ING1 and the closely related ING2 protein are believed to exert cellular effects primarily by altering gene expression through epigenetic mechanisms, specifically binding to, and targeting the HDAC complex to the H3K4Me3 mark (Martin, Baetz et al. 2006; Pena, Davrazou et al. 2006; Shi, Hong et al. 2006). If anything, some increase in gene expression might be expected if overexpression impaired the function of the Sin3A complex as previously proposed, due to altering stoichiometry. Although not to statistically significant levels, such an increase in response to ING1 overexpression was indeed noted in this study (Figure 19B).

ING1 overexpression also significantly reduced the number of metastatic tumors in the experimental mouse model as evident from BLI (Figure 21A). Animals with MDA-MB231 cells infected with ING1 + GFP adenovirus had significantly fewer metastatic growth sites than mice injected with MDA-MB231 cells infected with control GFP adenovirus and in fact only three mice in the group (n=12) had any signal detected at all after 28 days (Figure 21C). Experimental mice also showed increased survival compared to animals with GFP only expressing cells in this model developed for examining skeletal metastasis of MDA-MB231 cells specifically to the knee bone (Bondareva, Downey et al. 2009). Our findings demonstrated that ING1 overexpression completely abrogated the ability of MDA-MB231 cells to produce metastatic growths in the knee. Thus, mice with ING1 overexpressing breast cancer cells had no tumor burden in the knees, compared to

controls which had a clear burden as determined by the BLI, μCT imaging and bone histology studies (Figure 22). These results suggest that ING1b could effectively inhibit the metastatic spread of cancer cells leading to improved survival in our experimental metastasis mouse model.

All of the ING proteins affect histone acetylation in yeast through human cells (Loewith, Meijer et al. 2000; Kuzmichev, Zhang et al. 2002; Vieyra, Toyama et al. 2002) and ING2 serves as the major target of the HDAC inhibitor SAHA (Smith, Martin-Brown et al. 2010). Several additional HDAC inhibitors are in different phases of clinical trials where they have shown promising results for treating breast cancer as part of combination therapies (Luu, Morgan et al. 2008; Munster, Thurn et al. 2011). Since ING1 and ING2 are very closely related evolutionarily (He, Helbing et al. 2005) and functionally (Doyon, Cayrou et al. 2006), it is likely that both target the Sin3A HDAC complex to chromatin locales containing relatively higher density of the H3K4Me3 chromatin mark. This mechanism is consistent with recent observations that the epigenetic targeted drugs 5-azacytidine and the LBH589 HDAC inhibitor can act additively, or in some cases synergistically with ING1 in killing cells in breast cancer cells and in animal models (Thakur, Feng et al. 2012). Data generated in this study provide mechanistic insight into why breast cancer cells may be selectively sensitive to HDAC inhibitors compared to normal breast epithelium; down-regulation of ING1 would already reduce the ability of cancer cells to accurately target the Sin3A complex and treatment with HDAC inhibitors such as SAHA that selectively target ING2 and/or ING1 would be expected to have greater effects upon the epigenomes of cancerous versus normal epithelial cells. Since HDACs are also components of estrogen receptor

complexes and HDAC inhibitors have been reported to be able to restore sensitivity of breast cancer cells to tamoxifen (Hostetter, Licata et al. 2009), this may explain, in part, why ING1 levels are able to predict survival in non-luminal forms of breast cancer as we report here for the first time.

4.3 Stromal expression of ING1 predicts the survival of breast cancer patients

In this study we investigated the significance of ING1 expression in the stromal region of breast cancer patients and tested the prognostic/predictive value of stromal ING1 as a prognostic factor in the Calgary Tamoxifen Cohort. Prognostic markers are associated with outcomes independent from therapy whereas, predictive markers predict outcome in terms of survival of a specific therapy. As the patients in the cohort studied were treated with tamoxifen irrespective of the ER status; ING1 acts a predictive or prognostic marker is unclear. Results show that stromal ING1 correlates with clinico-pathological characters like tumor grade ($p=0.001$) and tumor size ($p=0.020$) in the luminal (ER+/HER2-) breast cancer group consisting of 443 patients in the cohort. Specifically, low stromal ING1 expression was associated with tumor grade and size, i.e. patients with lower expression of stromal ING1 had better prognosis. This is an interesting observation and in contrast to what was observed in the case of tumor ING1 expression. Therefore, it appears that high ING1 levels in tumor and low ING1 levels in stroma predict the best outcomes for patients.

We also investigated if stromal ING1 expression was associated with disease free survival and disease specific overall survival by analyzing survival outcomes using Kaplan Meier curves. Significant association with 5 year DFS were observed in both the

luminal group (p=0.0001) and in the total population (p=0.0001) of the cohort, with patients expressing low stromal ING1 having a better prognosis than patients with high stromal ING1. Similar results were obtained when the association with 7 year DSOS was analyzed, with both the luminal group (p=.0076) and total population (p=0.110) showing better prognosis than the low stromal ING1 category, although the relationship was less statistically significant. Patients from the non-luminal category were also analyzed for similar associations, but no significant results were obtained for DFS or DSOS in this case. This is interesting, suggesting that ING1 expression in different compartments of tissue (tumor/stroma) may have different roles to play in promoting or inhibiting the development of different sub-types of breast cancers.

Furthermore, multivariate analysis using Cox proportional hazards regression to adjust for important clinical covariates, confirmed that stromal ING1 expression was independently associated with DSS in breast cancer. When taking the total population of the cohort into account, stromal ING1 (HR 2.125, p=0.004) not only came out to be an independent prognostic marker for breast cancer, but had better predictive power than some of the already established biomarkers like HER2, ER and tumor size, which are commonly used in the clinic for determining an individual's risk of dying due to cancer. When the luminal only group was analyzed, similar results were obtained, where stromal ING1 (HR 2.32, p=0.002) came out as an independent prognostic marker in the cohort tested. In this particular population, stromal ING1 had better predictive power than tumor size which is a clinically used biomarker. These results indicate that stromal ING1 is not only associated with patient survival and clinico-pathological characters like tumor grade and size in breast cancer, but could also be developed into a biomarker for breast cancer

considering its better HR and predictive power than currently used clinical biomarkers. Further testing needs to be done in this regard by validating the present observation in a different breast cancer cohort, along with clinical testing, to establish stromal ING1 as a bona fide biomarker in breast cancer.

As this observation of association of stromal ING1 with patient survival was unanticipated for a typical type-II tumor suppressor, we wanted to determine the underlying reason for association of higher stromal ING1 expression with poor prognosis of patients in the luminal group of the cohort. Tumor cells in a patient are surrounded by a complex microenvironment that includes the extracellular matrix, diffusible growth factors and cytokines, and a variety of non-epithelial cells like endothelial cells, pericytes, smooth muscle cells, immune cells and fibroblasts collectively called as stroma. The concept of growth regulatory interactions between the stroma and adjacent epithelial cell population was first introduced by Schor *et al.* (Schor, Schor et al. 1985; Schor, Schor et al. 1985). This interaction is mediated by soluble autocrine/paracrine factors secreted from stromal cells that induce physiological changes such as increased proliferation, migration etc. in the adjacent epithelia. Specially, fibroblasts present in the stroma are known to produce several families of growth factors that are key mediators of stroma-tumor cell interactions. Since fibroblasts constitute the majority of the stromal cells within a breast carcinoma, we used a human mammary fibroblast cell line to determine the change in cytokines and growth factors produced by these cells upon modulating levels of ING1.

Since ING1b induced cell death in HMF3s cells, we used ING1a the longer isoform which is known to induce senescence (Soliman, Berardi et al. 2008) in our

experiments to determine the cytokine profile of these cells. Various studies have provided evidence that senescent human fibroblasts can promote the proliferation of pre-malignant and malignant epithelial cells in culture, and the formation of tumors in mice (Krtolica, Parrinello et al. 2001; Parrinello, Coppe et al. 2005; Olsen, Moreira et al. 2010). This is likely due to the fact that senescent fibroblasts show a senescence associated secretory phenotype (SASP), which is similar to the paracrine growth factors and cytokines made in tumors that can contribute to cancer progression. Contrary to our expectations, our results showed that there was a significant decrease in the number of pro-inflammatory and proliferative cytokines such as IL-6, IL-8, PDGFA, PDGFB, VEGF and GRO in HMF3s cells upon ING1a overexpression. Chemotactic cytokines promoting growth and recruitment of immune cells (neutrophils, monocytes and macrophage) like Eotaxin, Fractalkine and MCP-3 were also released at lower amounts compared to controls. However, IL-15 and IP-10 which are known to have anti-apoptotic and anti-angiogenic properties (Angiolillo, Sgadari et al. 1995; Malamut, El Machhour et al. 2010) also had lower levels upon ING1a expression in HMF3s cells, suggesting that these pathways may be activated by senescing fibroblasts.

Apart from the majority of cytokines and chemokines having reduced levels, some cytokines were increased upon ING1a expression. An increase in the levels of immune cell (granulocyte, monocyte and macrophage) promoting cytokines such as G-CSF, GM-CSF and MIP-1a was also observed along with increases in chemotactic and pro-inflammatory cytokine MCP-1.

In contrast to varied effects upon cytokines and chemokines, a much more directed effect was seen for matrix metalloproteases. Stromal cells secrete matrix

metalloproteases such as MMP-1, 2, 3, 9 and 10, all of which can promote epithelial transformation (Lynch and Matrisian 2002) and are known to have pro-angiogenic and metastatic properties (Itoh, Tanioka et al. 1998; Liu and Hornsby 2007). Previous studies have shown that senescent cells secrete increased levels of MMPs and the MMP family members that are consistently upregulated in fibroblasts undergoing senescence are MMP-1, 3 and 10 (Davalos, Coppe et al. 2010). Our previous study shows that ING1a induces senescence suggesting that these MMPs may contribute to epithelial cell transformation. When we overexpressed ING1a in HMF3s cells, a significant increase in the levels of these families of MMPs was observed indicating senescence induction in HMF3s cells due to ING1a expression. A reciprocal effect was observed in the case of inhibitors of MMPs (TIMPs) as the levels of TIMP-2, 3 and 4 showed a significant decrease in ING1a expressing cells indicating that both MMP production increased and inhibitor of MMP activity had decreased in a coordinated manner in these cells. To confirm that this was due to ING1a induced senescence in HMF3s cells, various independent markers of cellular senescence need to be tested.

These results clearly showed an increased amount of MMPs being secreted by the HMF3s cells expressing ING1a. To test if the MMPs secreted were active, we performed zymography with specific substrates for MMP-1 and MMP-2 to analyze their enzymatic activity *in vitro*. Activities on the zymogram corresponding to levels of MMP-1 and 2 previously observed were obtained confirming that the MMPs secreted by ING1a expressing HMF3s cells were biologically active in nature.

Next, in order to functionally investigate whether soluble factors produced by fibroblasts upon ING1a expression are able to induce changes in tumor cells, we co-

cultured HMF3s cells and MCF7 cells and studied their behavior in three dimensional cultures. The organoids formed when HMF3s cells expressing ING1a were co-cultured with MCF7 cells were highly disorganized as compared to GFP expressing co-cultured cells. This is an indication that the MMPs and cytokines secreted by ING1a expressing cells were able to induce morphological changes in the cancer cells resulting in disorganized and more aggressive colonies. The ability of ING1a expressing fibroblasts to stimulate the invasion of tumor cells into the matrix indicated that secreted factors produced by these cells in response to ING1a expression may be sufficient to induce invasiveness in these cells. This may explain the phenomenon believed to occur in tumor-stroma interactions in cancer patients, where senescent cancer associated fibroblasts release soluble factors which provides an environment that helps the tumors to grow more aggressively and to metastasize to form secondary tumors.

Future *in vivo* experiments in mice involving implantation of breast cancer cells with ING1a expressing fibroblasts could provide further pre-clinical information on the role of ING1 protein in stroma and its impact on tumor growth. It would also be interesting if stroma containing cancer associated fibroblasts in breast tumors were tested for cytokine and MMP profiles and then see if these correlate with ING1 expression. Such experiments could provide additional evidence for deciphering the role of ING1 in breast cancer biology.

Overall, these results from the cytokine and MMP profiling and the functional assays provide a possible explanation for the poor survival of breast cancer patients having elevated levels of ING1 in tumor associated stroma as observed in the AQUA analysis of patients having luminal types of breast cancer in the cohort we tested. Both

major isoforms of ING1, ING1a and ING1b have been reported to induce senescence in cells upon overexpression (Soliman, Berardi et al. 2008; Abad, Moreno et al. 2011; Li, Li et al. 2011) although ING1b also induces apoptosis at higher levels while ING1a appears to solely affect senescence. Therefore, we speculate that increased levels of ING1 in the stroma may induce senescence which allows the stromal cells to display a senescence associated secretory phenotype, releasing paracrine and cytokine growth factors and MMPs. This would result in more aggressive tumor formation in such patients leading to their documented poor survival.

Presently, a high incidence of breast cancer is observed in women worldwide. This is most likely due to the availability of widespread screening programs used to detect breast cancer, which otherwise may never get diagnosed. There is an inverse relation between the cost of treatment and patient survival as the breast cancer progresses to higher grades which makes screening and diagnosing cancers at earlier stages important, improving patient survival. Our study here provides substantial evidence for establishing ING1 as a probable biomarker for breast cancer. The study is limited by its retrospective nature and further validation needs to be done in retro/prospective patient cohorts that could provide further evidence and confidence in establishing ING1 as a *bona fide* biomarker in breast cancer. Overall, this study provides important pre-clinical information that may be helpful to evaluate the potential usefulness of the ING family of tumor suppressors in breast cancer prognosis and treatment.

PUBLICATIONS PRODUCED DURING THE COURSE OF THIS THESIS

- **Thakur S**, Feng X, Qiao Shi Z, Ganapathy A, Kumar Mishra M, et al. (2012) ING1 and 5-Azacytidine Act Synergistically to Block Breast Cancer Cell Growth. PLoS ONE 7(8): e43671

- Yu L, **Thakur S**, Leong-Quong RY, Suzuki K, Pang A, et al. (2013) Src Regulates the Activity of the ING1 Tumor Suppressor. PLoS ONE 8(4): e60943.

- Bose P*, **Thakur S***, Thalappilly S, Satpathy, Ahn BY, et al. (2013). ING1 induces apoptosis through direct effects at the mitochondria. Cell Death and Disease. e788.

- Bose P, **Thakur S**, Klimowicz A, Kornaga E, Nakoneshny, S, et al. (2014). Tumor cell apoptosis mediated by cytoplasmic ING1 is associated with improved survival in oral squamous cell carcinoma patients. Oncotarget 5(10):3210-9.

- Satpathy S*, Guerillon C*, Kim T, **Thakur S,** Peduex R, et al. (2014). Sumoylation of ING1b tumor suppressor regulates gene expression. Carcinogenesis doi:10.1093/carcin/bgu126

- **Thakur S***, Singla A*, Chen J, Yang Y, Salazar C, et al. (2014). Reduced ING1 levels in breast cancer promote metastasis. Oncotarget 5(12):4244-56

INTELLECTUAL PROPERTY RIGHTS

- Riabowol K*, Bose P*, Dort J* and **Thakur S***. (2014) ING1 in oral squamous cell carcinoma: A new approach to treatment. US patent filed May 2014.

* indicates equal contributions

References

(1997). AJCC Cancer Staging Manual. Philadelphia Lippincott-Raven.

Abad, M., A. Moreno, et al. (2011). "The tumor suppressor ING1 contributes to epigenetic control of cellular senescence." Aging Cell **10**(1): 158-171.

Anderberg, C., H. Li, et al. (2009). "Paracrine signaling by platelet-derived growth factor-CC promotes tumor growth by recruitment of cancer-associated fibroblasts." Cancer Res **69**(1): 369-378.

Andre, F., M. Campone, et al. (2010). "Phase I study of everolimus plus weekly paclitaxel and trastuzumab in patients with metastatic breast cancer pretreated with trastuzumab." J Clin Oncol **28**(34): 5110-5115.

Angiolillo, A. L., C. Sgadari, et al. (1995). "Human interferon-inducible protein 10 is a potent inhibitor of angiogenesis in vivo." J Exp Med **182**(1): 155-162.

Archer, S. Y. and R. A. Hodin (1999). "Histone acetylation and cancer." Curr Opin Genet Dev **9**(2): 171-174.

Atadja, P. (2009). "Development of the pan-DAC inhibitor panobinostat (LBH589): successes and challenges." Cancer Lett **280**(2): 233-241.

Atadja, P. W. (2011). "HDAC inhibitors and cancer therapy." Prog Drug Res **67**: 175-195.

Badve, S., D. J. Dabbs, et al. (2011). "Basal-like and triple-negative breast cancers: a critical review with an emphasis on the implications for pathologists and oncologists." Mod Pathol **24**(2): 157-167.

Ban, K. A. and C. V. Godellas (2014). "Epidemiology of breast cancer." Surg Oncol Clin N Am **23**(3): 409-422.

Baselga, J. (2010). "Treatment of HER2-overexpressing breast cancer." Ann Oncol **21 Suppl 7**: vii36-40.

Baselga, J., K. A. Gelmon, et al. (2010). "Phase II trial of pertuzumab and trastuzumab in patients with human epidermal growth factor receptor 2-positive metastatic breast cancer that progressed during prior trastuzumab therapy." J Clin Oncol **28**(7): 1138-1144.

Baselga, J., V. Semiglazov, et al. (2009). "Phase II randomized study of neoadjuvant everolimus plus letrozole compared with placebo plus letrozole in patients with estrogen receptor-positive breast cancer." J Clin Oncol **27**(16): 2630-2637.

Baselga, J. and S. M. Swain (2009). "Novel anticancer targets: revisiting ERBB2 and discovering ERBB3." Nat Rev Cancer **9**(7): 463-475.

Bates, R. C., D. I. Bellovin, et al. (2005). "Transcriptional activation of integrin beta6 during the epithelial-mesenchymal transition defines a novel prognostic indicator of aggressive colon carcinoma." J Clin Invest **115**(2): 339-347.

Berardi, P., M. Russell, et al. (2004). "Functional links between transcription, DNA repair and apoptosis." Cell Mol Life Sci **61**(17): 2173-2180.

Bhowmick, N. A., A. Chytil, et al. (2004). "TGF-beta signaling in fibroblasts modulates the oncogenic potential of adjacent epithelia." Science **303**(5659): 848-851.

Bhowmick, N. A., E. G. Neilson, et al. (2004). "Stromal fibroblasts in cancer initiation and progression." Nature **432**(7015): 332-337.

Bianconi, E., A. Piovesan, et al. (2013). "An estimation of the number of cells in the human body." Ann Hum Biol **40**(6): 463-471.

Boire, A., L. Covic, et al. (2005). "PAR1 is a matrix metalloprotease-1 receptor that promotes invasion and tumorigenesis of breast cancer cells." Cell **120**(3): 303-313.

Bondareva, A., C. M. Downey, et al. (2009). "The lysyl oxidase inhibitor, beta-aminopropionitrile, diminishes the metastatic colonization potential of circulating breast cancer cells." PLoS One **4**(5): e5620.

Borkosky, S. S., M. Gunduz, et al. (2009). "Frequent deletion of ING2 locus at 4q35.1 associates with advanced tumor stage in head and neck squamous cell carcinoma." J Cancer Res Clin Oncol **135**(5): 703-713.

Bose, P., S. Thakur, et al. (2013). "ING1 induces apoptosis through direct effects at the mitochondria." Cell Death Dis **4**: e788.

Bronzert, D. A., P. Pantazis, et al. (1987). "Synthesis and secretion of platelet-derived growth factor by human breast cancer cell lines." Proc Natl Acad Sci U S A **84**(16): 5763-5767.

Brown, R. and G. Strathdee (2002). "Epigenomics and epigenetic therapy of cancer." Trends Mol Med **8**(4 Suppl): S43-48.

Byers, T., S. Graham, et al. (1985). "Lactation and breast cancer. Evidence for a negative association in premenopausal women." Am J Epidemiol **121**(5): 664-674.

Byron, S. A., E. Min, et al. (2012). "Negative regulation of NF-kappaB by the ING4 tumor suppressor in breast cancer." PLoS One **7**(10): e46823.

Camerer, E., A. A. Qazi, et al. (2004). "Platelets, protease-activated receptors, and fibrinogen in hematogenous metastasis." Blood **104**(2): 397-401.

Camp, R. L., G. G. Chung, et al. (2002). "Automated subcellular localization and quantification of protein expression in tissue microarrays." Nat Med **8**(11): 1323-1327.

Campos, E. I., K. J. Cheung, Jr., et al. (2002). "The novel tumour suppressor gene ING1 is overexpressed in human melanoma cell lines." Br J Dermatol **146**(4): 574-580.

Campos, E. I., M. Y. Chin, et al. (2004). "Biological functions of the ING family tumor suppressors." Cell Mol Life Sci **61**(19-20): 2597-2613.

Canadian Cancer Statistics 2013. Toronto, ON: Canadian Cancer Society; 2013

Candido, E. P., R. Reeves, et al. (1978). "Sodium butyrate inhibits histone deacetylation in cultured cells." Cell **14**(1): 105-113.

Carvalho, I., F. Milanezi, et al. (2005). "Overexpression of platelet-derived growth factor receptor alpha in breast cancer is associated with tumour progression." Breast Cancer Res **7**(5): R788-795.

Cengiz, B., M. Gunduz, et al. (2007). "Fine deletion mapping of chromosome 2q21-37 shows three preferentially deleted regions in oral cancer." Oral Oncol **43**(3): 241-247.

Chaffer, C. L. and R. A. Weinberg (2011). "A perspective on cancer cell metastasis." Science **331**(6024): 1559-1564.

Chambers, A. F., A. C. Groom, et al. (2002). "Dissemination and growth of cancer cells in metastatic sites." Nat Rev Cancer **2**(8): 563-572.

Cheang, M. C., S. K. Chia, et al. (2009). "Ki67 index, HER2 status, and prognosis of patients with luminal B breast cancer." J Natl Cancer Inst **101**(10): 736-750.

Cheung, K. J., Jr. and G. Li (2002). "p33(ING1) enhances UVB-induced apoptosis in melanoma cells." Exp Cell Res **279**(2): 291-298.

Cheung, K. J., Jr., D. Mitchell, et al. (2001). "The tumor suppressor candidate p33(ING1) mediates repair of UV-damaged DNA." Cancer Res **61**(13): 4974-4977.

Chlebowski, R. T., L. H. Kuller, et al. (2009). "Breast cancer after use of estrogen plus progestin in postmenopausal women." N Engl J Med **360**(6): 573-587.

Chou, T. C. and P. Talalay (1984). "Quantitative analysis of dose-effect relationships: the combined effects of multiple drugs or enzyme inhibitors." Adv Enzyme Regul **22**: 27-55.

Cirri, P. and P. Chiarugi (2012). "Cancer-associated-fibroblasts and tumour cells: a diabolic liaison driving cancer progression." Cancer Metastasis Rev **31**(1-2): 195-208.

Comb, M. and H. M. Goodman (1990). "CpG methylation inhibits proenkephalin gene expression and binding of the transcription factor AP-2." Nucleic Acids Res **18**(13): 3975-3982.

Curtis, C., S. P. Shah, et al. (2012). "The genomic and transcriptomic architecture of 2,000 breast tumours reveals novel subgroups." Nature **486**(7403): 346-352.

Davalos, A. R., J. P. Coppe, et al. (2010). "Senescent cells as a source of inflammatory factors for tumor progression." Cancer Metastasis Rev **29**(2): 273-283.

De, P., D. Dryer, et al. (2013). "Canadian trends in liver cancer: a brief clinical and epidemiologic overview." Curr Oncol **20**(1): e40-43.

Debnath, J. and J. S. Brugge (2005). "Modelling glandular epithelial cancers in three-dimensional cultures." Nat Rev Cancer **5**(9): 675-688.

Doyon, Y., C. Cayrou, et al. (2006). "ING tumor suppressor proteins are critical regulators of chromatin acetylation required for genome expression and perpetuation." Mol Cell **21**(1): 51-64.

Eastman, A. and J. R. Rigas (1999). "Modulation of apoptosis signaling pathways and cell cycle regulation." Semin Oncol **26**(5 Suppl 16): 7-16; discussion 41-12.

Eckert, M. A. and J. Yang (2011). "Targeting invadopodia to block breast cancer metastasis." Oncotarget **2**(7): 562-568.

Edge, S. B. and C. C. Compton (2010). "The American Joint Committee on Cancer: the 7th edition of the AJCC cancer staging manual and the future of TNM." Ann Surg Oncol **17**(6): 1471-1474.

Evans, D. G. and A. Howell (2007). "Breast cancer risk-assessment models." Breast Cancer Res **9**(5): 213.

Farmer, P., H. Bonnefoi, et al. (2005). "Identification of molecular apocrine breast tumours by microarray analysis." Oncogene **24**(29): 4660-4671.

Feng, X., S. Bonni, et al. (2006). "HSP70 induction by ING proteins sensitizes cells to tumor necrosis factor alpha receptor-mediated apoptosis." Mol Cell Biol **26**(24): 9244-9255.

Feng, X., Y. Hara, et al. (2002). "Different HATS of the ING1 gene family." Trends Cell Biol **12**(11): 532-538.

Ferlay, J., Soerjomataram, et al. GLOBOCAN 2012 v1.0, Cancer Incidence and Mortality Worldwide : IARC CancerBase No. 11 [Internet]. Lyon, France: International Agency for Research on Cancer; 2013. Available from: http://globocan.iarc.fr, accessed on 15/07/2014.

Fidler, I. J. (1970). "Metastasis: guantitative analysis of distribution and fate of tumor embolilabeled with 125 I-5-iodo-2'-deoxyuridine." J Natl Cancer Inst **45**(4): 773-782.

Friedenreich, C. M., H. E. Bryant, et al. (2001). "Risk factors for benign breast biopsies: a nested case-control study in the Alberta breast screening program." Cancer Detect Prev **25**(3): 280-291.

Garkavtsev, I. and Y. Boucher (2005). "An intact ING1-P53 pathway can potentiate the cytotoxic effects of taxol." Cancer Biol Ther **4**(1): 48-49.

Garkavtsev, I., I. A. Grigorian, et al. (1998). "The candidate tumour suppressor p33ING1 cooperates with p53 in cell growth control." Nature **391**(6664): 295-298.

Garkavtsev, I., A. Kazarov, et al. (1996). "Suppression of the novel growth inhibitor p33ING1 promotes neoplastic transformation." Nat Genet **14**(4): 415-420.

Garkavtsev, I., S. V. Kozin, et al. (2004). "The candidate tumour suppressor protein ING4 regulates brain tumour growth and angiogenesis." Nature **428**(6980): 328-332.

Gerber, P. A., A. Hippe, et al. (2009). "Chemokines in tumor-associated angiogenesis." Biol Chem **390**(12): 1213-1223.

Giannoni, E., F. Bianchini, et al. (2010). "Reciprocal activation of prostate cancer cells and cancer-associated fibroblasts stimulates epithelial-mesenchymal transition and cancer stemness." Cancer Res **70**(17): 6945-6956.

Gong, W., M. Russell, et al. (2006). "Subcellular targeting of p33ING1b by phosphorylation-dependent 14-3-3 binding regulates p21WAF1 expression." Mol Cell Biol **26**(8): 2947-2954.

Gong, W., K. Suzuki, et al. (2005). "Function of the ING family of PHD proteins in cancer." Int J Biochem Cell Biol **37**(5): 1054-1065.

Gozani, O., P. Karuman, et al. (2003). "The PHD finger of the chromatin-associated protein ING2 functions as a nuclear phosphoinositide receptor." Cell **114**(1): 99-111.

Gradishar, W. J. (2010). "Adjuvant endocrine therapy for early breast cancer: the story so far." Cancer Invest **28**(4): 433-442.

Green, A. R., D. G. Powe, et al. (2013). "Identification of key clinical phenotypes of breast cancer using a reduced panel of protein biomarkers." Br J Cancer **109**(7): 1886-1894.

Gunduz, M., L. B. Beder, et al. (2008). "Downregulation of ING3 mRNA expression predicts poor prognosis in head and neck cancer." Cancer Sci **99**(3): 531-538.

Gunduz, M., H. Nagatsuka, et al. (2005). "Frequent deletion and down-regulation of ING4, a candidate tumor suppressor gene at 12p13, in head and neck squamous cell carcinomas." Gene **356**: 109-117.

Gunduz, M., M. Ouchida, et al. (2002). "Allelic loss and reduced expression of the ING3, a candidate tumor suppressor gene at 7q31, in human head and neck cancers." Oncogene **21**(28): 4462-4470.

Han, X., X. Feng, et al. (2008). "Tethering by lamin A stabilizes and targets the ING1 tumour suppressor." Nat Cell Biol **10**(11): 1333-1340.

Hanahan, D. and R. A. Weinberg (2000). "The hallmarks of cancer." Cell **100**(1): 57-70.

Hartmann, L. C., T. A. Sellers, et al. (2005). "Benign breast disease and the risk of breast cancer." N Engl J Med **353**(3): 229-237.

He, G. H., C. C. Helbing, et al. (2005). "Phylogenetic analysis of the ING family of PHD finger proteins." Mol Biol Evol **22**(1): 104-116.

Helbing, C. C., C. Veillette, et al. (1997). "A novel candidate tumor suppressor, ING1, is involved in the regulation of apoptosis." Cancer Res **57**(7): 1255-1258.

Henke, J. I., D. Goergen, et al. (2008). "microRNA-122 stimulates translation of hepatitis C virus RNA." EMBO J **27**(24): 3300-3310.

Herman, J. G. and S. B. Baylin (2003). "Gene silencing in cancer in association with promoter hypermethylation." N Engl J Med **349**(21): 2042-2054.

Higgins, M. J. and J. Baselga (2011). "Targeted therapies for breast cancer." J Clin Invest **121**(10): 3797-3803.

Hostetter, C. L., L. A. Licata, et al. (2009). "Timing is everything: order of administration of 5-aza 2' deoxycytidine, trichostatin A and tamoxifen changes estrogen receptor mRNA expression and cell sensitivity." Cancer Lett **275**(2): 178-184.

Hunter, D. J., G. A. Colditz, et al. (2010). "Oral contraceptive use and breast cancer: a prospective study of young women." Cancer Epidemiol Biomarkers Prev **19**(10): 2496-2502.

Inamdar, N. M., K. C. Ehrlich, et al. (1991). "CpG methylation inhibits binding of several sequence-specific DNA-binding proteins from pea, wheat, soybean and cauliflower." Plant Mol Biol **17**(1): 111-123.

Itoh, T., M. Tanioka, et al. (1998). "Reduced angiogenesis and tumor progression in gelatinase A-deficient mice." Cancer Res **58**(5): 1048-1051.

Janssen, H. L., H. W. Reesink, et al. (2013). "Treatment of HCV infection by targeting microRNA." N Engl J Med **368**(18): 1685-1694.

Jechlinger, M., A. Sommer, et al. (2006). "Autocrine PDGFR signaling promotes mammary cancer metastasis." J Clin Invest **116**(6): 1561-1570.

Jenuwein, T. and C. D. Allis (2001). "Translating the histone code." Science **293**(5532): 1074-1080.

Jiang, C. and B. F. Pugh (2009). "Nucleosome positioning and gene regulation: advances through genomics." Nat Rev Genet **10**(3): 161-172.

Johnston, S., J. Pippen, Jr., et al. (2009). "Lapatinib combined with letrozole versus letrozole and placebo as first-line therapy for postmenopausal hormone receptor-positive metastatic breast cancer." J Clin Oncol **27**(33): 5538-5546.

Johnstone, R. W. (2002). "Histone-deacetylase inhibitors: novel drugs for the treatment of cancer." Nat Rev Drug Discov **1**(4): 287-299.

Johnstone, R. W. and J. D. Licht (2003). "Histone deacetylase inhibitors in cancer therapy: is transcription the primary target?" Cancer Cell **4**(1): 13-18.

Kaadige, M. R. and D. E. Ayer (2006). "The polybasic region that follows the plant homeodomain zinc finger 1 of Pf1 is necessary and sufficient for specific phosphoinositide binding." J Biol Chem **281**(39): 28831-28836.

Kameyama, K., C. L. Huang, et al. (2003). "Reduced ING1b gene expression plays an important role in carcinogenesis of non-small cell lung cancer patients." Clin Cancer Res **9**(13): 4926-4934.

Kang, Y., P. M. Siegel, et al. (2003). "A multigenic program mediating breast cancer metastasis to bone." Cancer Cell **3**(6): 537-549.

Kaplan, R. N., R. D. Riba, et al. (2005). "VEGFR1-positive haematopoietic bone marrow progenitors initiate the pre-metastatic niche." Nature **438**(7069): 820-827.

Katsuno, Y., S. Lamouille, et al. (2013). "TGF-beta signaling and epithelial-mesenchymal transition in cancer progression." Curr Opin Oncol **25**(1): 76-84.

Kaufman, B., J. R. Mackey, et al. (2009). "Trastuzumab plus anastrozole versus anastrozole alone for the treatment of postmenopausal women with human epidermal growth factor receptor 2-positive, hormone receptor-positive metastatic breast cancer: results from the randomized phase III TAnDEM study." J Clin Oncol **27**(33): 5529-5537.

Kelsey, J. L., M. D. Gammon, et al. (1993). "Reproductive factors and breast cancer." Epidemiol Rev **15**(1): 36-47.

Kim, T. Y., Y. J. Bang, et al. (2006). "Histone deacetylase inhibitors for cancer therapy." Epigenetics **1**(1): 14-23.

Kiziltepe, T., T. Hideshima, et al. (2007). "5-Azacytidine, a DNA methyltransferase inhibitor, induces ATR-mediated DNA double-strand break responses, apoptosis, and synergistic cytotoxicity with doxorubicin and bortezomib against multiple myeloma cells." Mol Cancer Ther **6**(6): 1718-1727.

Klironomos, G., V. Bravou, et al. (2010). "Loss of inhibitor of growth (ING-4) is implicated in the pathogenesis and progression of human astrocytomas." Brain Pathol **20**(2): 490-497.

Kobayashi, L. C., I. Janssen, et al. (2013). "Moderate-to-vigorous intensity physical activity across the life course and risk of pre- and post-menopausal breast cancer." Breast Cancer Res Treat **139**(3): 851-861.

Kouzarides, T. (2007). "Chromatin modifications and their function." Cell **128**(4): 693-705.

Krop, I. E., M. Beeram, et al. (2010). "Phase I study of trastuzumab-DM1, an HER2 antibody-drug conjugate, given every 3 weeks to patients with HER2-positive metastatic breast cancer." J Clin Oncol **28**(16): 2698-2704.

Krtolica, A., S. Parrinello, et al. (2001). "Senescent fibroblasts promote epithelial cell growth and tumorigenesis: a link between cancer and aging." Proc Natl Acad Sci U S A **98**(21): 12072-12077.

Ku, N. O., D. M. Toivola, et al. (2010). "Cytoskeletal keratin glycosylation protects epithelial tissue from injury." Nat Cell Biol **12**(9): 876-885.

Kuendgen, A. and M. Lubbert (2008). "Current status of epigenetic treatment in myelodysplastic syndromes." Ann Hematol **87**(8): 601-611.

Kumamoto, K., K. Fujita, et al. (2009). "ING2 is upregulated in colon cancer and increases invasion by enhanced MMP13 expression." Int J Cancer **125**(6): 1306-1315.

Kuo, Y. C., C. H. Su, et al. (2009). "Transforming growth factor-beta induces CD44 cleavage that promotes migration of MDA-MB-435s cells through the up-regulation of membrane type 1-matrix metalloproteinase." Int J Cancer **124**(11): 2568-2576.

Kuzmichev, A., Y. Zhang, et al. (2002). "Role of the Sin3-histone deacetylase complex in growth regulation by the candidate tumor suppressor p33(ING1)." Mol Cell Biol **22**(3): 835-848.

Lambe, M., C. Hsieh, et al. (1994). "Transient increase in the risk of breast cancer after giving birth." N Engl J Med **331**(1): 5-9.

Land, C. E., M. Tokunaga, et al. (2003). "Incidence of female breast cancer among atomic bomb survivors, Hiroshima and Nagasaki, 1950-1990." Radiat Res **160**(6): 707-717.

Lederle, W., B. Hartenstein, et al. (2010). "MMP13 as a stromal mediator in controlling persistent angiogenesis in skin carcinoma." Carcinogenesis **31**(7): 1175-1184.

Levental, K. R., H. Yu, et al. (2009). "Matrix crosslinking forces tumor progression by enhancing integrin signaling." Cell **139**(5): 891-906.

Li, J., M. Martinka, et al. (2008). "Role of ING4 in human melanoma cell migration, invasion and patient survival." Carcinogenesis **29**(7): 1373-1379.

Li, M., Y. Jin, et al. (2009). "Reduced expression and novel splice variants of ING4 in human gastric adenocarcinoma." J Pathol **219**(1): 87-95.

Li, N., Q. Li, et al. (2011). "The tumor suppressor p33ING1b upregulates p16INK4a expression and induces cellular senescence." FEBS Lett **585**(19): 3106-3112.

Li, X., T. Nishida, et al. (2010). "Decreased nuclear expression and increased cytoplasmic expression of ING5 may be linked to tumorigenesis and progression in human head and neck squamous cell carcinoma." J Cancer Res Clin Oncol **136**(10): 1573-1583.

Li, Z., Y. Xie, et al. (2010). "Tumor-suppressive effect of adenovirus-mediated inhibitor of growth 4 gene transfer in breast carcinoma cells in vitro and in vivo." Cancer Biother Radiopharm **25**(4): 427-437.

Liu, D. and P. J. Hornsby (2007). "Senescent human fibroblasts increase the early growth of xenograft tumors via matrix metalloproteinase secretion." Cancer Res **67**(7): 3117-3126.

Liu, J. Y., B. Q. Wu, et al. (2003). "[Effects of two variants of ING1 expression on tumor cell growth regulation]." Zhonghua Bing Li Xue Za Zhi **32**(1): 48-51.

Loewith, R., M. Meijer, et al. (2000). "Three yeast proteins related to the human candidate tumor suppressor p33(ING1) are associated with histone acetyltransferase activities." Mol Cell Biol **20**(11): 3807-3816.

Lohr, F., D. Y. Lo, et al. (2001). "Effective tumor therapy with plasmid-encoded cytokines combined with in vivo electroporation." Cancer Res **61**(8): 3281-3284.

Lu, F., D. L. Dai, et al. (2006). "Nuclear ING2 expression is reduced in human cutaneous melanomas." Br J Cancer **95**(1): 80-86.

Luu, T. H., R. J. Morgan, et al. (2008). "A phase II trial of vorinostat (suberoylanilide hydroxamic acid) in metastatic breast cancer: a California Cancer Consortium study." Clin Cancer Res **14**(21): 7138-7142.

Lynch, C. C. and L. M. Matrisian (2002). "Matrix metalloproteinases in tumor-host cell communication." Differentiation **70**(9-10): 561-573.

Maga, G. and U. Hubscher (2003). "Proliferating cell nuclear antigen (PCNA): a dancer with many partners." J Cell Sci **116**(Pt 15): 3051-3060.

Malamut, G., R. El Machhour, et al. (2010). "IL-15 triggers an antiapoptotic pathway in human intraepithelial lymphocytes that is a potential new target in celiac disease-associated inflammation and lymphomagenesis." J Clin Invest **120**(6): 2131-2143.

Mandili, G., A. Khadjavi, et al. (2012). "Characterization of the protein ubiquitination response induced by Doxorubicin." FEBS J **279**(12): 2182-2191.

Marks, P., R. A. Rifkind, et al. (2001). "Histone deacetylases and cancer: causes and therapies." Nat Rev Cancer **1**(3): 194-202.

Martin, D. G., K. Baetz, et al. (2006). "The Yng1p plant homeodomain finger is a methyl-histone binding module that recognizes lysine 4-methylated histone H3." Mol Cell Biol **26**(21): 7871-7879.

Matsuo, Y., N. Ochi, et al. (2009). "CXCL8/IL-8 and CXCL12/SDF-1alpha co-operatively promote invasiveness and angiogenesis in pancreatic cancer." Int J Cancer **124**(4): 853-861.

McMillin, D. W., J. M. Negri, et al. (2013). "The role of tumour-stromal interactions in modifying drug response: challenges and opportunities." Nat Rev Drug Discov **12**(3): 217-228.

Minn, A. J., G. P. Gupta, et al. (2005). "Genes that mediate breast cancer metastasis to lung." Nature **436**(7050): 518-524.

Mulder, K. W., X. Wang, et al. (2012). "Diverse epigenetic strategies interact to control epidermal differentiation." Nat Cell Biol **14**(7): 753-763.

Munster, P. N., K. T. Thurn, et al. (2011). "A phase II study of the histone deacetylase inhibitor vorinostat combined with tamoxifen for the treatment of patients with hormone therapy-resistant breast cancer." Br J Cancer **104**(12): 1828-1835.

Nagashima, M., M. Shiseki, et al. (2001). "DNA damage-inducible gene p33ING2 negatively regulates cell proliferation through acetylation of p53." Proc Natl Acad Sci U S A **98**(17): 9671-9676.

Nagashima, M., M. Shiseki, et al. (2003). "A novel PHD-finger motif protein, p47ING3, modulates p53-mediated transcription, cell cycle control, and apoptosis." Oncogene **22**(3): 343-350.

Nouman, G. S., J. J. Anderson, et al. (2003). "Downregulation of nuclear expression of the p33(ING1b) inhibitor of growth protein in invasive carcinoma of the breast." J Clin Pathol **56**(7): 507-511.

O'Shaughnessy, J., C. Osborne, et al. (2011). "Iniparib plus chemotherapy in metastatic triple-negative breast cancer." N Engl J Med **364**(3): 205-214.

Ohmori, M., M. Nagai, et al. (1999). "Decreased expression of p33ING1 mRNA in lymphoid malignancies." Am J Hematol **62**(2): 118-119.

Oki, E., Y. Maehara, et al. (1999). "Reduced expression of p33(ING1) and the relationship with p53 expression in human gastric cancer." Cancer Lett **147**(1-2): 157-162.

Oki, Y., E. Aoki, et al. (2007). "Decitabine--bedside to bench." Crit Rev Oncol Hematol **61**(2): 140-152.

Olmeda, D., M. Jorda, et al. (2007). "Snail silencing effectively suppresses tumour growth and invasiveness." Oncogene **26**(13): 1862-1874.

Olsen, C. J., J. Moreira, et al. (2010). "Human mammary fibroblasts stimulate invasion of breast cancer cells in a three-dimensional culture and increase stroma development in mouse xenografts." BMC Cancer **10**: 444.

Orimo, A., P. B. Gupta, et al. (2005). "Stromal fibroblasts present in invasive human breast carcinomas promote tumor growth and angiogenesis through elevated SDF-1/CXCL12 secretion." Cell **121**(3): 335-348.

Ota, I., X. Y. Li, et al. (2009). "Induction of a MT1-MMP and MT2-MMP-dependent basement membrane transmigration program in cancer cells by Snail1." Proc Natl Acad Sci U S A **106**(48): 20318-20323.

Paget, S. (1989). "The distribution of secondary growths in cancer of the breast. 1889." Cancer Metastasis Rev **8**(2): 98-101.

Parrinello, S., J. P. Coppe, et al. (2005). "Stromal-epithelial interactions in aging and cancer: senescent fibroblasts alter epithelial cell differentiation." J Cell Sci **118**(Pt 3): 485-496.

Pena, P. V., F. Davrazou, et al. (2006). "Molecular mechanism of histone H3K4me3 recognition by plant homeodomain of ING2." Nature **442**(7098): 100-103.

Petersen, O. W., L. Ronnov-Jessen, et al. (1992). "Interaction with basement membrane serves to rapidly distinguish growth and differentiation pattern of normal and malignant human breast epithelial cells." Proc Natl Acad Sci U S A **89**(19): 9064-9068.

Phillips, G. D., C. T. Fields, et al. (2014). "Dual targeting of HER2-positive cancer with trastuzumab emtansine and pertuzumab: critical role for neuregulin blockade in antitumor response to combination therapy." Clin Cancer Res **20**(2): 456-468.

Pietras, K. and A. Ostman (2010). "Hallmarks of cancer: interactions with the tumor stroma." Exp Cell Res **316**(8): 1324-1331.

Prat, A., J. S. Parker, et al. (2010). "Phenotypic and molecular characterization of the claudin-low intrinsic subtype of breast cancer." Breast Cancer Res **12**(5): R68.

Pratt, A. J. and I. J. MacRae (2009). "The RNA-induced silencing complex: a versatile gene-silencing machine." J Biol Chem **284**(27): 17897-17901.

Prentice, R. L., B. Caan, et al. (2006). "Low-fat dietary pattern and risk of invasive breast cancer: the Women's Health Initiative Randomized Controlled Dietary Modification Trial." JAMA **295**(6): 629-642.

Raguz, S. and E. Yague (2008). "Resistance to chemotherapy: new treatments and novel insights into an old problem." Br J Cancer **99**(3): 387-391.

Rakha, E. A., J. S. Reis-Filho, et al. (2010). "Breast cancer prognostic classification in the molecular era: the role of histological grade." Breast Cancer Res **12**(4): 207.

Razin, A. and H. Cedar (1977). "Distribution of 5-methylcytosine in chromatin." Proc Natl Acad Sci U S A **74**(7): 2725-2728.

Razin, A. and A. D. Riggs (1980). "DNA methylation and gene function." Science **210**(4470): 604-610.

Richie, R. C. and J. O. Swanson (2003). "Breast cancer: a review of the literature." J Insur Med **35**(2): 85-101.

Robertson, J. F., A. Llombart-Cussac, et al. (2009). "Activity of fulvestrant 500 mg versus anastrozole 1 mg as first-line treatment for advanced breast cancer: results from the FIRST study." J Clin Oncol **27**(27): 4530-4535.

Ropero, S. and M. Esteller (2007). "The role of histone deacetylases (HDACs) in human cancer." Mol Oncol **1**(1): 19-25.

Roy, R., J. Yang, et al. (2009). "Matrix metalloproteinases as novel biomarkers and potential therapeutic targets in human cancer." J Clin Oncol **27**(31): 5287-5297.

Russo, J., R. Moral, et al. (2005). "The protective role of pregnancy in breast cancer." Breast Cancer Res **7**(3): 131-142.

Sanchez-Abarca, L. I., S. Gutierrez-Cosio, et al. (2010). "Immunomodulatory effect of 5-azacytidine (5-azaC): potential role in the transplantation setting." Blood **115**(1): 107-121.

Satpathy, S., C. Guerillon, et al. (2014). "SUMOylation of the ING1b tumor suppressor regulates gene transcription." Carcinogenesis.

Satpathy, S., A. Nabbi, et al. (2013). "RegulatING chromatin regulators: post-translational modification of the ING family of epigenetic regulators." Biochem J **450**(3): 433-442.

Schito, L., S. Rey, et al. (2012). "Hypoxia-inducible factor 1-dependent expression of platelet-derived growth factor B promotes lymphatic metastasis of hypoxic breast cancer cells." Proc Natl Acad Sci U S A **109**(40): E2707-2716.

Schor, S. L., A. M. Schor, et al. (1985). "Skin fibroblasts obtained from cancer patients display foetal-like migratory behaviour on collagen gels." J Cell Sci **73**: 235-244.

Schor, S. L., A. M. Schor, et al. (1985). "Adult, foetal and transformed fibroblasts display different migratory phenotypes on collagen gels: evidence for an isoformic transition during foetal development." J Cell Sci **73**: 221-234.

Scott, M., P. Bonnefin, et al. (2001). "UV-induced binding of ING1 to PCNA regulates the induction of apoptosis." J Cell Sci **114**(Pt 19): 3455-3462.

Serra, V., M. Scaltriti, et al. (2011). "PI3K inhibition results in enhanced HER signaling and acquired ERK dependency in HER2-overexpressing breast cancer." Oncogene **30**(22): 2547-2557.

Shao, Z. M., M. Nguyen, et al. (2000). "Human breast carcinoma desmoplasia is PDGF initiated." Oncogene **19**(38): 4337-4345.

Sharma, S., T. K. Kelly, et al. (2010). "Epigenetics in cancer." Carcinogenesis **31**(1): 27-36.

Shi, X., T. Hong, et al. (2006). "ING2 PHD domain links histone H3 lysine 4 methylation to active gene repression." Nature **442**(7098): 96-99.

Shimada, H., T. L. Liu, et al. (2002). "Facilitation of adenoviral wild-type p53-induced apoptotic cell death by overexpression of p33(ING1) in T.Tn human esophageal carcinoma cells." Oncogene **21**(8): 1208-1216.

Shinoura, N., Y. Muramatsu, et al. (1999). "Adenovirus-mediated transfer of p33ING1 with p53 drastically augments apoptosis in gliomas." Cancer Res **59**(21): 5521-5528.

Slamon, D. J., G. M. Clark, et al. (1987). "Human breast cancer: correlation of relapse and survival with amplification of the HER-2/neu oncogene." Science **235**(4785): 177-182.

Smith-Warner, S. A., D. Spiegelman, et al. (1998). "Alcohol and breast cancer in women: a pooled analysis of cohort studies." JAMA **279**(7): 535-540.

Smith, K. T., S. A. Martin-Brown, et al. (2010). "Deacetylase inhibitors dissociate the histone-targeting ING2 subunit from the Sin3 complex." Chem Biol **17**(1): 65-74.

Soliman, M. A., P. Berardi, et al. (2008). "ING1a expression increases during replicative senescence and induces a senescent phenotype." Aging Cell **7**(6): 783-794.

Soriano, A. O., H. Yang, et al. (2007). "Safety and clinical activity of the combination of 5-azacytidine, valproic acid, and all-trans retinoic acid in acute myeloid leukemia and myelodysplastic syndrome." Blood **110**(7): 2302-2308.

Stratton, M. R. and N. Rahman (2008). "The emerging landscape of breast cancer susceptibility." Nat Genet **40**(1): 17-22.

Surveillance, Epidemiology, and End Results (SEER) Program Populations (1969-2012) (www.seer.cancer.gov/popdata), National Cancer Institute, DCCPS, Surveillance Research Program, Surveillance Systems Branch, released March 2014.

Suzuki, K., D. Boland, et al. (2011). "Domain recognition of the ING1 tumor suppressor by a panel of monoclonal antibodies." Hybridoma (Larchmt) **30**(3): 239-245.

Suzuki, M. M. and A. Bird (2008). "DNA methylation landscapes: provocative insights from epigenomics." Nat Rev Genet **9**(6): 465-476.

Szyf, M. (1994). "DNA methylation properties: consequences for pharmacology." Trends Pharmacol Sci **15**(7): 233-238.

Takahashi, M., T. Ozaki, et al. (2004). "Decreased expression of the candidate tumor suppressor gene ING1 is associated with poor prognosis in advanced neuroblastomas." Oncol Rep **12**(4): 811-816.

Tallen, G., S. Farhangi, et al. (2009). "The inhibitor of growth 1 (ING1) proteins suppress angiogenesis and differentially regulate angiopoietin expression in glioblastoma cells." Oncol Res **18**(2-3): 95-105.

Tallen, G., I. Kaiser, et al. (2004). "No ING1 mutations in human brain tumours but reduced expression in high malignancy grades of astrocytoma." Int J Cancer **109**(3): 476-479.

Tallen, G. and K. Riabowol (2014). "Keep-ING balance: Tumor suppression by epigenetic regulation." FEBS Lett **588**(16): 2728-2742.

Tallen, G., K. Riabowol, et al. (2003). "Expression of p33ING1 mRNA and chemosensitivity in brain tumor cells." Anticancer Res **23**(2B): 1631-1635.

Taube, J. H., J. I. Herschkowitz, et al. (2010). "Core epithelial-to-mesenchymal transition interactome gene-expression signature is associated with claudin-low and metaplastic breast cancer subtypes." Proc Natl Acad Sci U S A **107**(35): 15449-15454.

Thakur, S., X. Feng, et al. (2012). "ING1 and 5-azacytidine act synergistically to block breast cancer cell growth." PLoS One **7**(8): e43671.

Thakur, S., A. K. Singla, et al. (2014). "Reduced ING1 levels in breast cancer promotes metastasis." Oncotarget **5**(12): 4244-4256.

Thalappilly, S., X. Feng, et al. (2011). "The p53 tumor suppressor is stabilized by inhibitor of growth 1 (ING1) by blocking polyubiquitination." PLoS One **6**(6): e21065.

Thiery, J. P. and J. P. Sleeman (2006). "Complex networks orchestrate epithelial-mesenchymal transitions." Nat Rev Mol Cell Biol **7**(2): 131-142.

Tokunaga, E., Y. Maehara, et al. (2000). "Diminished expression of ING1 mRNA and the correlation with p53 expression in breast cancers." Cancer Lett **152**(1): 15-22.

Toullec, A., D. Gerald, et al. (2010). "Oxidative stress promotes myofibroblast differentiation and tumour spreading." EMBO Mol Med **2**(6): 211-230.

Toyama, T. and H. Iwase (2004). "p33ING1b and estrogen receptor (ER) alpha." Breast Cancer **11**(1): 33-37.

Toyama, T., H. Iwase, et al. (1999). "Suppression of ING1 expression in sporadic breast cancer." Oncogene **18**(37): 5187-5193.

Toyama, T., H. Iwase, et al. (2003). "p33(ING1b) stimulates the transcriptional activity of the estrogen receptor alpha via its activation function (AF) 2 domain." J Steroid Biochem Mol Biol **87**(1): 57-63.

Trichopoulos, D., B. MacMahon, et al. (1972). "Menopause and breast cancer risk." J Natl Cancer Inst **48**(3): 605-613.

Tsai, J. H. and J. Yang (2013). "Epithelial-mesenchymal plasticity in carcinoma metastasis." Genes Dev **27**(20): 2192-2206.

Tutt, A., M. Robson, et al. (2010). "Oral poly(ADP-ribose) polymerase inhibitor olaparib in patients with BRCA1 or BRCA2 mutations and advanced breast cancer: a proof-of-concept trial." Lancet **376**(9737): 235-244.

Umbricht, C. B., E. Evron, et al. (2001). "Hypermethylation of 14-3-3 sigma (stratifin) is an early event in breast cancer." Oncogene **20**(26): 3348-3353.

Unoki, M., K. Kumamoto, et al. (2009). "ING proteins as potential anticancer drug targets." Curr Drug Targets **10**(5): 442-454.

Valentin, M. D., S. D. da Silva, et al. (2012). "Molecular insights on basal-like breast cancer." Breast Cancer Res Treat **134**(1): 21-30.

Ventura, A. and T. Jacks (2009). "MicroRNAs and cancer: short RNAs go a long way." Cell **136**(4): 586-591.

Vieyra, D., D. L. Senger, et al. (2003). "Altered subcellular localization and low frequency of mutations of ING1 in human brain tumors." Clin Cancer Res **9**(16 Pt 1): 5952-5961.

Vieyra, D., T. Toyama, et al. (2002). "ING1 isoforms differentially affect apoptosis in a cell age-dependent manner." Cancer Res **62**(15): 4445-4452.

Vuong, D., P. T. Simpson, et al. (2014). "Molecular classification of breast cancer." Virchows Arch **465**(1): 1-14.

Wagner, M. J. and C. C. Helbing (2005). "Multiple variants of the ING1 and ING2 tumor suppressors are differentially expressed and thyroid hormone-responsive in Xenopus laevis." Gen Comp Endocrinol **144**(1): 38-50.

Walsh, T. and M. C. King (2007). "Ten genes for inherited breast cancer." Cancer Cell **11**(2): 103-105.

Walzak, A. A., N. Veldhoen, et al. (2008). "Expression profiles of mRNA transcript variants encoding the human inhibitor of growth tumor suppressor gene family in normal and neoplastic tissues." Exp Cell Res **314**(2): 273-285.

Wang, Q. S., M. Li, et al. (2010). "Down-regulation of ING4 is associated with initiation and progression of lung cancer." Histopathology **57**(2): 271-281.

Wang, Y., D. L. Dai, et al. (2007). "Prognostic significance of nuclear ING3 expression in human cutaneous melanoma." Clin Cancer Res **13**(14): 4111-4116.

Wang, Y. and F. C. Leung (2004). "An evaluation of new criteria for CpG islands in the human genome as gene markers." Bioinformatics **20**(7): 1170-1177.

Wu, J. C. and D. V. Santi (1985). "On the mechanism and inhibition of DNA cytosine methyltransferases." Prog Clin Biol Res **198**: 119-129.

Xie, Y., W. Sheng, et al. (2011). "Enhanced antitumor activity by combining an adenovirus harboring ING4 with cisplatin for hepatocarcinoma cells." Cancer Gene Ther **18**(3): 176-188.

Xie, Y., H. Zhang, et al. (2008). "Adenovirus-mediated ING4 expression suppresses lung carcinoma cell growth via induction of cell cycle alteration and apoptosis and inhibition of tumor invasion and angiogenesis." Cancer Lett **271**(1): 105-116.

Xing, Y. N., X. Yang, et al. (2011). "The altered expression of ING5 protein is involved in gastric carcinogenesis and subsequent progression." Hum Pathol **42**(1): 25-35.

Yamamoto, S., T. Sobue, et al. (2003). "Soy, isoflavones, and breast cancer risk in Japan." J Natl Cancer Inst **95**(12): 906-913.

Yang, J. and R. A. Weinberg (2008). "Epithelial-mesenchymal transition: at the crossroads of development and tumor metastasis." Dev Cell **14**(6): 818-829.

Yasui, Y. and J. D. Potter (1999). "The shape of age-incidence curves of female breast cancer by hormone-receptor status." Cancer Causes Control **10**(5): 431-437.

Ythier, D., E. Brambilla, et al. (2010). "Expression of candidate tumor suppressor gene ING2 is lost in non-small cell lung carcinoma." Lung Cancer **69**(2): 180-186.

Zhang, B., X. Pan, et al. (2007). "microRNAs as oncogenes and tumor suppressors." Dev Biol **302**(1): 1-12.

Zhang, F., N. Baumer, et al. (2011). "The inhibitor of growth protein 5 (ING5) depends on INCA1 as a co-factor for its antiproliferative effects." PLoS One **6**(7): e21505.

Zhang, H. K., K. Pan, et al. (2008). "Decreased expression of ING2 gene and its clinicopathological significance in hepatocellular carcinoma." Cancer Lett **261**(2): 183-192.

Zhang, X., L. S. Xu, et al. (2004). "ING4 induces G2/M cell cycle arrest and enhances the chemosensitivity to DNA-damage agents in HepG2 cells." FEBS Lett **570**(1-3): 7-12.

Zhu, Y., H. Lv, et al. (2011). "Enhanced tumor suppression by an ING4/IL-24 bicistronic adenovirus-mediated gene cotransfer in human non-small cell lung cancer cells." Cancer Gene Ther **18**(9): 627-636.

Zhu, Z., J. Lin, et al. (2005). "Inhibitory effect of tumor suppressor p33(ING1b) and its synergy with p53 gene in hepatocellular carcinoma." World J Gastroenterol **11**(13): 1903-1909.